RISØ DK9500091 Risø-R-780(EN)

Indoor Deposition and the Protective Effect of Houses against Airborne Pollution

Christian Lange

Risø National Laboratory, Roskilde, Denmark
May 1995

Indoor Deposition and the Protective Effect of Houses against Airborne Pollution

Risø-R-780(EN)

Christian Lange

Risø National Laboratory, Roskilde, Denmark
May 1995

Abstract The protective value of a house during a release of toxic materials has been investigated to the atmosphere. A review of the relevant literature revealed wide agreement on dose reduction factors from 0.5 to 0.2. According to the literature indoor deposition rather than filtration by the building envelope was the main cause of the reduction, but very little information on indoor deposition exists.

The main topic for this work has been the measurement of indoor deposition using monodisperse particles in the size range 0.5 to 5.5 μm, labelled with neutron activatable tracers. The decay of aerosol concentration was measured and average deposition velocities were recorded in four houses. The results were consistent with increasing deposition velocities for increasing particle size and increasing degree of furnishing.

Neutron activatable particles have been used for measurements of skin deposition velocities to a human volunteer. The deposition velocity was found to be $7.4 \pm 1.1 \times 10^{-4}$ ms^{-1} for the 0.5 μm particles and $57 \pm 14 \times 10^{-4}$ ms^{-1} for the 2.5 μm particles. These values of skin deposition velocities imply that the amount of pollutants deposited to the skin of a dressed person is more than an order of magnitude larger than the amount deposited in the lungs, and that skin deposition is an important pathway for toxics that can penetrate through the skin.

Beryllium-7 was used as a tracer in a series of experiments. The activity distribution of this isotope was determined using a Berner low pressure impactor. Median diameters ranged from 0.7 to 1.1 μm and it was found that the activity distribution followed the mass distribution of the accumulation mode for atmospheric particles. I/O measurements have been made with two impactors. The results showed that the reduction in indoor air concentration was largest for supra micron particles.

This report is submitted in partial fulfilment of the requirements for a Ph.D. degree at the Technical University of Denmark, DTU.

ISBN 87-550-2024-0
ISSN 0106-2840

Grafisk Service, Risø, 1995

Contents

List of Tables

List of Figures

Nomenclature

Latin letters:

a	Constant, $a=(g \ \|\Delta T\| / (4 \nu^2 T_\infty))^{1/4}$.
C	Pollutant concentration[mass/m3] or [Bq/m3].
C_c	Cunninghams correction factor [ ].
C_i	Indoor concentration [mass/m3] or [Bqm^{-3}].
C_m	Momentum exchange coefficient, 1.146.
C_o	Outdoor concentration [massm^{-3}] or [Bqm^{-3}].
C_s	Thermal slip coefficient, 1.147.
C_t	Temperature jump coefficient, 2.20.
C_∞	Pollutant concentration in the core of the room [mass m^{-3}].
d_p	Particle aerodynamic diameter.
D	Diffusion coefficient [m^{2}s^{-1}].
D_e	Eddy diffusion coefficient [m^2s^{-1}].
D_l	Mass loading of indoor surfaces[gm^{-2}].
f	Filter factor for building envelope [ ].
F	Flow rate, [m^{3}s^{-1}].
g	Acceleration of gravity, 9.8 ms^{-1}.
H	Height of room [m].
k	Boltzmann's constant, 1.38x10^{-23} JK^{-1}.
k_g	Thermal conductivity of air [Wm^{-1}K^{-1}].
k_n	Von Karman's constant [ ].
k_p	Thermal conductivity of particles [Wm^{-1}K^{-1}].
K	Thermophoresis coefficient [ ].
K_r	Turbulence intensity parameter [s^{-1}].
Kn	Knudsen number, $Kn = 2\lambda/d_p$.
Lw	Lewis number, α/D.
Re_x	Reynolds number for flow over a surface [ ].
Ra_H	Rayleigh number based on height, $Ra_H=(g \beta \ \|\Delta T\| H^3)/(\alpha \nu)$.
s_g	Surface orientation coefficient, [ ].
S	Total indoor surface area. [m^2]
S_i	Area of the i'th surface, [m^2].
t	Time, [s].
T	Temperature, [K].
T_s	Surface temperature, [K].
T_∞	Air temperature in the core of the room, [K].
U	Fluid velocity parallel to a surface, [ms^{-1}].
v_{CP}	Deposition velocity according to the theory of Corner and Pendlebury, [ms^{-1}].
v_d	Deposition velocity, [ms^{-1}].
v_D	Deposition velocity due to diffusion to the wall from a convective flow, [ms^{-1}].
v_g	Gravitational settling velocity, [ms^{-1}].
v_t	Migration velocity associated with thermophoresis, [ms^{-1}].
V	Volume of room, [m^3].
x	Distance along surface, [m].
y	Distance normal to surface, [m].

Greek letters:

α	Thermal diffusivity of air, [m^2s^{-1}].
β	Coefficient of thermal expansion, [K^{-1}].
δ	Fluid boundary layer thickness, [m].
ΔT	Temperature difference, $\Delta T = T_s - T_\infty$.
θ	Normalized temperature, $\theta = (T - T_\infty)/(T_s - T_\infty)$.
λ	Mean free path of air molecules, 65 nm at 298K and 1 atm.
λ_r	Air exchange rate, [h^{-1}].
λ_c	Cleaning constant. Fraction of room/house air cleaned per unit time, [h^{-1}].
λ_d	Deposition decay constant, [h^{-1}].
λ_R	Resuspension constant, [h^{-1}].
λ_n	Radioactive decay constant, [h^{-1}].
λ_t	Concentration decay constant [h^{-1}].
μ	Dynamic viscosity of air, [$kgm^{-1}s^{-1}$].
ν	Kinematic viscosity of air, [m^2s^{-1}].
ρ_p	Particle density, [kgm^{-3}].
τ	Relaxation time of particle, [s].
ω	Normalized pollutant concentration, $\omega = C/C_\infty$.

Acronyms

AD	Aerodynamic Diameter.
AMAD	Activity Median Aerodynamic Diameter
APS	Aerodynamic Particle Sizer
BLPI	Berner Low Pressure Impactor
BRE	Building Research Establishment in Watford, United Kingdom.
DRF	Dose Reduction Factor
EML	Environmental Measurements Laboratory in New York
GFA	Glass Fibre *filter paper*
GMD	Geometric Mean Diameter.
GSD	Geometric Standard Deviation.
I/O	Indoor/Outdoor
MMAD	Mass Median Aerodynamic Diameter
NAA	Neutron activation analysis.
NMSIMPLX	Nealder&Mead Simplex algorithmen for size distribution analysis
PIXE	Proton induced x-ray emission.
RH27	Risø Huse 27 *a test site*
RIMI	Risø's Integrated MIlieu site: meteorological measurements centre

Preface

This is the final version of a thesis that was submitted to the Technical University of Denmark, DTU, in October 1994 in partial fulfilment of the requirements for the degree Ph.D. Lector Uffe Korsbech at DTU has been the responsible supervisor and Senior Scientist Jørn Roed from Risø National Laboratory has been the daily supervisor. Dr. John Garland from AEA, Technology in Great Britain has been acting as external censor.

The work has been funded by Risø National Laboratory, the Danish Research Academy and the Commission of the European Communities.

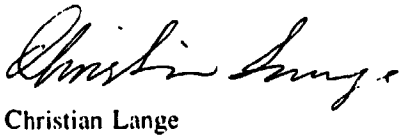

Christian Lange

Risø National Laboratory

May 1995

1 Introduction

When an accident occurs that involves releases to the atmosphere of toxic materials the first action of the civil defense authorities is to urge people to go indoors and close the windows and doors. It is assumed that the house will offer some protection against the inhalation of airborne gases and particles. But in 1975 the Rasmussen Report/WASH 1400(1975) disclaimed any protective value of houses in case of a release from a nuclear power plant. The authors stated that no measurements have shown such a protective value and that sooner or later the concentration levels indoor would equal the outdoor levels because all houses have air exchange with the atmosphere. In response to this statement a research project was initiated at Risø to measure the actual ratio of indoor to outdoor inhalation dose.

As part of an investigation the possible consequences of an accident on the nuclear power plant Barsebäck situated only 20 kilometres from Copenhagen a study on the reduction of inhalation doses indoors was initiated in 1978. Risø participated in this project together with the Danish technology institute. Risøs work was terminated in 1985 with a report by Roed et al (1985) which concluded that a dose reduction of 50 to 75 percent could be achieved by indoor residence during an accident. Later, Risø have started a research project together with Imperial College in London to further investigate the mechanisms governing the indoor/outdoor ratio of pollutants and thus determining the protective value of houses. The first results of this project showed that indoor deposition was a very important parameter. As a result a Ph.D. project with special focus on this topic was started at Risø.

1.1 Sources

When toxic materials are transported away from an accident site by the wind they will be in the form of a plume of gases and particles small enough to stay in the air. When discussing the protective value of a house the first question is, what are the properties of the gases and particles in the plume.

Gases are generally divided into two groups: reactive gases and non-reactive gases. Any gas with a negligible deposition velocity is considered to be a non-reactive gas. Noble gases are examples of a non-reactive gases. None reactive gases enter houses with litle or no filtration through the building envelop have a negligible deposition velocity, so the only way to reduce indoor inhalation is by ventilation of the building after a cloud passage. Lung deposition of these gasses is also negligible and usually, doses caused by these gases are quite small.

A reactive gas is a gas which has a sticking probability significantly larger than zero when bouncing into a surface. This leads to deposition on indoor surfaces, filtration by the building envelop and attachment to ambient aerosols. An example of a 'gas' with 100 % sticking probability is radon progeny which within few minutes after creation will deposit on indoor surfaces or attach to ambient aerosols. An other example of a reactive gas is elemental Iodine, which reacts with surfaces and ambient aerosol, but here it is more of chemical equilibrium/reaction that takes places and deposition velocities depend strongly on surface composition. In general sheltering in a house is expected to reduce inhalation dose of reactive gases.

All non-gaseous pollutants will either form particles or be attached to ambient aerosols and will be subject to atmospheric transport as such. Atmospheric

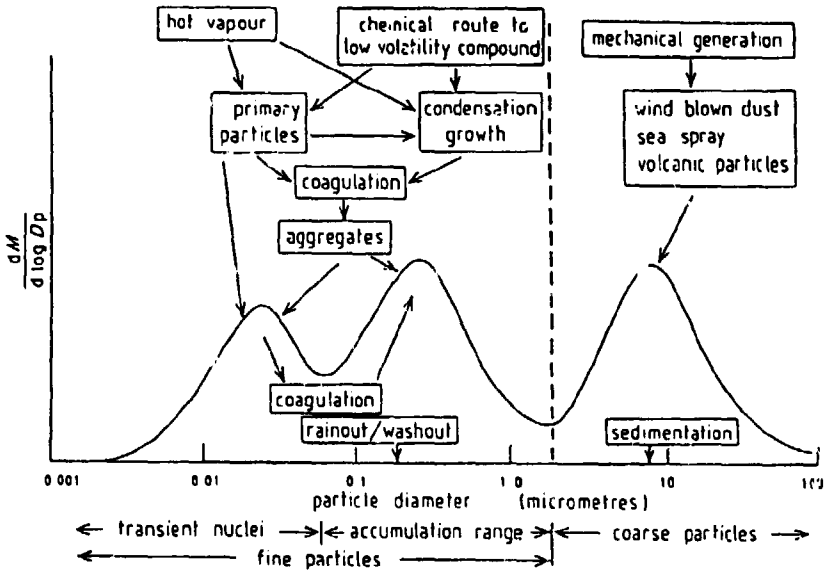

Figure 1.1. Schematic diagram of the size distribution and formation mechanisms of atmospheric aerosol. Whitby(1978). Y-axis is mass increment expressed per increment in log particle diameter and the area under the curve is thus proportional to mass. The accumulation mode and the coarse mode often contains equal amounts of mass whereas the nuclei mode only contains negligible mass but has the highest number concentration.

particles cover a wide size range: 10 nm to approximately 50 μm. During transport in a cloud, many processes will change the size distribution of the aerosols: smaller particles will grow larger and the larger particles will be lost by sedimentation. Figure 1.1 gives an idealized picture of the many mechanisms that governs atmospheric particles. The figure show the classification into three categories, as proposed by Willeke and Whitby(1975). This is generally accepted as a good description of atmospheric aerosols. The three categories are described below:

1. **Nuclei mode**/transient mode: these small particles are the result of vapour condensation and gas to particle conversion processes. They are the primary particles produced during a fire or a combustion. Combustion products and volatile compounds from the burning material condensate in the smoke when temperature drops. High particle concentration in the smoke will cause very rapid coagulation as coagulation for a given particle size is proportional to the number concentration squared. Dropping number concentrations and increasing particle size decreases coagulation, but even in normal continental air with particle concentrations from 10^9-10^{10} m^{-3} half life for particles in this mode will be a few hours at most before they coagulate or are attached to larger particles. Size range: 3 nm to 70 nm.

2. **Accumulation mode:** When particles have grown into this mode further growth is slow. Loss mechanisms, dry deposition and scavenging also have a minimum in this size range making it the atmospheric mode which usually contains the most mass. The size distribution of these particle can be described by a log-normal function with a mass mean between 0.5 and 1.0 μm. Particles in this mode have a mean residence time of 15 to 22 days in the atmosphere, Poet et al.(1972), making it the dominant mode for long range transport. Size range: 70 nm to 2 μm.

3. **Coarse mode**/Giant mode: Particles in this mode are usually produced by mechanical processes or by the blowing winds. Resuspension of soil dust due to traffic, agricultural activity or strong winds is a typical source of giant mode particles. Dried sea spray produces salt particles and can be the biggest contribution to airborne mass in coastal areas. Non flammable fuel fragments can be carried away during a fire. Sedimentation is the dominant loss term for large particles and the mean residence time in the atmosphere ranges from hours to a few days. Size range: 2 μm to 50 μm.

Nuclear Aerosols after the Chernobyl Accident

During and soon after the Chernobyl accident in 1986 activity distributions were measured for a range of radionuclides by size fractionating ambient aerosol and determining the radionuclides associated with each fraction. These measurements were made with impactors that collects particles according to their aerodynamic size. Usually the radionuclide activities were determined by gamma spectrometry. The resulting activity distributions are characterised by their activity median aerodynamic diameter, AMAD.

There were clear differences in the distributions depending on the properties of the chemical elements and the processes which created the particles. Tschiersch and Georgi(1987) measured activity distributions with an 8-stage Berner impactor from Hauke GmBH. They found similar distributions for Cs-137, Ru-103 and Te-132 as can be seen in figure 1.2 The AMAD ranged from 0.5 μm to 0.85 μm with a tendency to increasing AMAD with increasing distance from the point of release. They explained this by a slow growth due to coagulation during transport. Particulate I-131 showed a different distribution: the size range was broader and had a lower AMAD ranging from 0.4 μm to 0.5 μm (upper right corner of Figure 1.2). The distribution followed the surface distribution of the local aerosol, which is roughly equivalent to the attachment distribution of an aerosol. It was believed that I-131 was mainly transported as a gas in equilibrium with the local ambient aerosol. Reineking et al.(1987) and Jost et al.(1986) found the same pattern of size distribution. In addition they measured the total Iodine activity with charcoal filters and estimated that between 15 and 23 % of the activity was attached to particles. This agree what would be expected from the photochemical processes described by Jenkin et al.(1985), with the important exception that Jenkin et al. do not take dissociation from the particles into account which must happen if the similar ratios between gaseous and particulate iodine in different areas are to be explained. Reineking also noted that the activity distributions (except for iodine) resembled that of long-lived radionuclides in the atmosphere, e.g. Be-7 and Pb-210.

Another group of aerosols measured after Chernobyl were the so called 'hot'-particles. Osuch et al.(1989) divided these particles into two groups. Group A consisted of particles believed to have been created by condensation of especially [illegible] very soon after evaporation from the reactor core. Group B consisted of fuel fragments. Both groups consisted of relatively large particles (0.5 to 150 μm, Sandalls et al.(1993)) and therefore most of these particles was deposited in the vicinity of the power plant, but hot particles from the Chernobyl accident have been found as far away as Germany, Reineking et al.(1987).

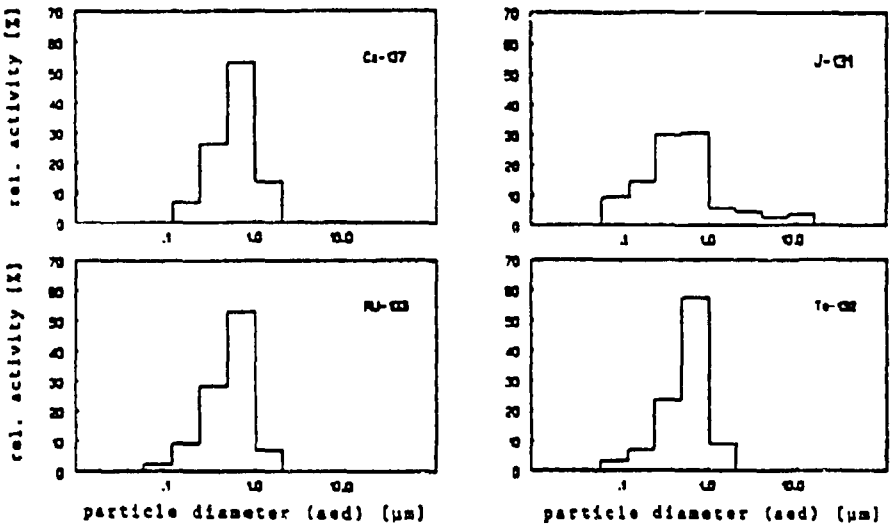

Figure 1.2. Size distribution of four isotopes from Chernobyl measured with a Berner impactor on the 6th of May in Neuherberg near Munich From Tschiersch and Georgi (1987).

Rulik et al.(1989) measured the Chernobyl aerosols using a Sierra high volume impactor. The higher flow rate made it possible to detect more isotopes but with poorer resolution/accuracy. The measurements confirmed that the AMAD of Cs-137, Ru-103 and Te-132 were somewhat below 1.0 µm. They also showed a second group, termed refractory elements, which had an AMAD of 1 to 4 µm. This group was associated with fuel fragments, such as Ce-144, Ce-141, La-140, Ba-140, Zr-95 and Nb-95.

In the impactor measurements by Reineking et al.(1987) decay of refractory elements were only detected in the two 'hot' particles found. This indicates that the measurements of refractory elements by Rulik et al.(1989) and Roed and Cannell(1987) probably was associated with 'hot' particles. Similar the contamination close to Chernobyl power plant of fuel fragments must be believed to have occurred through quite large particles (20 to 40 µm) as the activity is concentrated relatively close around the power plant.

In general, most particulate pollutants will be found in the second mode of particles, the accumulation mode, but close to the site of an accident both smaller and larger particles will have an important role, so the entire size range from 25 nm to 50 µm is of importance.

1.2 A Simple Box Model Relating Indoor and Outdoor Concentrations

To establish a platform for discussion, it is useful to establish an equation describing the problem and to identify the parameters of interest. This requires a definition of the mechanisms determining indoor concentration of pollutants of outdoor origin and their interaction. First it will be useful to define a term that describe our objective, namely a measure of the reduction in inhalation dose achievable by sheltering indoors.. Since inhalation dose is directly proportional to air concentration (for a given particle size) the dose reduction factor, *DRF*, can be defined theoretically as the ratio between the indoor pollutant concentration, C_i,

and the outdoor pollutant concentration, C_o, integrated from the start of the cloud passage, t_o, to infinity:

$$DRF = \frac{\int_{t_o}^{\infty} C_i dt}{\int_{t_o}^{\infty} C_o dt} \quad (1)$$

In order to derive an expression for the *DRF* we need to consider the many processes that take place in the indoor environment which determine or influence the ratio of indoor/outdoor concentration: the various processes are indicated diagrammatically in Figure 1.3. A simple differential equation can be derived by equating the change in indoor concentration per unit time with the difference between the production and loss of particles.

Equation (2) describes the processes represented in Figure 1.3. This equation is based on the premise that the indoor environment can be described as a single compartment with good internal mixing. Often the inhabitants will occupy only one room in the house and there will be cross ventilation from other rooms in the building. A set of differential equations can be set up describing a multi chamber system, as in Roed(1985) or Nazaroff & Cass(1989), but for simple description aiming at identifying the important parameters a one box model will do. This equation is:

$$\frac{dC_i}{dt} = f\lambda_r C_o - \lambda_r C_i - \lambda_d C_i - \lambda_c C_i + \lambda_R D_i - \lambda_r C_i \quad (2)$$

where the change in indoor air concentration, C_i, per unit time is given by the difference between ingression, $f\lambda_r C_o$, and losses due to exfiltration, $\lambda_r C_i$, cleaning, $\lambda_c C_i$, radioactive decay, $\lambda_o C_i$, resuspension from indoor surfaces, $\lambda_R D_i$ and indoor deposition, $\lambda_d C_i$.

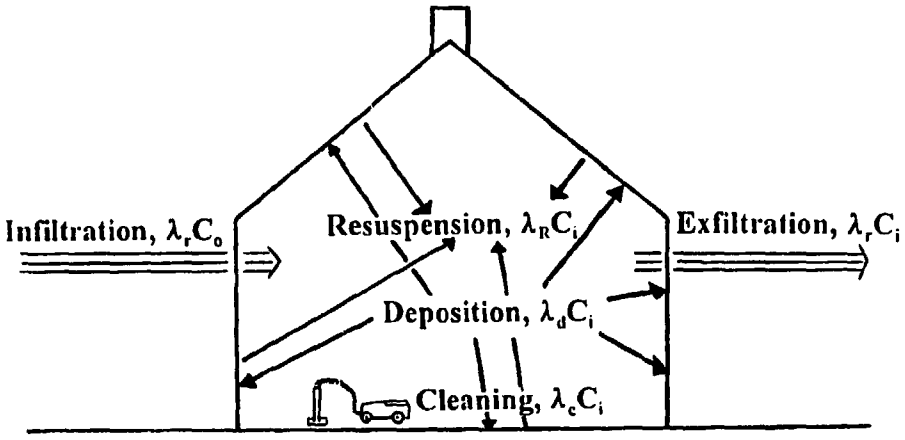

Figure 1.3. Diagram of processes involved in indoor/outdoor ratios.

The air that infiltrates from the outside which is filtered by the building envelope, f. Both the air exchange rate, λ_v, and the filter factor of the building envelope, f, depends on the construction of the house and must be expected to vary widely with the regional climate (Buildings in in warmer climates often have a higher air-exchange). The air-exchange rate will also depend on outdoor wind speeds and the temperature difference over the building envelop. The filter factor is expected according to the nature of the pollutant (i.e., size of particle and reactivity of gases). The air escaping from the building is also filtered over the building envelop but this has no effect on the equations as the outdoor volume can be considered as infinite compared to indoors.

The losses due to deposition inside a building are given by a room or building specific deposition constant, λ_d, multiplied by the indoor air concentration, C_i. This constant can be calculated from specific deposition velocities to eacn surface, $v_{d,i}$, multiplied by the area of that surface, S_i, and divided by the total volume, V, of the inclosure:

$$\lambda_d = \frac{\sum_{i=1}^{n} v_{d,i} S_i}{V} \tag{3}$$

where the deposition velocity is defined as the pollutant flux to a surface divided by the concentration of the pollutants over the surface and the sum is for n surfaces.

For a radioactive plume containing short-lived radionuclides the concentration indoors will decline due to radioactive decay, λ_n. For isotopes with half lives longer than one day this is of little importance since ventilation will be the governing loss-term, but for short-lived isotopes the decay can be included as an extra loss term similar to deposition or cleaning. The half-live of most radionuclides are well known and if the *DRF* for a specific radionuclide is sought it will be easy to incorporate this into the equations. For the general case this term will be omitted.

Another factor to take into account is resuspension from indoor surfaces, that is re-entrainment into the air of previously deposited particles. This can be expressed as a resuspension factor, λ_R, that can be specific for each surface and is dependent on the prehistory of the deposits. The amount of resuspended matter per unit time is proportional to the mass loading of the indoor surfaces, D_i. Very little is known about indoor resuspension. For short term emergency planning resuspension can be neglected, but it might be an important pathway for long-term dose. Resuspension from indoor surfaces has not been included in this study.

The use of domestic vacuum cleaners for removing radioactivity from indoor air in emergencies has been discussed as a possible counter measure by Roed et al.(1991). The air cleaning constant is obtained from the flow-rate, F, multiplied by the filter efficiency, ε, of the equipment and divided by the volume of the room, V:

$$\lambda_c = \frac{\varepsilon F}{V_i} \tag{4}$$

Looking at the basic processes of infiltration, exfiltration and deposition equation (2) can be reduced to the following first order inhomogeneous linear differential equation:

$$\frac{dC_i(t)}{dt}+(\lambda_r+\lambda_d)C_i(t)=f\lambda_r C_o(t) \qquad (5)$$

The equilibrium ratio between the indoor and outdoor air concentrations can be found by setting the change in indoor air concentration per unit time to zero. The I/O ratio in the equilibrium state is identical with the long term *DRF* given by equation (8). To simulate the passage of a radioactive cloud the outdoor concentration can be described as a step function, which is initially zero. It rises to a constant level at time t_0 and falls to zero again at time t_1. Using this function for $C_o(t)$, equation (5) can be solved analytically using a formula from Jenser(1981). The solution is given in equations (6) & (7). During passage of the cloud the indoor air concentration will increase towards the equilibrium ratio with an exponentially declining function:

$$C_i(t)=f\frac{\lambda_r}{\lambda_r+\lambda_d}C_o(1-e^{-(\lambda_r+\lambda_d)t}),\ t_0\le t\le t_1 \qquad (6)$$

After the cloud has passed the indoor concentration will decline exponentially towards zero:

$$C_i(t)=Ae^{-(\lambda_r+\lambda_d)t},\ A=C_i(t_1),\ t>t_1 \qquad (7)$$

The rise and fall of the indoor pollutant concentration as given by equation (6) and (7) is shown in Figure 1.4.

The *DRF* can now be found analytically by integrating the indoor and outdoor air concentrations and dividing the results. The result of this calculation is that the time integrated *DRF* equals the equilibrium ratio as shown in Figure 1.4 and by equation (8):

$$DRF=\frac{\int_{t_0}^{\infty}C_i(t)dt}{\int_{t_0}^{\infty}C_o(t)dt}=f\frac{\lambda_r}{\lambda_r+\lambda_d} \qquad (8)$$

This is a general result for all shapes of passing clouds, because all shapes can be approximated with a sequence of step functions and for all step functions the differential equation can be solved analytically with the same result for the *DRF*. This, of course, is based on the assumption that λ_r and λ_d are constants. The air exchange rate, λ_r, may change if the weather conditions change, but in all circumstances the value used in modelling will be an average value, which again will give us an average value for the dose reduction factor. When we want to examine the effect of varying the air-exchange rate we need to calculate the *DRF* by integration of the indoor and outdoor concentration levels. The deposition constant, λ_d, will vary with the particle size, but for each size class and type of pollutant the expression will be valid. This result has been presented by many authors, e.g. Kocher(1980), Roed et al.(1991), but many authors, e.g. Engelmann(1992) and Siren(1992), have given a more optemistic expression for the *DRF* by including ventilation of the house right after the passage of an rectangular cloud and thus reducing the contribution to dose from the 'tail' after passage, as given by equation (7).

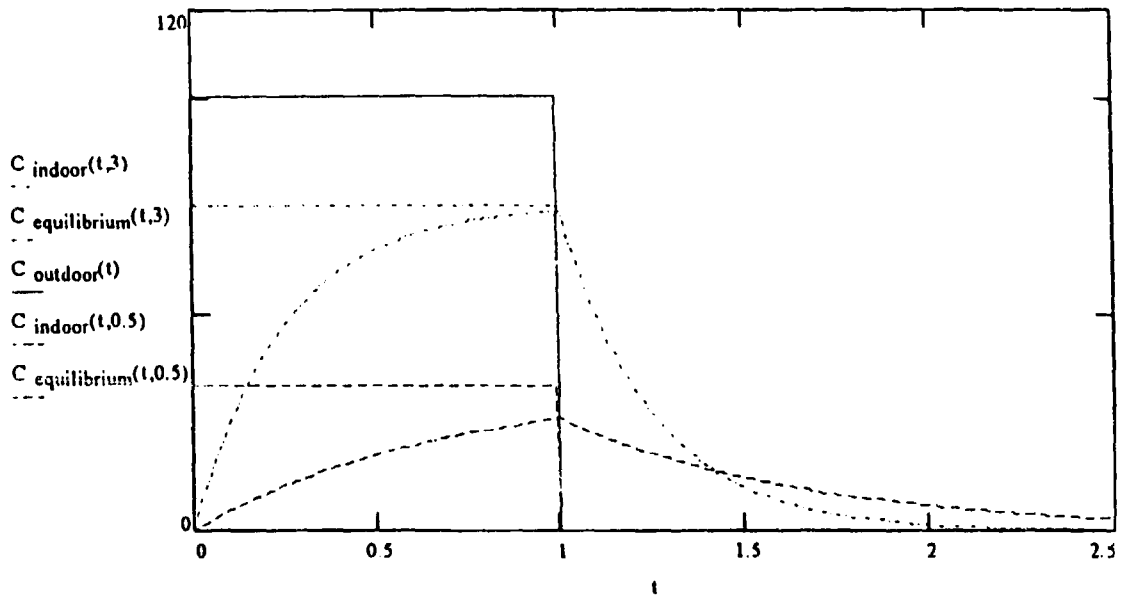

Figure 1.4. Rectangular shaped cloud passage with rise and fall of indoor air concentration as function of the air exchange rate. Curves are shown for $\lambda_v = 3\lambda_d$, *solid lines, and* $\lambda_v = 0.5\lambda_d$, *dashed lines. In both cases f equals 1.0 and the outdoor air concentration is 100. The rectangular curve shows the equilibrium between outdoor and indoor concentration. The graphs illustrate that the area under the equilibrium curve corresponds to the area under the exponential curves in both cases, i.e. it corresponds to the total inhalation dose.*

A factor which is not taken into account in this simple box model is the effect of air-conditioning systems. Air conditioning is rare in houses in Northern Europe, but in warmer parts of the world it is common and depending on the design of the individual system it can both enhance or decrease the *DRF*. The design of these systems varies and no general formulae can be applied for the effect of such systems.

After these considerations on infiltration of airborne pollution into houses three important parameters can be identified from equation (8):

1. Air exchange rates, λ_v.
2. Filter factors of the building envelope, *f*.
3. Deposition constants, λ_d.

With these three parameters in mind, the literature on relative indoor and outdoor concentrations was reviewed. The review is presented in section 1.3.

1.3 Indoor/Outdoor Concentration of Airborne Pollutants: A Review.

One method of estimating the benefit of staying indoors during a release of radioactivity to the atmosphere is to monitor the indoor/outdoor ratio of everyday pollutants. The observed pollutants must be of outdoor origin such as beryllium-7 or sulphur-dioxide, SO_2. Several such studies have been reported.

Dingle et al.(1958) described a study where the concentration of ragweed

pollen, 18-20 μm geometric diameter particles, was monitored indoors and outdoors together with the air-exchange rate. The effect of factors such as opening of windows and outdoor wind speed were examined. The I/O ratio ranged from 0.15 to 0.5 and correlations with the air-exchange rate and with the outdoor wind speed were observed. The penetration of pollen increased with increased outdoor wind speeds as did the air-exchange rate.

A series of papers has been published on the indoor/outdoor ratio of SO_2. Biersteker et al.(1965) carried out an investigation in Rotterdam in the early 1960s. The I/O ratio of SO_2 and the mass concentration were measured in 60 different homes. Air-exchange was not measured. Data were correlated with smoking habits of inhabitants, type of heating and the year of construction of the house and an increased SO_2 level were found in older homes, in homes of smokers and in homes were the heating system emitted SO_2. An I/O ratio of 0.20 was found for SO_2 in homes of newer construction with no internal sources.

Andersen(1972) reviewed measurements of I/O ratios of SO_2. The results of Biersteker et al. and 13 others were compared together with his own measurements. The I/O ratios ranged from 0.2 to 1.0. Important factors such as particle size and air-exchange rates were not considered in the review.

Dockery and Spengler(1981) studied I/O ratios of SO_2 and respirable particulate matter in 68 homes in six American cities. Indoor concentrations were described in terms of outdoor concentrations, air-exchange rates and indoor sources using the following formula:

$$C_i = fC_o + \frac{1}{\lambda_r} P \tag{9}$$

This formula was derived from an equation similar to equation (2), with the assumption that the deposition constant was much smaller than the air-exchange rate. The deposition constant was claimed to be less than 0.5 h^{-1} for particles larger than 1 μm and less than 0.05 h^{-1} for particles smaller than 1 μm, which was smaller than the average air-exchange rate of the houses, 1.5 h^{-1}.

$$\frac{\lambda_r}{\lambda_r + \lambda_d} \rightarrow 1 \quad for \ \lambda_r \gg \lambda_d \tag{10}$$

This reduction implies that filtration of the building envelop is the mechanism that causes lower concentration indoors. A term, P, expressed in amount of pollutant produced per volume per time was added to describe the effect of indoor sources. The model had correlation of 0.68 when fitted with the measured particle I/O ratios and 0.79 when fitted with the SO_2 I/O ratios. For particles a large contribution from indoor sources were found from the regression.

I/O ratios have been measured for many chemicals other than SO_2. Halpern(1978) examined of I/O ratios for lead. Colome and Spengler(1979) made I/O measurements of elements detectable by neutron activation. Yocom et al.(1971) and later Yocom(1982) made a review of indoor-outdoor air quality relationships. The reviews do not contain any values of air exchange rates or any formulas for prediction/explanation of I/O ratios. These references are examples of the many I/O measurements that do not try to interpretate the measured data and to understanding of the processes that determines the I/O ratio of atmospheric pollutants.

Alzona et al.(1979) investigated I/O ratios for airborne metals using X-ray florescence. The mean I/O value range from 0.1 to 0.42 depending on the element. Filtration by the building envelop, indoor deposition and resuspension were the parameters considered in the modelling of the results. Filtration by the

building envelop was considered to be of minor importance since experiments performed with windows open, where filtration should be close to zero, still yielded a 50% reduction of indoor concentration levels. Experiments where pumps were moved out of the test room and filters were changed with a minimum of human presence did not show any difference from earlier experiments. and from this they concluded that resuspension due to human and mechanical activity probably was of minor importance for the I/O ratio They suggested the following equation to model the I/O ratio:

$$\frac{C_i}{C_o} = f\frac{\lambda_r}{\lambda_d} \quad as\ \lambda_r + \lambda_d \approx \lambda_d \quad when\ \lambda_d \gg \lambda_r \tag{11}$$

since they found that the deposition constants that explained their results was much higher than the measured air exchange rates.

Using Be-7 as a tracer Christensen and Mustonen(1987) measured *DRF*s in four Finnish and one Norwegian house. The *DRF*s ranged from 0.23 to 0.45 in the Finnish houses and from 0.40 to 0.86 in the Norwegian house. No measurements were made of the air- exchange rate and the reduction in concentration was attributed to the filter factor f. The report did not discuss indoor deposition.

Measurements from Nuclear Accidents

A few measurements were made during or immediately after accidental release from nuclear power plants. After the Windscale accident in 1957 measurements of indoor/outdoor external gamma exposure rates were made in buildings nearby, Megaw(1961). These measurements were used to verify experiments where the indoor deposition velocity and the I/O ratio for a cloud of sub-micron particles were measured. v_d was found to be app. 1.5×10^{-3} ms^{-1} and the I/O ratio ranged from 0.34 to 0.78 for the particle cloud.

Roed and Cannell(1987) presented an experiment aimed at measuring the filter factor of the building envelop, f, and the average indoor deposition velocity, v_d, using Be-7 as a tracer. As the first cloud of radioactive material from the Chernobyl accident passed over Denmark this experiment was running and I/O ratios were measured for a series of radionuclides. *DRF*s were found to be in the range of 0.27 to 0.49 for particulate Iodine and Cesium with an air exchange rate of 0.4 h^{-1}.

Work Focused on Nuclear Accidents

Kocher(1980) modelled the inhalation dose indoors using a formula similar to equation (8). He assumed no filtration, i.e. f=1, and calculated the *DRF* for air-exchange rates of 0.2, 1.0 and 5.0 h^{-1} and average indoor deposition velocities of 10^{-2} and 10^{-4} ms^{-1}. In the absence of any information on actual values for indoor deposition, a maximum and a minimum value were chosen, based on knowledge of outdoor deposition velocities.

Koch and Tadmor(1988) calculated the actual effect of sheltering after a given release. They assumed an inhalation dose reduction of 0.65 for houses. They believed that ventilation of the house immediately after the cloud have passed could reduce the inhalation dose even further.

Cohen and Cohen(1979) measured I/O ratios at 20 sites in Pittsburg using X-ray fluorescence of Ca, Fe, Zn, Pb and Br. From measurements in the literature of the typical size distributions of each element they divided the result into a submicron

and supra micron set. For the submicron particles their best estimate was a DRF of 0.5 and for larger particles they found a DRF of 0.25.

Brown(1989) reviewed a series of measurements and model work on DRFs and concluded that a DRF value of 0.3 to 0.5 was appropriate, recommending 0.5 as a conservative value for accident consequence models such as COSYMA and RHODOS. She mentioned ventilation after passage of the cloud as a possible improvement but did not include that in the estimate of the DRF.

Engelmann(1991) modelled the effectiveness of sheltering and calculated DRFs for 2 μm particles as an example. He ignored the tail after cloud passage (as given by equation 7) since he thought that it could be removed by increased ventilation of the house after the passage of the cloud. He criticised other authors for equating the DRF with the long term I/O ratio and stressed that realistic rather than conservative values should be used in accident consequence assessment codes since this could be important when considering evacuation versus sheltering. He used a f value of 1, a λ_d of 0.81 h^{-1}derived from $v_d = 1.3 \times 10^{-4}$ ms^{-1}, as found in Sehmel (1984), and $\lambda_r = 0.5$ corresponding to an older house and predicted a *DRF* of 0.35 for a cloud passage of long duration. Engelmann(1992) later presented measurements of the *DRF* for cars. In this paper he includes equation 7, but ignores it again in his calculation of the *DRF* since he assumed rapid ventilation immediately after the cloud had passed.

Studies of Air Exchange Rates

Air-exchange rate has been studied for many reasons. It is an important factor influencing the quality of indoor air, in heat conservation calculations and when looking at ingress of outdoor pollutants. The Technological Institute of Denmark, Collet(1976) have researched this area for many years. The air-exchange rate has been found to be a function of pressure difference over the building envelop by applying positive and negative pressure to houses. The pressure difference is roughly proportional to the temperature difference and to the square of the wind speed. The air-exchange rate is proportional to the pressure difference. For a given house equation (12) has been found to describe the air exchange by Coblentz and Achenbach(1963). Others, Kvisgaard et al.(1988), have used a similar expression with the wind speed squared. k_1, k_2, and k_3 are empirical constants, ΔT is the temperature difference over the building envelop and U is the outdoor wind speed:

$$\lambda_r = k_1 + k_2 \Delta T + k_3 U \qquad (12)$$

Average air-exchange rates in older Danish houses are typically between 0.4 and 1.0 h^{-1}, Kvisgaard et al.(1988). For newly-constructed Danish houses an average value of 0.2 h^{-1} has been found. In these houses the air exchange rate is increased by mechanical ventilation through heat exchangers to 0.4 h^{-1} in order to improve the indoor air quality. Such mechanical ventilation should be turned off in during the passage of a cloud in order to minimize the air-exchange.

Similar studies have been made at the Helsinki Technical University. Siren(1992) calculated the ingress of gaseous pollutants into houses using the building characteristics and the weather conditions. He calculated only the *DRF* for penetration during the passage of the cloud and ignored the contribution from the 'tail' after passage (as given by equation (7)). He proposed to further improve the *DRF* by turning off the heating in the winter thus reducing the temperature difference driven air-exchange rate but this would only be of importance for a cloud passage of longer duration.

Summary

All the reports and papers of the literature review agreed on the basic processes as shown in Figure 1.3 and represented in equation (2). They then reduced this equation to an expression that best described their problem using appropriate approximations. Some authors, Engelmann(1992), Siren(1992), ignored the fraction of inhalation dose received after passage of the cloud (as described by equation (7)) others mention it and then but omit it with reference to ventilation immediately after the passage of the cloud (e.g. Engelmann(1991)) and some include it (e.g. Kocher(1980) and Roed(1991)).

Some papers (e.g. Christensen and Mustonen(1987), Roed(1985)) focused on f as the important factor and remove deposition from the equations due to an assumption that it is of minor importance, but most authors (e.g. Engelmann(1991), Roed and Cannell(1987), Kocher(1980) and Alzona(1979)) equate f to 1 in accordance with experimental experience.

Most articles acknowledge the importance of the air exchange rate. Some have made their own measurements and others quote reviews on air exchange rates. Values range from 0.07 to 5.0 h^{-1} for all the articles. Typical values in Danish houses range from 0.25 to 1.0 h^{-1}. Technological institutes in various countries have described the air-exchange rate of houses as a function of construction and weather conditions and for Danish houses accurate descriptions are available.

With f set to 1 and precise knowledge of the air-exchange rate, the deposition constant and the average indoor deposition velocities can be calculated as shown by Roed(1987). None of the other reviewed articles derived such values for indoor deposition from the measured I/O ratios. Some of the articles used values of λ_d for predictions of the *DRF* (Kocher(1980) and Engelmann(1991)) but they stated generally that knowledge is very limited in this area.

The conclusions of this review are that the *DRF* or I/O ratios generally lie between 0.2 and 0.5 with larger reductions for coarse particles. It is clear that the Rasmussen report(1975) was being too pessimistic on this point. All authors of the recent articles agreed that indoor deposition and not filtration by the building envelop is the mechanism that is responsible for lower indoor concentrations, but only one paper derived the average indoor deposition velocities that would explain the observed *DRF*. They also agreed that little knowledge and practically no measurements exist on indoor deposition.

1.4 Objectives

In order to predict the *DRF* for specific of pollutants as a function of their size and chemical properties more information is needed on indoor deposition of gases and particles of different sizes. It is the goal of this thesis to provide such knowledge with focus on particles in the size range 0.35 to 5.5 μm.

Two measurement techniques are available and have been used to investigate the problem from different views. Atmospheric beryllium-7, which is of purely outdoor origin, has been used at Risø for many years to investigate long term I/O ratios. Three investigations have been made with this tracer and will be described in Chapter 3. During this project an effort to determine the activity size distribution of this tracer and to investigate the connection between the tracer and the ambient atmospheric aerosol distribution have been done to increase the knowledge of the tracer. The experiment by Roed & Cannell(1987) have been repeated to verify the findings regarding the filtering effect, f, of building envelops and estimate indoor deposition constants, λ_d. Using two low-pressure impactors and the experimental design developed by Roed and Cannell(1987)

particle size specific I/O ratios have been measured in a house with four different air-exchange configurations. In general, the Be-7 tracer have been used measure overall I/O ratios and an effort have been made to dissolve the results into a filter factor and a deposition velocity.

To verify the deposition velocities estimate from the Be-7 measurements a technique using artificial aerosols with neutron activatable rare-earth incorporated as tracer have been used to measure indoor deposition velocities in Danish houses. This technique were presented by Roed et al.(1991). During this project an effort have been made to develop this technique to include sub-micron particles so that deposition velocities could be measured for particle sizes similar to those of Be-7. Experiments have been planned and performed in three houses and results are presented in Chapter 4.

As a spin-off from the technique using aerosols with neutron activatable tracers, deposition velocities have been measured to individual indoor surfaces. Here especially the deposition to human skin was found to be of interest and attention have been given to this topic and results are presented in Chapter 5.

2 Modelling of Indoor Deposition

This chapter describes the present theories for indoor deposition. The indoor environment has a complex and not very well defined air flow. The models describing the deposition indoors stipulate a rectangular box and either a convective flow or a homogeneously turbulent flow. W.W. Nazaroff and G.R. Cass's review paper 'Mass-transport Aspects of Pollutant removal at Indoor Surfaces' gives an introduction to the present state of modelling and have been an important source on the topic. In this paper methods for calculating indoor deposition for different flow regimes are presented. The formulas given by Nazaroff and Cass have been programmed in turbo pascal in order to facilitate calculation of deposition velocities and to produce graphs for comparison with experimental results.

G.A. Sehmel(1973) presented one of the few papers where deposition velocities to individual surfaces, floor, wall and ceiling, were measured (in a wind tunnel) and his paper has been an important source as the presented results are the only reference found that gives deposition velocities to individual surfaces, and thus can be used for comparison with the measurements of deposition velocities to individual surfaces presented in chapter 5.

2.1 Basic Principles for Calculation of Rate Constants of Indoor Deposition

Aerosols have a great variety of shapes and sizes depending on how they were formed and on their subsequent history. To measure these particles in a uniform and comparable way a special quantity has been introduced known as the aerodynamic diameter. The aerodynamic diameter of a particle is the diameter of a unit density spherical particle, which has the same settling velocity as the physical particle. The impactor and APS particle sizer instruments used to size the tracer particles used during this research project give information on their aerodynamic diameter. The Las-x particle sizer that have been used to size the sub-micron particles used gives information on the geometric size of the particles

and some difference in the size obtained with this instrument must expected depending on the density and shape of the particles. When calculating the theoretical behaviour of these particles using the formulas presented in this chapter their measured aerodynamic diameter should be used together with an unit density assumption no matter what their actual density is or knowledge of the density of the particles should be used to calculate the actual diameter of the particle.

The deposition constant for an aerosol in a room can be calculated by dividing the sum of the product of the deposition velocity and the area of each surface of the room by the volume of the room. Equation (3) shows the formula for this calculation. The deposition velocity, v_d, to each surface in a room can be approximated as the sum of the deposition velocities of the different processes, Nazaroff and Cass(1989):

$$v_d = v_t + v_D + s_g v_g \tag{13}$$

where v_t is the drift velocity caused by thermophoresis and can be both an enhancing or reducing effect, v_D is the drift caused by Brownian motions of the particles and it will always be directed towards the region where the concentration is lowest, v_g is the motion due to gravity and the effect depends on the orientation of the surface and s_g is an orientation parameter for each surface which determines whether the contribution from gravity should be added, $s_g = 1$, neglected, $s_g = 0$ or subtracted, $s_g = -1$. The subtraction of gravity from the deposition to a ceiling is probably a fair assumption when balance between different 'slow' forces is considered (such as brownian diffusion and gravety), but for larger particles where inertial processes and interception is of importance gravity might be of little significance to deposition on a ceiling and a subtraction will not be justified.

Diffusion

When gases or particles are distributed in air, the random movements due to Brownian motion, or impaction of the air molecules on the particle surfaces, will always result in a net transport towards areas of lower concentration. The drift velocity is proportional to the gradient of the pollutant concentration, ∇C:

$$v_D = -\frac{D}{C_\infty}\nabla C \tag{14}$$

where C_∞ is the pollutant concentration in the centre of the room, and D is the constant of proportionality known as the diffusion coefficient. D has been measured for many gases and has been found to be in the range 0.7 to 7.6 x 10^{-5} m^2s^{-1}, Nazaroff and Cass(1989). For particles, a general expression has been derived for D, see for example Reist(1984):

$$D = \frac{kTC_c}{3\pi\mu d_p} \tag{15}$$

where k = 1.38x10^{-23} JK^{-1} is Boltzmann's constant, T is the temperature of the air, μ is the dynamic viscosity of air (1.81x10^{-5} $kgm^{-1}s^{-1}$ at 293 K) and d_p is the particle diameter. C_c is a slip coefficient that varies according to the particle Knudsen number, $Kn = 2\lambda/d_p$, where λ = 0.065 µm at 298 K is the free mean path of air molecules. An empirical expression for the slip coefficient is given by Davies(1945), based on experimental work where the motion of oil droplets in air

and glass beads in fluids was studied:

$$C_c = 1 + Kn[1.257 + 0.400e^{-\frac{1.10}{Kn}}] \quad (16)$$

In general, diffusion is not important for the mixing of air in a room. Reist(1984) gave an example where he calculated the average time it would take for a 0.25 µm particle to move from the centre to the wall of a spherical flask, 5 cm in diameter, assuming diffusion to be the only mixing process. The result of 35.5 days shows that diffusion is only important for particles so small that the diffusion coefficient, D, approaches that of molecules or when considering small volumes very close to a surface. Particles in the air in a room will be moved around by convective air flows, which are created by the temperature differences between walls and the air, the air exchange and by mechanical motions, e.g. fans, humans. Within a given room, the mixing is normally sufficient for the particle concentration to be essentially uniform (see for example Figure 4.8) except very close to the surfaces where diffusion is one of the mechanisms that transports particles through a boundary layer close to the surface where the concentration can be assumed to be zero for particles with a 100 % 'sticking probability' (that is all particles that touch a surface adhere to that surfaces). The deposition velocity due to diffusion can then be found as the diffusion coefficient divided by the thickness of the boundary layer.

Thermophoretic Deposition Velocity

Thermophoresis is the term used to describe a process where airborne particles tend to move from warmer areas toward colder areas. For small particles (compared with the free mean path of air molecules) the behaviour is explained by the difference in kinetic energy of air molecules impacting from the hot and cold side, but for larger particles, the thermophoretic effect also depends on the thermal conductivity of the air and the particles. The resulting drift/deposition velocity is proportional to the balance between the viscous drag and the thermophoretic force. The thermophoretic force is proportional to the temperature gradient, ∇T, divided by the temperature, T_∞, in the centre of the room:

$$v_t = -K\frac{\nu}{T_\infty}\nabla T \quad (17)$$

where ν is the kinematic viscosity of air (1.5×10^{-5} m^2s^{-1} at 293 Kelvin) and the proportionality factor K is determined from the interpolation formula of Talbot et al.(1980):

$$K = 2C_s \frac{(\frac{k_g}{k_p} + C_t Kn)[1 + Kn(1.2 + 0.41e^{-\frac{0.88}{Kn}})]}{(1 + 3C_m Kn)(1 + 2\frac{k_g}{k_p} + 2C_t Kn)} \quad (18)$$

kg and kp are the thermal conductivities of the air and the particles. The coefficients have the following values: C_m = 1.146, C_s = 1.147 and C_t = 2.20. For particles in air with d_p of less than 3 µm and k_g/k_p in the range of 0.01-0.5, K varies between 0.1 and 0.6, Nazaroff and Cass(1989).

Gravitational Settling Velocity

The gravitational settling velocity for particles is usually derived by equalling the fluid drag, F, with the gravitational force, $m\,g$, and isolating the equilibrium velocity. The resistance of a fluid is given by Stokes equation. When the particle size becomes comparable to the free mean path of the air molecules the resistance force is reduced by Cunningham's slip correction factor and a modified version of Stokes equation is derived:

$$F=3\pi\mu v_p d_p/C_c \tag{19}$$

where v_p is the velocity of the particle and C_c is the slip correction factor. When this expression is equalled to the force of gravity, $m\,g$, the following expression for the equilibrium or settling velocity, v_g, is derived:

$$v_g=\tau g,\ \tau=\frac{d_p^2\rho_p C_c}{18\mu} \tag{20}$$

where ρ_p is the particle density, g is the acceleration of gravity, v_g is the velocity a particle will have relative to air under steady state conditions and τ is the relaxation time of the particle. τ is a parameter often used to characterize the behaviour of a particle due to inertia or gravity.

Particle Impaction

As the density of particles is usually much greater than that of air, particles will have a tendency to continue along their original path due to the inertia when the air flow suddenly changes direction. This might cause the particles to impact on the object that forced the air flow to change direction, in which case the phenomenon is called inertial impaction. The probability of impaction is described by the Stokes number, Stk:

$$Stk=\frac{U\tau}{W} \tag{21}$$

where U is the flow velocity. $U\tau$ is the distance the particle will move in the original direction of the flow when the air flow turns through 90 degrees. W depends on the geometry of the original flow in relation to the impaction surface. For a Berner impactor, W is the radius of the nozzle. Another effect of particle inertia is inertial mixing in a turbulent boundary layer.

Boundary Layer Theory

When air flows over a surface, a laminar (i.e. free of turbulence/no air motion orthogonal to the main flow) boundary layer will increase in thickness in the direction of the flow. Davies(1966) derived a formula for the laminar boundary layer thickness, δ, over a surface with an initial uniform flow, as a function of the distance, x, along the surface from the place where it starts:

$$\delta=5x/\sqrt{Re_x},\ Re_x=U_\infty x/\nu \tag{22}$$

where Re_x is called the Reynolds number of the flow and is defined by analogy with the Reynolds number for particles flowing through air, or air flowing through tubes.

U_0 is the velocity of the main air stream and ν is the kinematic viscosity of air. The Reynolds number gives information on the type of flow, and for Reynolds numbers larger than about 10^5 a transition to a turbulent boundary layer occurs. When turbulence is introduced in the boundary layer it will enhance mixing and thus deposition as described in the section below on deposition from turbulent air.

The pollutant concentration and air velocity gradient within a laminar boundary layer is assumed to be constant. With this assumption the air velocity profile, $U(y)$, within the boundary layer can be represented by:

$$U(y)=\frac{U^*}{k_v}\ln\left(\frac{y+y_0}{y_0}\right) \tag{23}$$

where U is the wind speed, y is the distance from the surface, y_0 is the roughness length, U^* is the friction velocity of the surface material, and k_v is von Karman's constant, which is commonly cited in the literature as 0.4. This profile has been verified experimentally in a series of wind tunnel experiments (e.g. Chamberlain(1991)).

At the solid surface, where the air motion is negligible and the concentration is zero, when 100 % attachment of the gas or aerosol is assumed. The deposition velocity due to diffusion through a laminar boundary layer will be given by D/δ, where δ is the thickness of the boundary layer; the concentration gradient can be assumed to be constant in the boundary layer.

2.2 Deposition from Convective Flows

Nazaroff and Cass(1987) and later Gadgil et al.(1992) presented a numerical solution of the flow regime in a two-dimensional rectangular enclosure generated by differences in surface temperature. By including diffusion in these equations deposition velocities were predicted for unattached and attached radon progeny. Nazaroff(1989) incorporated the numerical results of these calculations into his computer code MIAQ4. With information on either (user defined) the temperature difference between the air and the surfaces or the mean air flow velocity over the surface, deposition velocities were calculated. The flow generated by the temperature difference between the surface and the air, ΔT, is characterized by its Rayleigh number, Ra, obtained from Ede(1967):

$$Ra_H=\frac{\beta g|\Delta T|H^3}{\alpha\nu} \tag{24}$$

where H is the height or length of the surface, α is the thermal diffusivity of air, and β is the coefficient of thermal expansion ($1/T$ for an ideal gas). For Rayleigh numbers larger than 10^9 transition to turbulence begins. In general this will happen over radiators and at the end of flows along walls with a significant temperature differences to the air. The results of the numerical calculations are presented in the form of a dimensionless flux, $[\omega'(0)/Lw^{1/3}]$, and can be converted to a deposition velocity to a vertical surface by using the following formula, Nazaroff and Cass(1989):

$$v_d=\frac{4}{3}a\alpha^{1/3}D^{2/3}H^{-1/4}[\omega'(0)/Lw^{1/3}] \tag{25}$$

where H is the height of the wall, $Lw = \alpha/D$ is the Lewis number and a is given by:

$$a=[\frac{g|\Delta T|}{4\nu^2 T_m}]^{1/4} \qquad (26)$$

Equation (25) has been used to calculate deposition velocities for a range of diffusivities (particle sizes) and surface-to-air temperature differences. In Figure 2.1, the deposition velocity is presented as a function of particle size for three temperature differences. All the curves approximate to the curve for purely gravitational losses when particle size rises above 2 - 3 μm, that the average v_d that is found when from the deposition constant calculated from the gravitational settling to the floor.

The equations presented by Nazaroff and Cass(1989) did not include particle inertia as it was assumed that the low velocities of air in the indoor environment would mean that this effect of minor importance. Several authors, Sehmel(1973), Byrne(1994) and Schneider et al.(1994), have presented an increase in deposition velocity to vertical surfaces when particle size becomes greater than 1 μm. This is in line with the theoretical considerations presented by Reist(1984) and illustrated in Figure 2.2. First a decreasing deposition velocity can be seen as the diffusion coefficient decreases with increasing particle size. At some point between one or two micrometer the impaction/inertial mixing will act to increase the deposition velocity to vertical surfaces. Larger particles (above 20 μm) will not follow the small eddies in turbulent air and mixing will decrease, and at some particle size deposition to a vertical surface will start to decline again. As impaction is proportional to the air speed angular to the surfaces it is possible that the local maximum in Figure 2.2 is negligible in the relatively still indoor air, but the experimental results presented in this study and by others are not in line with such an assumption.

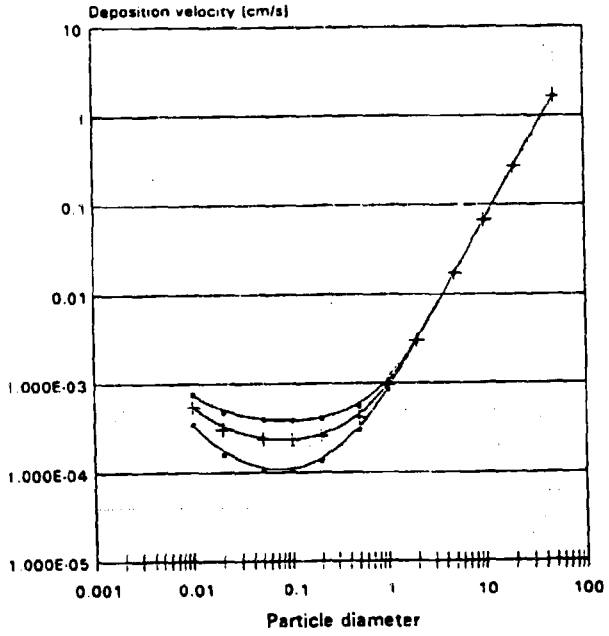

Figure 2.1 Average deposition velocities as function of temperature differences between air and surface. The deposition velocity have been calculated for each surface in the room using the formulas from Nazaroff and Cass(1989) and the average deposition velocity have been calculated after equation (3) for three different values of the temperature difference.

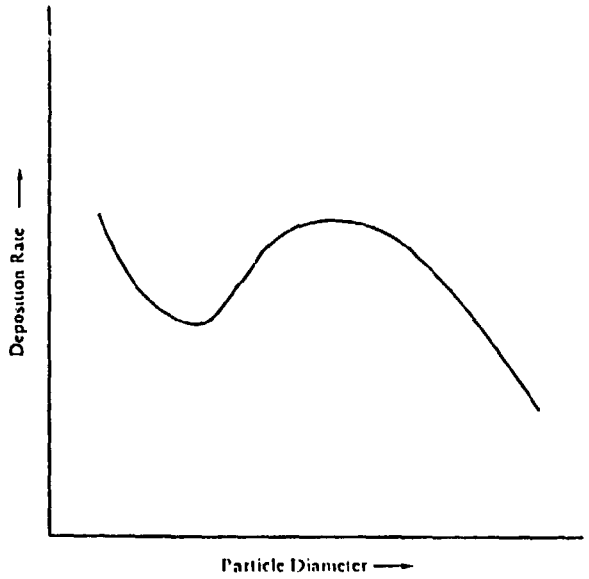

Figure 2.2. Schematic diagram of deposition velocity to a vertical surface as a function particle diameter. First the deposition velocity, v_d, declines as diffusion decreases with particle size, At some point (app. 1 μm) the inertia of the particles becomes important and the deposition to a vertical surface starts to increase. At some particle size (app. 20 μm) the deposition starts to decrease again as the larger particles becomes immobile and stop to follow the small eddies. From Reist(1984).

2.3 Deposition from a Homogeneously Mixed Core

Corner and Pendlebury(1951) calculated deposition velocities to the floor, walls and ceiling of a room with a homogeneously turbulent mixed core and with an assumption of a boundary layer near the surface with a constant gradient of the mean air velocity *du/dy* parallel to the wall within the boundary layer. The calculation were compared with measurements by Langsroth and Gillespie(1947) performed in a test chamber with still and moving air and the model showed qualitative agreement both regarding the magnitude of deposition and the effect of stirring. Mean air velocities in the test chamber were up to 0.8 ms^{-1}. Particle transport was assumed to occur only by Brownian motion, sedimentation and eddy diffusion. The eddy diffusion in the boundary layer was assumed to be proportional to the square of the distance from the surface, $D_e = K_e y^2$. They solved a differential equation for the flow in the boundary layer for each surface orientation, similarly to Fick's second law, Reist(1984):

$$\frac{dC}{dt} = \frac{d}{dy}\left[(K_e y^2 + D)\frac{dC}{dy}\right] + s_R v_R \frac{dC}{dy}, \quad 0 \le y \le \delta \tag{27}$$

where K_e is the turbulence intensity parameter measured in s^{-1} given by $k_0^2 du/dy$ where $k_0 = 0.4$ is von Karman's constant. Nazaroff and Cass(1989) summarized their results and extended it to include the case of reactive gases. For vertical surfaces, the deposition velocity derived by Corner and Pendlebury(1951), v_{CP}, was represented as follows:

$$v_{CP} = \frac{2}{\pi}\sqrt{DK_e} \tag{28}$$

and for ceilings:

$$v_{CP}=v_k/(e^{\frac{\pi}{2}\frac{v_s}{\sqrt{DK_c}}}-1) \tag{29}$$

and for floors:

$$v_{CP}=v_k/(1-e^{-\frac{\pi}{2}\frac{v_s}{\sqrt{DK_c}}}) \tag{30}$$

Crump and Seinfeld(1983) extended this model to derive expressions for a chamber of any given shape. They also solved the equation for the general case, $D_e = K_e y^n$. Holub et al.(1988) and Okuyama et al.(1985) have used this result with a value of n of 2.61 and 2.7 respectively.

The equations (28) to (30) have the drawback that they do not include the effect of particle inertia. Therefore the deposition to the walls and ceiling falls to zero when the particle size increases and this can be seen in Figure 2.3. In Figure 2.4 it can been seen that for increasing particle size, all curves follow the same path. The common path represents the gravitational settling at the floor (given by v_g) averaged to all surfaces in the room as the contribution from deposition to other surfaces falls to zero.

A series of references that have used a solution equation (27) to derive an imperical formulae for there experimetal results dealing with turbulent deposition is shown in Table 2.1 below. For all the references in the table the prediction of the experimental result consists of curve-fitting with different parameters. References 2, 3 and 6 all used a fitted value of n. The other papers used a fixed n of 2 and found the turbulence intensity that gave the best fit for their results. Reference 5 used an empirical formula based on the basic aerosol mechanisms.

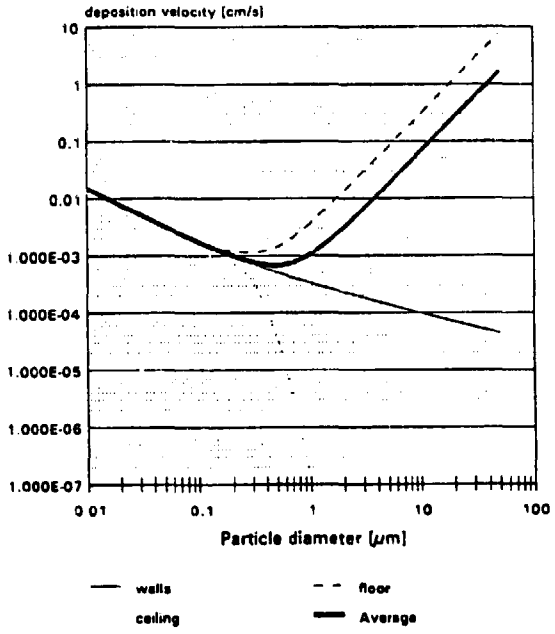

Figure 2.3 Deposition velocities calculated from equation (28) to (30) for k_e = 1 and the average deposition velocity, bold line, calculated from the individual deposition velocities using equation (3). It can be seen that deposition to the walls and ceiling keeps declining when only diffusion and gravitational settling is considered.

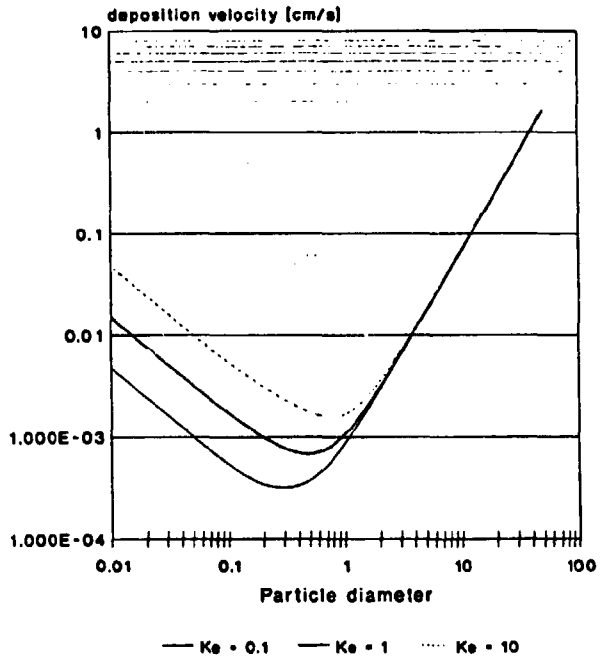

Figure 2.4. Average deposition velo ·ies as function of particle size plotted for three values of k_ϵ. It can be seen that independently of the chosen k_ϵ value the average deposition velocity is almost identical when the particle size exceeds 2 μm.

Table 2.1. Review of papers which have measured deposition constant in various test chambers and wind tunnels. The results have been fitted with different models of turbulent deposition based equation (27).

No	Reference	n in $D_\epsilon=k_\epsilon x^n$	k_ϵ, turbulence intensity	Remarks
1.	Crump et al.(1983)	2, fixed	0.028 s^{-1}& 0.068 s^{-1}, fitted	
2.	Holub et al.(1988)	2.61, fitted	0.0071 s^{-1}, fitted 107 s^{-1} calculated from fan speeds.	3.9 m^3 test tank
3.	Okuyama et al.(1985)	2.7, fitted	Calculated from fan speeds	Volume 2.6 litre test tank
4.	Schneider et al.(1994)	2, fixed	one dimensionless k_ϵ value and a set of friction velocities was fitted.	Wind tunnel
5.	Sehmel(1973)		Purely empirical formula used to fit data.	Wind tunnel
6.	Shimada et al.(1988)	2.7, fit from 3	Calculated	

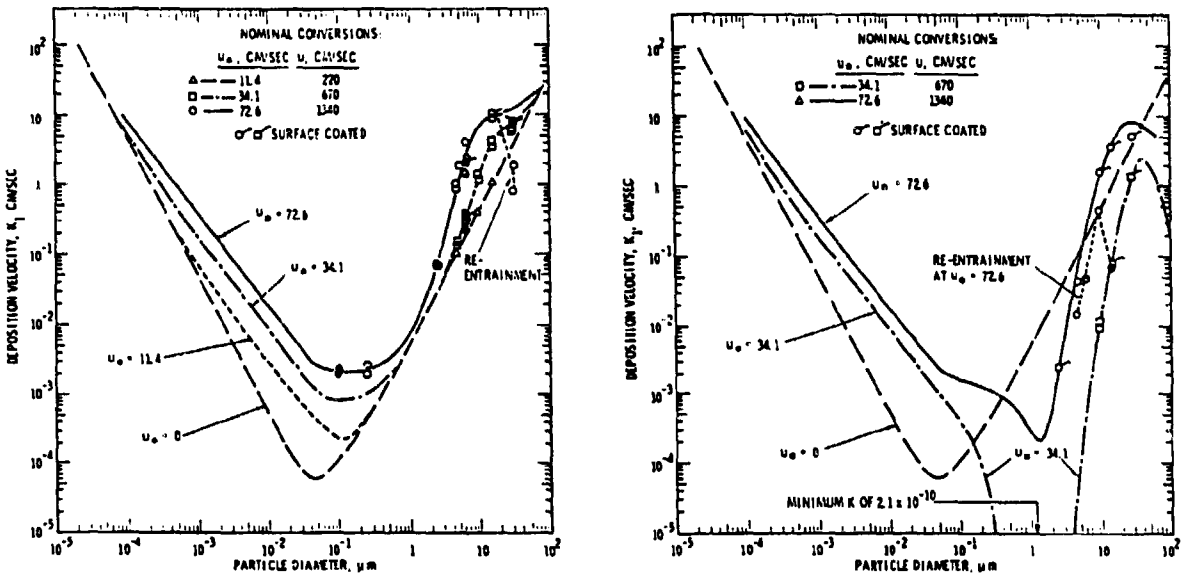

Figure 2.5 a & b. Experimental results fitted with empirical models for deposition to walls and ceiling of a wind tunnel. From Sehmel(1973). On Figure a (to the left) and Figure b the theoretical deposition velocity due to liffusion can be seen in the left side. It declines with increasing particle size as the diffusion coefficient decreases with particle size. When particle size reach app. 0.1 μm gravity starts to act and the deposition to the floor increases and it decreases to the ceiling. The dashed curve shows the deposition due to inertial impaction at both ceiling and floor

In Figures 2.5 a & b the experimental results obtained by Sehmel(1973) are plotted together with the curves of the derived empirical formulae. These curves show the pattern predicted by Reist(1984) and which can be seen in Figure 2.2. It is interesting to note that with only small changes in particle size, relatively large changes are predicted in deposition velocity in some critical regions.

2.4 Measurements in Houses

Only a few references have been found in the literature concerning measurements of indoor deposition. Most of them concerned radon progeny and the deposition constant was calculated from the balance between radon, unattached and attached progeny and the air exchange rate. In a review paper by Porstendörfer and Reineking(1992) average indoor deposition velocities of 1-2 x 10^{-4} ms^{-1} for attached progeny with an AMAD of about 200 nm were quoted from a series of papers.

Yamasaki and Suzuki(1992) and Kojima et al.(1993) studied the dependence of the equilibrium ratio between attached and unattached radon progeny on the deposition velocities of the two species. For the attached fraction a deposition constant of 0.3 h^{-1} was found and for the unattached fraction a value of 30 h^{-1} was obtained.

Offermann et al.(1985) studied tobacco smoke in a room. Corrections for changes in the size distribution due to Brownian coagulation were made by numerical computations. The remaining loss rate was attributed to uniform deposition to all surfaces. For particle sizes from 0.07 to 0.91 μm, deposition velocities from 2.7 x 10^{-6} to 1.3 x 10^{-4} ms^{-1} were found.

2.5 Theoretical Considerations on the Filtering Effect of Building Envelops.

In order to estimate the importance of filtration during the penetration of particles into a house some simple calculations have been made. The two loss mechanisms considered are diffusion and impaction. The geometry considered is a 20 centimeter deep long gap in a wall. It is assumed that most of the air-exchange will occur in gaps between 0.1 and 10 millimeter in width and that airspeeds during penetration will be between 0.1 and 10 ms^{-1}.

Diffusion losses have been calculated as a first order appoximation by dividing the diffusion coefficient, D, from equation (15) with the gap width, the surface to volume ratio of the gap, and the residence time of the particles in the gap (gap depth divided by the air speed). Diffusion losses will be highest for narrow gaps (small distance to travel) and slow air speeds (long residence time) as can be seen from the curves in figure 2.6. As a 'worst case', considering high diffusion losses a gap width of 0.1 millimeter and an air speed of 0.1 ms^{-1} gives a filtration of less than 10% for particles larger than 0.1 μm. From these considerations it is a fair assumption that diffusion losses will insignificant for particles larger than 0.1 μm.

For impaction losses it is assumed that a 90° turn exists in the gap. The *stk* number can then be calculated from equation (21). The greatest losses will here occur for narrow gap and high air speeds. Three sets of calculation are shown in figure 2.7. Here the greatest losses are found for a gab width of 0.1 μm and an air speed of 10 ms^{-1}, yielding a *stk* number of 0.031. So due to impaction we can assume fairly little filtration for particles smaller than 10 μm, but here other mechanisms will also be of importance. Results presented in Chapter 5 and by Chamberlain et al.(1984) show a significant increase in losses to rough surfaces of supra-micron particles, which makes the calculations insufficiant for these particles. As a conclusion the filtering effect of an building envelop will be small (less than 10%) for particles in the size range 0.1 to 1 μm.

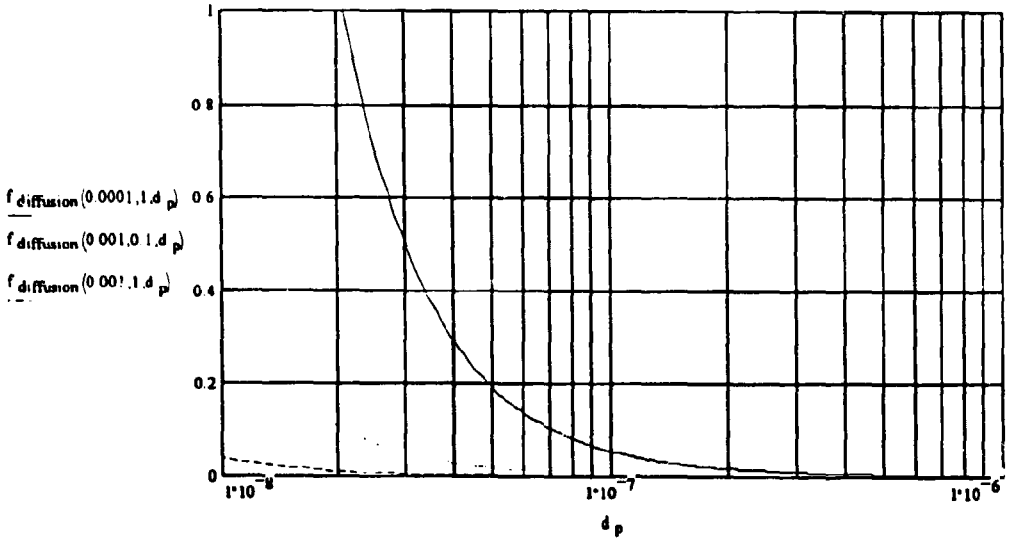

Figure 2.6 Diffusion losses, $f_{diffusion}(W,U,d_p)$, as a function of gap width, W, air velocity, U, and particle diameter. The particle diameter is given in meters along the x-axis.

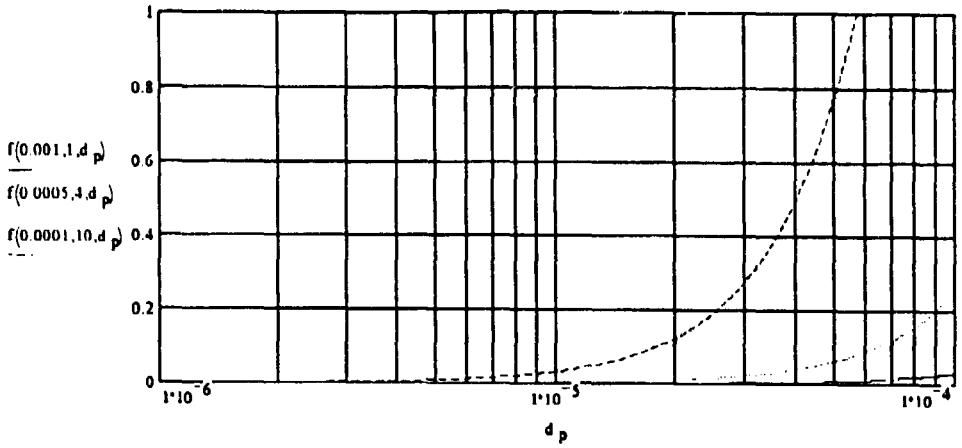

Figure 2.7. Impaction losses, $f(W,U,d_p)$, as a function of gap width, W, air velocity, U, and particle diameter d_p. The particle diameter is given in meters along the x-axis.

2.6 Conclusion

The paper by Nazaroff and Cass(1989) discussed various models for the prediction of deposition velocities from both laminar convective flow and turbulent flow. With access to the numerical solutions of the flow equations, as given in the source code to the computer model MIAQ4 by Nazaroff(1989) or by reading the Figure in the paper, it is possible to calculate deposition velocities from measurable environmental parameters, such as the room air temperature and the surface temperatures. Unfortunately, the models fail when the particle size exceeds one µm. For particle diameters greater than 1 µm the models predict that deposition velocities decrease for all surfaces except floors, when particle size increases. Several authors (e.g. Sehmel(1973), Chamberlain et al.(1984)) have found that the deposition velocity to walls starts to increase, when the particle size rises above app. 1 µm due to particle inertia. A maximum is reached for a particle size around 10 µm and then the deposition velocity starts to decline. Nazaroff and Cass omitted this from their equations as they believed it would be of minor importance due to the small air velocities observed indoors.

The effect of particle inertia has been allowed for in several models on turbulent deposition in enclosed vessels by inclusion in the term for the eddy diffusion in equation (15), but these models require a knowledge of parameters such as the turbulence intensity parameter, k_ϵ, which has no direct connection with the simple physical parameters in a room. Two references, Okuyama et al.(1985) and Holub et al.(1988), gave empirical formulae for the calculation of the turbulence intensity from fan blade speeds in small vessels, but this is not applicable to a living room where many other mechanisms cause air motion.

The experimental work done so far concerning indoor deposition has mostly focused on radon progeny, which is attached to smaller particles, 0.01 to 0.2 µm. This is somewhat smaller than the particle sizes that are expected to carry most of the airborne radioactivity after a nuclear accident as discussed in chapter 1.

For the particle size range studied during this project, 0.5 to 5.5 µm, it is concluded that no model exist that can accurately predict deposition in houses. However, a well-defined theory exists for the behaviour of aerosols and the pattern of the results obtained in this study can be interpreted according to that theory.

3 Measurements Using Beryllium-7 as Tracer

Beryllium-7 has been used at Risø to monitor long term I/O ratios in Danish houses for many years. In the spring of 1991 Kim Pilegård, the senior scientist in the office next to our laboratory, purchased an 11 stage Berner impactor from Hauke, and this enable us to start an investigation of the activity size distribution of Be-7. When I started at Risø the gamma counting analysis of this sample run had just been completed. I took on the job to calculate the important parameters for the measured size distribution using the techniques described by Parker C. Reist in his book 'Introduction to Aerosol Science'. During my stay at the Environmental Measurements Laboratory EML, in New York, Dr. E. O. Knutson introduced me to the computer programs he had developed for analysis activity size distributions of radon progeny and these programs I have used since to analyze our measurement data. During the last three years the measurement series have been expanded with an examination of the correlation between the mass distribution of atmospheric aerosol and the activity size distribution and the height dependence of the size distributions.

In the summer of 1993 a second Berner impactor was purchased and it now became possible to measure indoor and outdoor Be-7 concentrations simultaneously for different size classes, an experiment we had wanted to do since the acquisition of the first impactor. An experiment was started right away in a house in the village of Fersley. From the I/O ratios obtained average deposition velocities were calculated for particle sizes from 0.35 to 2.8 μm.

3.1 Measurement Technique with a Berner Impactor

The Berner low pressure impactor, BLPI, has been described by Berner and Lürzer(1980). The BLPI, Hauke Aeras 25-23/0.015 model, which is used in this study, has ten ordinary stages and a eleventh stage at the inlet where the particles larger than 16 μm impacts. It has been tested by Hillamo and Kauppinen(1991). They found that the impactor operated in accordance with the manufacturers specification with steep cut functions and with cut sizes identical to those specified by the manufacturer for stages 5 to 10 inclusive. For the low pressure stages, an increasing difference was found between the measured values and the specified values. For stage 1 a 50 % cut-off diameter of 30 nm was found instead of the specified 15 nm. For the measurements presented here this was of minor importance as mass and activity concentration in the last three stages was minimal. The Berner impactor has come to have widespread use as a scientific aerosol sampling instrument. It has the advantage of narrow cut sizes for each stage giving it a high resolution compared to many other impactors such as Sierra and Anderson. The BLPI 25 version covers the size range from 15 (30) nm to 16 μm. One advantage of impactors, in contrast to other aerosol sizing equipment, is that the size-fractionated material is collected on the impaction surfaces for subsequent analysis, by say PIXE, NAA, chemical analysis, gravimetric analysis and gamma ray spectrometry.

Impaction Surfaces

Prior to using an impactor, the materials to be used as a collector in the various stages must be carefully considered. It is essential to collect the particles on a surface which

will not interfere with subsequent measurements and which will retain its efficiency for long periods (several days). The collector material must not contain significant amounts of the element or material to be determined. Similarly, the material must not give rise to interferences when treated as a forerunner to analysis: for example neutron activation must not produce a radioactive nuclide which will interfere with the subsequent gamma ray analysis. For gravimetric measurements a surface that does not absorb humidity is preferable. For chemical analysis a collection material with no content of the species of interest is needed. Typically lead, zinc, iron, sulphates, etc. The selected impaction surface must also have the ability to keep impacted particles firmly attached.

To test the effectiveness of different impaction surfaces as collectors six different materials was tested using monodisperse silica particles of 2 and 4 μm aerodynamic diameter. One sample were made for each particle size and collector type. The impactor inlet were placed in front of the outlet of the silica particle disperser and approximately 100 mg of silica powder were dispersed in a 10 minutes period. The size distributions were obtained by gravimetric analysis as described in the next section and are shown in Figure 3.1 a & b.

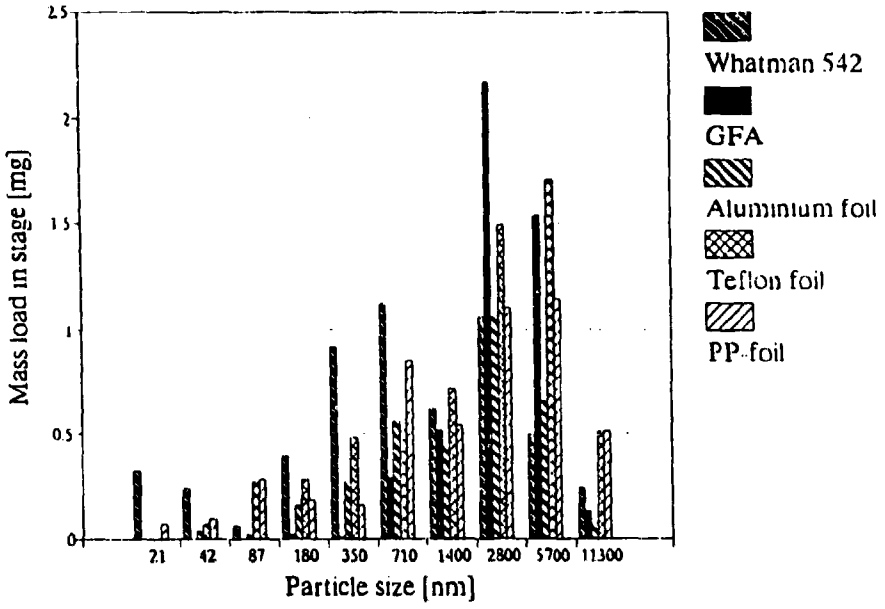

Figure 3.1 a. Five different sampling surfaces tested with 2 μm silica particles. As these particles are spherical, a higher fraction of particles must be expected to carry over to the next stages than would be the case for atmospheric particles.

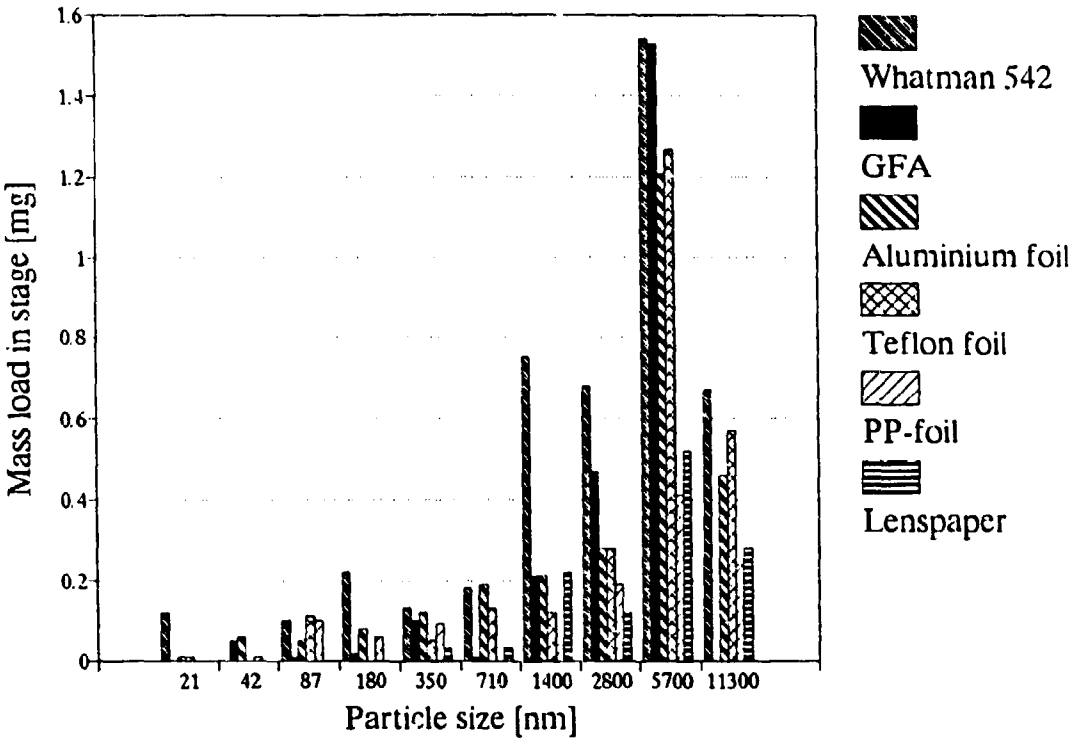

Figure 3.1 b. Six different sampling surfaces tested with 4 μm silica particles. As these particles are spherical, a higher fraction of particles must be expected to carry over to the next stages than would be the case for atmospheric particles.

Table 3.1. Properties of collection surfaces tested for use with a Berner impactor. The collection efficiency was determined from the distributions in Figures 3.1 a & b. The ratings for gravimetric analysis were based on personal experience with the collectors using a scale with a 10 μg resolution. The content of trace elements of metals was determined for all the collectors except the lens paper by Pilegaard(1994) and only the teflon and the PE foil had a negligible background. The teflon foil is thus assumed to be suitable for neutron activation analysis, NAA, but this has not been proven.

Surface type	Collection efficiency	Gravimetric analysis	PIXE or NAA	Chemical analysis
Glass fibre Whatman A	Good	Bad	Bad	Bad
Cellulose Whatman 542	Bad	Bad	Good	Medium
Aluminium foil	Medium	Good	Bad	Medium
Poly-Ethylene, PE, foil	Bad	Good	Good	Good
Teflon foil	Medium /good	Good	Good(?)	Good
Lens paper	medium	Medium	-	-

Schumann et al.(1988) examined the collection efficiency of impactors and found that for particles larger than 1 μm adhesive coating with greases or some other sticking material is preferable to enhance the 'sticking probability'. As very long sample periods were to be used in this study none of the recommended oils by Schumann et al. could be used as they would evaporate within a few days in a low pressure impactor.

Gravimetric Analysis

To facilitate comparability of results and minimize the uncertainties, a fixed measurement protocol has been maintained for all the gravimetric measurements. Before sampling the collector surfaces were dried in an air oven for 30 minutes and then in a desiccator for 2 to 4 days before they were weighed. After the sampling period, the filters were weighed again using the same procedure. The scale used had a resolution of 10 μg. To minimize the influence of absorption of humidity during weighing the collectors were weighed in the same order before and after sampling and a fixed time interval was maintained between each measurement. At the end of each series of measurements, a control collector that had been dried together with the samples was also weighed. If the reading for the control collector differed by more than a few hundred microgrammes all the samples were redried and reweighed. The control proved to be particularly useful when Whatman 542 was used as a collector since problems arose due to the uptake of humidity from the air in the weighing room. When teflon foils were used as collectors the scale was much more stable and easier to read. No redrying have been necessary when using teflon foils as collector surfaces.

A subjective evaluation of the suitability for gravimetric analysis of the different collection surfaces tested during this study is given in Table 2.1.

Gamma Spectrometry

When the collector surfaces were analyzed for Be-7 a 21 % or 35 % Ge(Li) gamma detector was used. Counting time ranged from 1 to 2 days for the centre stage and up to a week for the low activity stages. The standard deviation of these measurements varied from 6 - 8 % for the centre stage to 100 % for the less activity stages. In some of the experiments, filters 1 to 3 and 8, 9 and 10 were counted together to improve the counting statistics.

When neutron activation analysis was used to detect the tracer particles described in the next Chapter 4 the count time was five to ten minutes and the standard deviation was usually better than ±1 %. When neutron analysis was to be used for analysis Whatman 542 should be preferred as collection surface as can be seen from the review in Table 2.1.

Analysis of Results

Generally, particle size distributions will often fit a log-normal distribution rather than a normal distribution. That is, when the frequency function of the particle size data is plotted against the log of the particle diameter instead of the diameter it will resemble a normal distribution. By analogy with a normal distribution the geometric mean and the geometric standard deviation become:

$$\log d_g = \frac{\sum n_i \log d_i}{\sum n_i} \tag{31}$$

known as the geometric mean diameter, GMD, and:

$$\log \sigma_g = \sqrt{\frac{\sum n_i (\log d_g - \log d_i)^2}{\sum (n_i) - 1}} \tag{32}$$

where σ_g is known as the geometric standard deviation, GSD. m_i is the amount collected (i.e. mass or activity) at the stage with a logarithmic mean sample diameter of d_i. It is important to note that neither of these two numbers gives any information by themselves on whether or not a log-normal function is a good description of the measured data.

Another method is to plot the frequency function of the measured data on log-normal paper. A log-normal plot of the 1991 impactor data shown in Figure 3.2, can be seen in Figure 3.3. If a log-normal distribution is a good description of the measured data then the plot should follow a straight line. The median diameter can be found as the 50 % cut size and the GSD can be calculated from the following ratios, Reist(1984):

$$\sigma_g = \frac{84.13\%diameter}{50\%diameter} = \frac{50\%diameter}{15.87\%diameter} \tag{33}$$

where the diameters is found by reading the log-normal plot at the stated percentage lines. This is a convenient method of determining the median diameter and the GSD and it has the advantage that the linearity of the plot will show whether a log-normal distribution is a good representation of the data. The major disadvantage is that drawing a straight line is not an objective procedure.

As a third method for analysing impactor data, a computer program, NMSIMPLX, fitting the data with a log-normal distribution using a Nelder & Mead simplex method has been produced by Earl O. Knutson(1994) at EML in New York. This program provides a more objective method of determining the GMD and the GSD for the data and it calculates error terms for these values based on error estimates for the individual data points. Reineking et al.(1984) have described the method. A sum, X^2, of the square of the difference between the measured value, $A_{measured}$ and a fitted number, A_{fitted}, devided by the standard deviation of the measured values, $SD(A_{measured})$, is minimized by the program:

$$X^2 = \sum_{i=1}^{n} \left(\frac{A_{measured} - A_{fitted}}{SD(A_{measured})} \right)^2 \tag{34}$$

where n is the number of measurement points. If a log-normal distribution is a good description of the measured data then the average difference between the measured value and the fitted value should be equal to the standard deviation of the data points and thus the average X^2 value for one data point should be unity and the X^2 sum should be of the same magnitude as the number of measurement points. For a series of measurements, the average X^2 value should be close to the average number of data points. Stages 10 through 3 of the Berner impactor measurements were fitted a log-normal distribution using the NMSIMPLX program and the X^2 sum should be around 8 (the number of data points/stages) if a log-normal distribution is a good representation of the data.

The NMSIMPLX program has four advantages. It calculates a median diameter and a GSD with an error estimate based on the standard deviation of each measured point. The X^2 value gives a figure for the appropriateness of the fit. It also takes into account the collection efficiency curve of each impactor stage. Fourthly, it is an objective way to analyze the data.

3.2 Sizing of Be-7 Labelled Particles with a Berner Impactor

Beryllium-7 is created mainly in the stratosphere when the atoms, C-12, N-14 and O-16, are spallated by cosmic rays into two smaller atoms, one of which is Be-7. Be-7 is radioactive and decays with a half-life of 51.6 days: this makes it the only radioactive isotope formed by this process with a half-life long enough to reach ground level air Be-7 content in the atmosphere has been monitored for more than 20 years in Denmark as part of a bigger programme for monitoring radionuclides in the atmosphere The average levels range from 1000 to 4000 μBqm^{-3}, Aarkrog et al.(1993). Be-7 has been used as a natural tracer in various experiments: Roed(1985), Roed & Cannell(1987) and Christensen and Mustonen(1987) used Be-7 to monitor the ingress of airborne particles into buildings. It is especially suited for such studies since it is of almost purely outdoor origin. Kritz and Rosner(1991) used Be-7 as a tracer in studies of air mass origins and Dibb and Jaffrezo(1995) used it as a tracer in a study of snowfall in Greenland It has also been used to check the filter efficiency and flow rate of high volume air samplers at Risø National Laboratory.

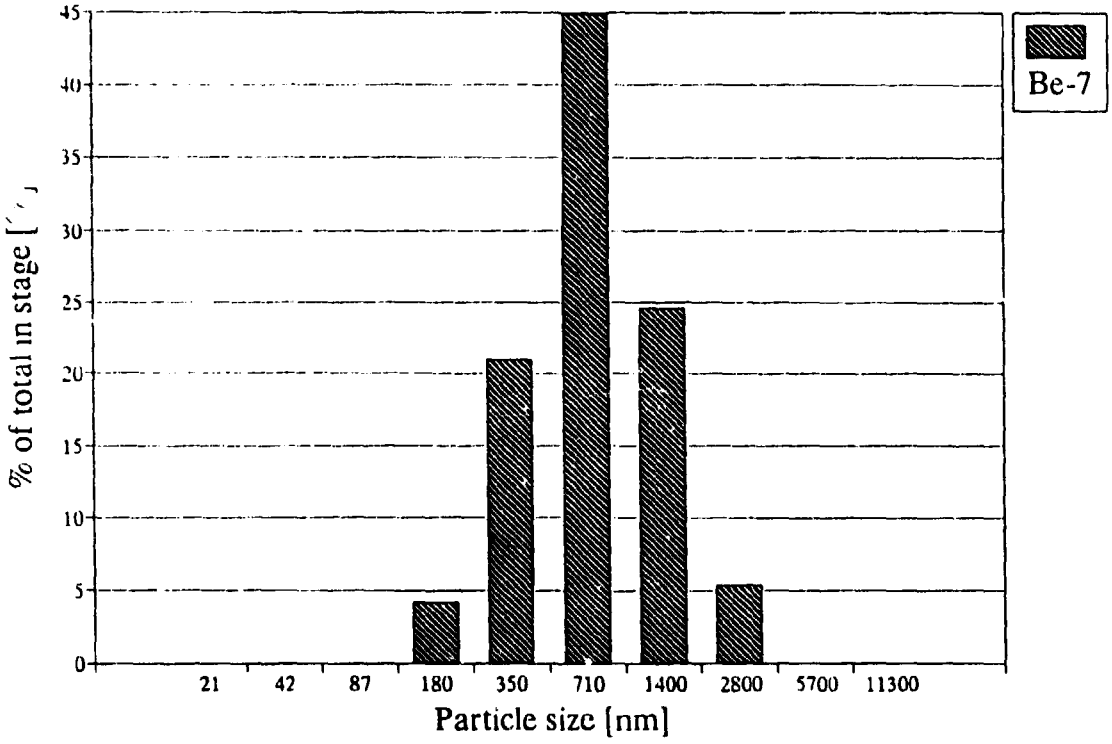

Figure 3.2. Size distribution of Be-7 measured 3 meters above ground in 1991. The data is presented by plotting the pertage of the total collected present in each stage. This distribution had a GMD of 0.79 μm and GSD of 1.7 as can be seen in Table 3.2.

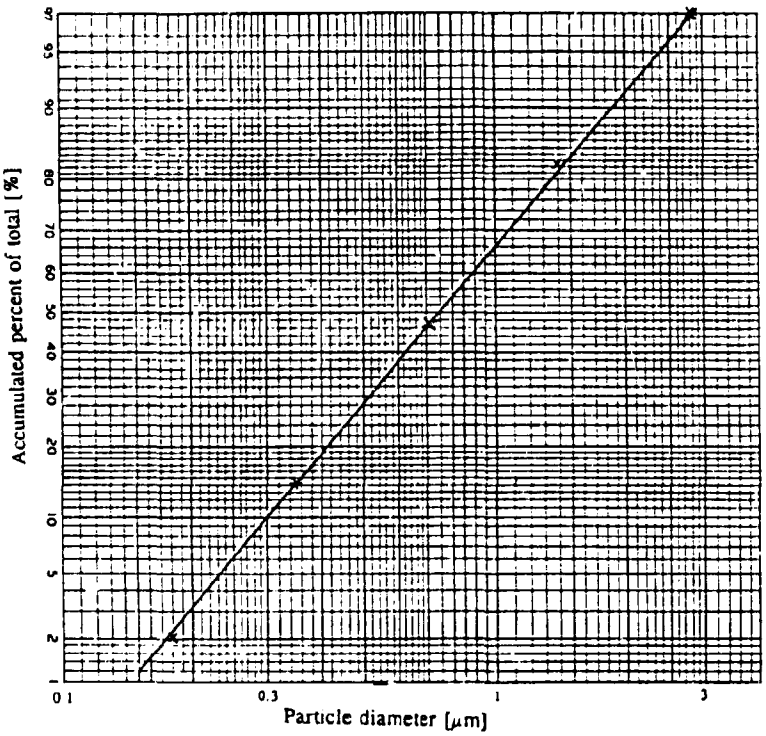

Figure 3.3. Log-normal plot of the 1991 measurement. As can be seen on the Figure the Be-7 activity distribution followed a straight line when plotted on log-normal paper and a log-normal distribution was thus a good description of the data.

In order to obtain knowledge about the size distribution of the particles for which the indoor/outdoor concentration ratios have been determined previously and during this study, a Berner impactor has been used to measure the size distribution of Be-7 and the mass distribution of ambient atmospheric aerosol The results for Be-7 give information on the size of the particles used in the experiments and the mass distribution measurements give information on the connections between Be-7 labelled particles and the ambient aerosol.

Method

Particles were collected with a 10-stage Berner Impactor from Hauke in six periods of about 40 days each. In the first collection, Whatman Glass Fibre A filter paper was used as a collecting surface but to facilitate gravimetric analysis Whatman 542 filter papers were used during the next three impactor runs. The poor performance of the Whatman filter papers collector lead to the investigation of a series of collectors, see Figures 3.1 a & b and Table 3.1. Based on the results of this investigation teflon foil was chosen for all later measurements. Gravimetric and gamma ray analysis were carried out. The results were analyzed by plotting on log normal paper and by using the NMSIMPLX program and the obtained GMD and GSD are displayed in Table 3.2.

Table 3.2. Summary of impactor measurements, mass and Be-7. -LN = not log-normal. In the test in '91, mass was not measured. [1] 10[-1]x Counts per second instead of Bq. Plot means that the value was found by reading a plot on log-normal paper. The last four columns present results calculated with the NMSIMPLX computer program.

Name	Type	GMD Plot [nm]	GSD Plot [ ]	Total amount [Bq] or [μgm^{-3}]	GMD *NMSIMPLX* [nm]	GSD *NMSIMPLX* [ ]	Amount *NMSIMPLX* [Bq] or [μgm^{-3}]	X^2 [ ]
91	Be-7	740	2.01	166.43[1]	786±37	1.72±0.07	168.24±6.4	1.35
A	Be-7	540	2.52	2.52	518±33	2.04±0.11	2.33±0.24	5.31
A	Mass	800	3.72	51.87	1045± 2	2.62±0.02	44.63±0.23	3413
B	Be-7	1180	2.32	3.97	1143±42	2.03±0.07	3.88±0.29	4.25
B	Mass	1040	3.47	27.86	1035± 5	2.17±0.01	23.94±0.22	821
C	Be-7	740	2.60	6.77	981±17	2.17±0.04	5.97±0.18	70.6
C	Mass	-LN	-LN	14.32	1052± 6	3.47±0.04	10.89±0.26	432
D	Be-7	780	2.66	6.12	932±24	2.29±0.05	6.03±0.25	9.73
D	Mass	-LN	-LN	29.00	4635±22	2.31±0.01	22.47±0.22	2180
E	Be-7	970	2.51	22.65	1039±23	2.22±0.05	23.16±1.06	6.23
E	Mass	1310	3.76	22.60	1011±5	2.31±0.02	18.91±0.22	954

The 1991 measurement was made at Risø with the inlet of the impactor approximately 3 meters above the ground and the size distribution is shown in Figure 3.2. The 'A' experiment was conducted inside a house in Vellerup and the result is shown in Figure 3.5. All other experiments were made at the RIMI test site near Risø and the size distributions have been shown in figures 3.4 b-e, 3.6 a-b and 3.7 a-b. The RIMI station features a 10-meter mast with anemometry equipment. It is situated 2 km from Risø in the middle of a field in a flat area. The nearest significant source of airborne particles is a highway (10,000 cars per day) at a distance of one kilometer. A full description of this meteorological research station is given by Hummelshøj(1992).

Serie B 3/4 - 7/5 1992

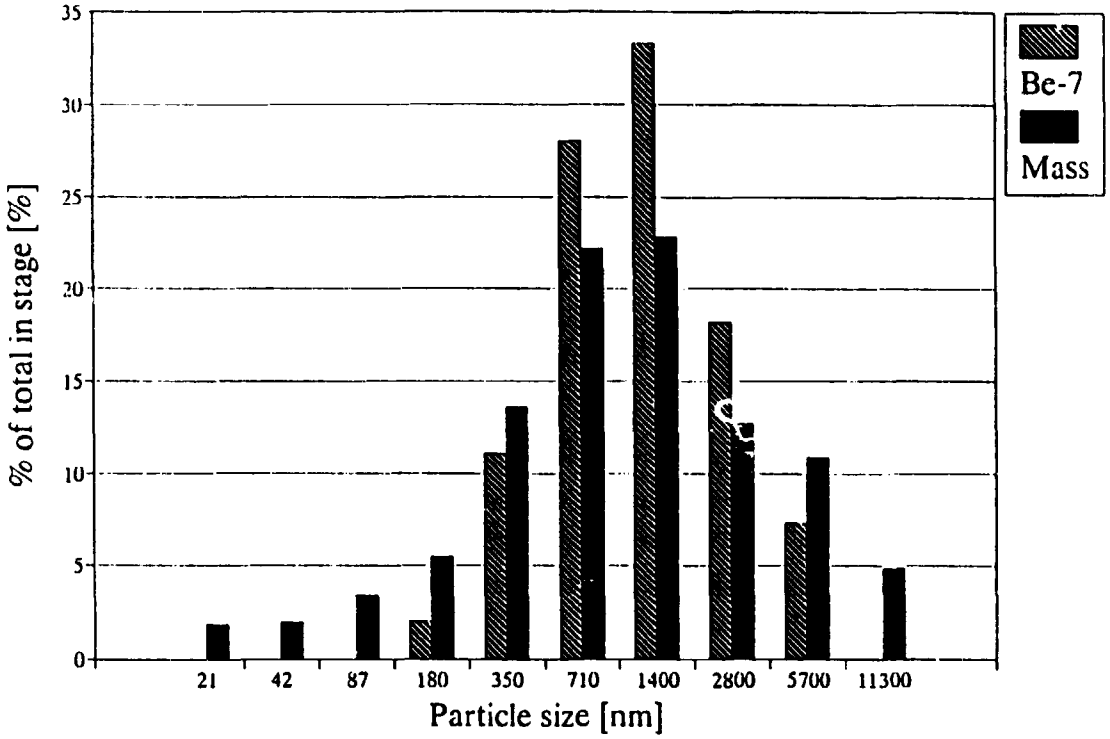

Serie C 13/5 - 22/6 1992

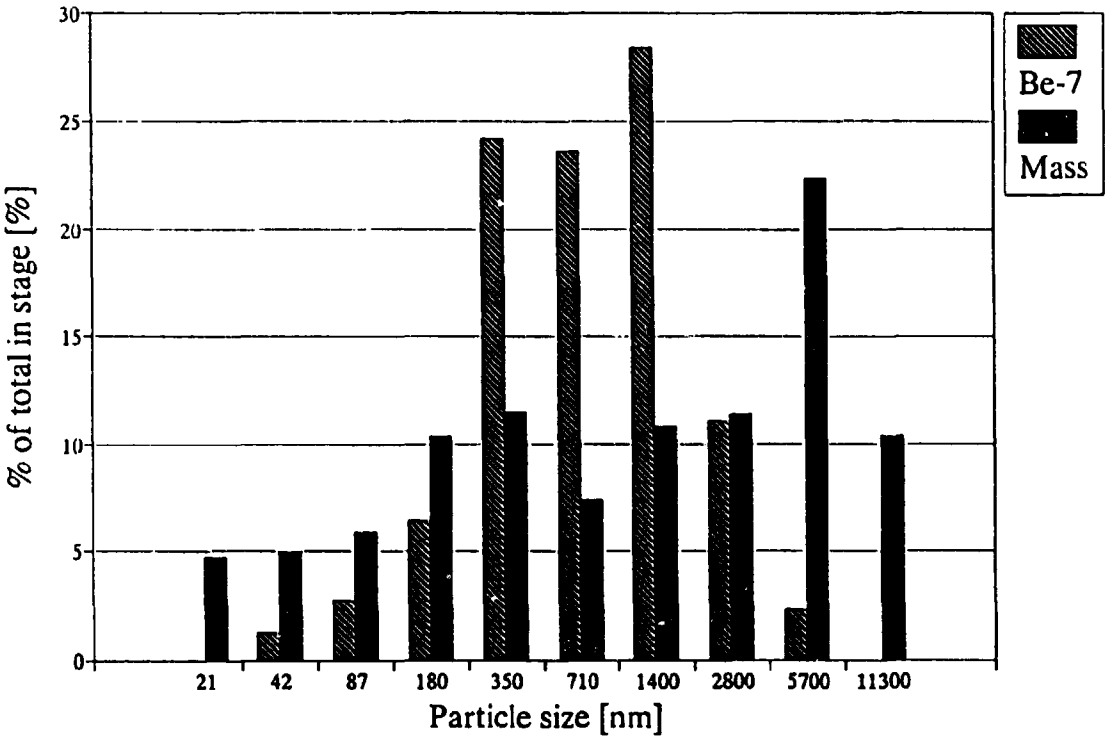

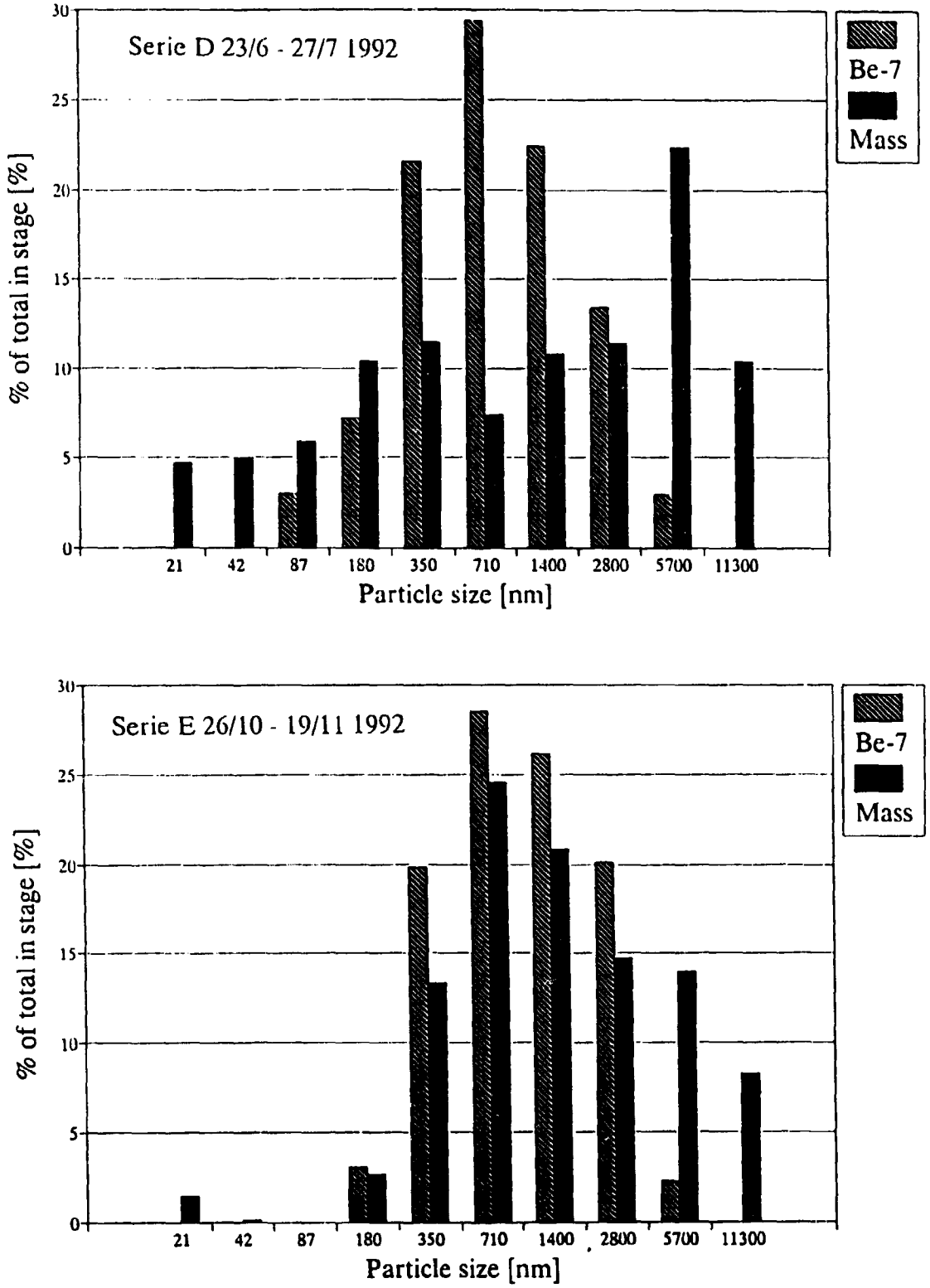

Figure 3.4 b-e. Mass distribution and activity distribution of Be-7 at the RIMI research station near Risø. The x-axis is the logarithmic mean of the cut-off diameter of the current and previous stage. On the y-axis the percentage of the total collected material deposited in each stage in pictured. With this unit the shape of the two distributions can be compared.

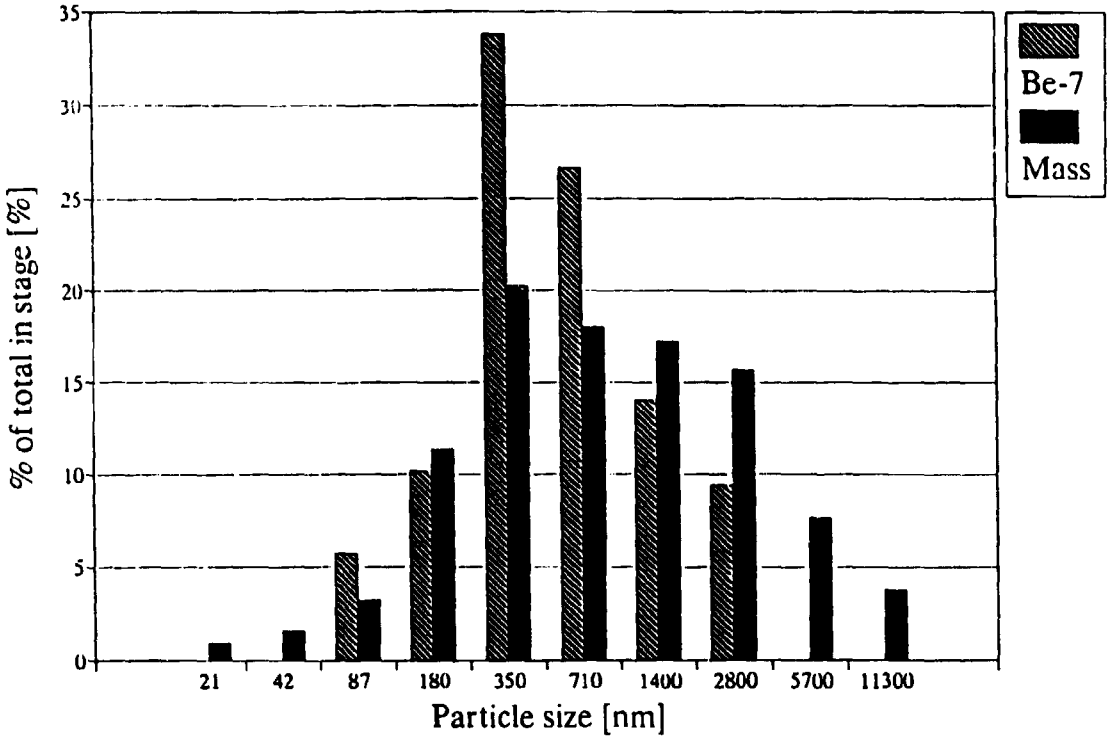

Figure 3.5. Indoor mass and Be-7 size distribution measured in a summer cottage in Vellerup in the spring of 1992. The house had a natural air-exchange during the sampling which lasted 42 days. The Be-7 activity distribution had median size of 520 nm which is clearly lower than in the outdoor measurements suggesting a higher loss-rate of bigger particles during ingression. The total mass collected was twice the average mass load found in the outdoor measurements and especially for the smaller particles an excess mass were found suggesting the presence of internal sources.

Discussion

The average amount of suspended particulate matter found in the four outdoor tests (B - E) was 24.65 μgm^{-3} (Table 3.3). The total sampling time was 5 months. This corresponds well to the levels of particulate matter in rural air found by others, such as Whitby(1978) and Hummelshøj(1992). All mass distributions, Figures 3.4 b - e, 3.6 a and 3.7 a, had a peak between 0.7 and 1.4 μm and that was associated with the accumulation mode of atmospheric particles. A second peak between 2 and 6 μm was also recorded and in two experiments, Figure 3.4 b & d, this peak exceeded the first peak. These larger particles were associated with the coarse mode of atmospheric particles. An experiment in March 1993 with two impactors, one lend borrowed from GSF in Munich, at different heights supported the belief that this mode was associated with resuspended particles close to the ground (Figure 3.6). During this experiment there was agricultural activity in the field surrounding the RiMI test station during the sampling period. A repetition in 1994 of the experiment in a period with no local activity showed no difference in the mass distributions at the two heights as can be seen in Figure 3.7 a. In general, a log-normal distribution is not a good description of the mass data as the large X^2 values in Table 3.2 show.

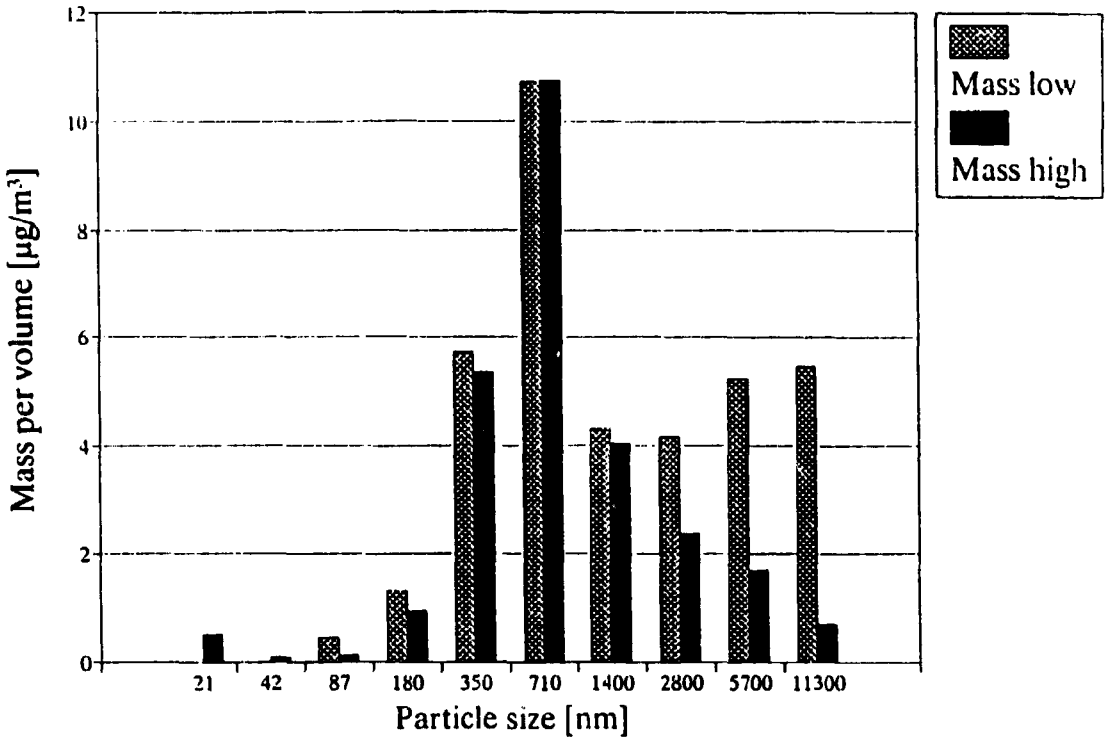

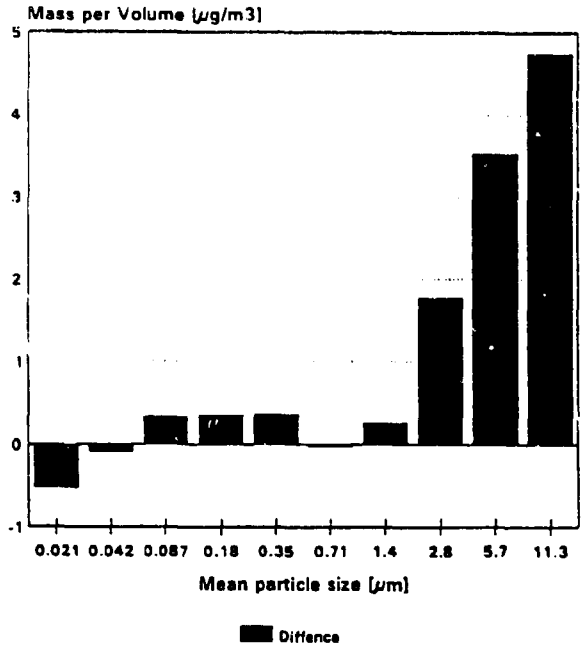

Figure 3.6 a & b. Mass distribution at 1 m and 10 m above ground measured at the RIMI meteorological station at Lille Valby near Risø. The two mass distribution have been measured with a 10-stage and a 8-stage Berner impactor. To adjust for the different flow rates of the equipment the collected have been divided by the volume of sampled air. Both here and in Figure 3.7 the mass peak at 0.71 µm is identical for the two heights. In this figure a second mode of larger particles can be seen closer to the ground. This is attributed to resuspended particles due to agricultural activities in the field surrounding the test site.

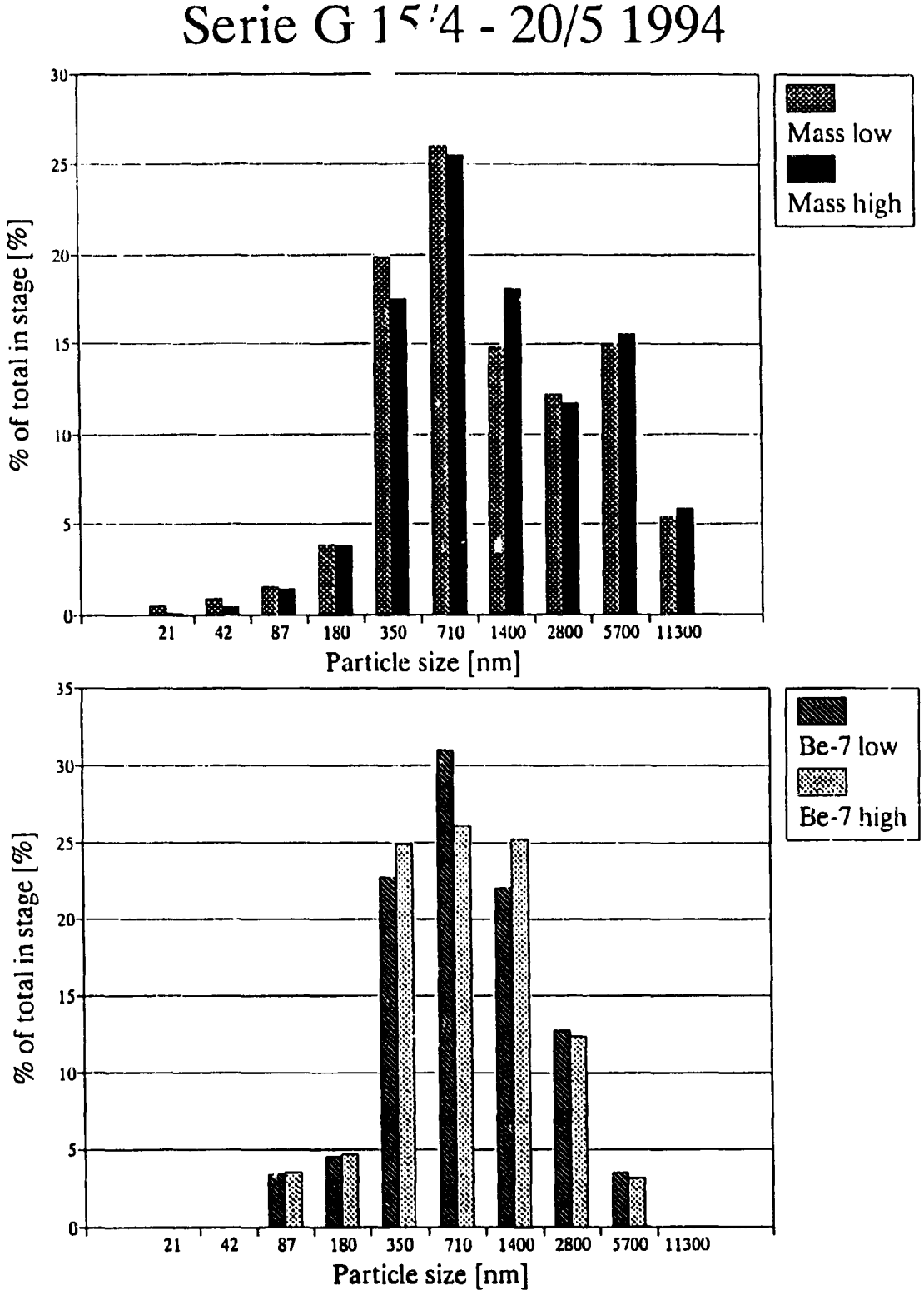

Figure 3.7 a & b. 1994 measurements in 1 and 10 meters height. Mass and Be-7. During a second experiment with impactors in two heights no significant difference was observed between the two distributions neither for Be-7 or the mass measurements.

Table 3.3. Size-fractionated average mass concentrations in rural air in Denmark. Mass concentrations in each stage of the impactor averaged for the measurements at the RIMI research station. The uncertainty on each measurement was estimated to be 200 µg or app. 0.2 µg m^{-3}.

Sta-ge	A [µg/m^3]	B [µg/m^3]	C [µg/m^3]	D [µg/m^3]	E [µg/m^3]	Av(B-E). [µg/m^3]
1	0.48	0.54	0.89	1.00	0.15	0.64
2	0.86	0.58	0.94	0.31	0.04	0.47
3	1.73	1.01	0.11	0.93	0.21	0.56
4	6.07	1.62	1.96	2.02	0.61	1.55
5	10.80	3.99	2.16	3.02	3.04	3.06
6	9.61	6.51	1.39	3.83	5.61	4.34
7	9.19	6.71	2.03	3.81	4.77	4.33
8	8.33	3.74	2.14	4.32	3.37	3.39
9	4.10	3.22	0.42	6.19	3.19	3.26
10	2.03	1.43	1.95	4.88	1.89	2.53
Tot:	53.21	29.34	16.15	30.31	22.8	24.65

In all six experiments, the Be-7 counts had a clear log-normal distribution with a GMD of 0.7 µm to 1.0 µm (figures 3.4 b-e, 3.7 and Table 3.2). The size distribution of Be-7 correlated with the first peak of the mass distribution but not with the surface distribution. This supports the findings of Reineking et al.(1985), namely, that the Be-7 distribution follows that of an 'aged' ambient aerosol and has a size distribution similar to Pb-210 labelled particles and sulphur particles. In other words, although attachment is the process that leads to the creation of particles labelled with Be-7, the subsequent coagulation and rain-out/wash-out of the aerosol forms an activity distribution that resembles the mass distribution of the accumulation mode. Measurements with high volume samplers by Reineking et al.(1990) and Bondietti and Papastefanou(1986) showed GMD values of 510 nm and 400 nm, respectively.

For the Be-7 data, the NMSIMPLX program gave good results with all but one X^2 value close to the number of measurement points. The fitted distributions had GMD's close to those found by plotting. The GSD was smaller than those found manually and that was expected because NMSIMPLX takes the collection efficiency function of each impactor stage into account. In contrast to this, all fits of the mass distribution had large X^2 values and a uni-modal log-normal distribution was not a good fit. Fitting the mass distribution with bimodal log-normal distributions gave reasonable values of X^2 with the first peak at 311 to 462 nm and the second peak at 1431 to 3840 nm.

As the measured activity levels of Be-7 in Denmark corresponded to an average concentration of 10^5 atoms per m^3 of air and the particle concentration was in the range 10^9 to 10^{10} m^{-3}, it can be seen that only very few particles were actually labelled with Be-7.

In addition to the outdoor samples an indoor impactor run was made in the spring of 1992 to investigate whether differences in the indoor and the outdoor size distributions could be seen. The Be-7 activity distribution had median size of 520 nm which is clearly lower than in the outdoor measurements suggesting a higher loss-rate of bigger particles during ingression or due to a higher deposition velocity of larger particles. The total mass collected was twice the average mass load found in the out measurements and especially for the smaller particles an excess mass were found suggesting the presence of internal sources. It was believed that the enhanced indoor mass concentration was due to the presence of the air sampling equipment, the impactor pump and the pumps used for making reference measurements of the Be-7 level.

3.3 The Vellerup Experiment

Roed & Cannell(1987) described an experiment where both the filter factor of the building envelop, f, and the deposition constant, λ_d, were measured using Be-7 as a tracer. The experiment was carried out in three phases. In the first phase, air was conducted into the house with a centrifugal blower thus maintaining an overpressure in the house and making sure that air only entered the house through the blower. Secondly air was sucked out of the house at the same rate that it had been blown in thus creating a reduced pressure in the house. In this phases all air leaving the house went through the blower due to the reduced pressure. The assumption that all air entered or left the house through the blower was verified by comparing the flow-rate of the blower with the air-exchange of the house measured with SF_6 tracer gas. In the first phase there should be no filtration or interception by building envelop as all air entered through the blower and the tracer concentration in the incoming air was determined at the outlet of theblower. In the second phase all incoming air entered through the building envelop was thus suspectable to filtrated by the building envelop. As the air exchange rate is identical in the two situations f can be calculated from a difference in the I/O ratio when the deposition constant is assumed to be identical in the two situations. In the third configuration the house was monitored with the natural air-exchange rate. Using the value for f determined by the first two measurements the deposition constant, λ_d, and the average deposition velocity, v_d, were calculated. For Be-7 f was found to be unity, i.e. no filtration, and the average deposition velocity was 7.1×10^{-5} m s^{-1}.

Following the same experimental procedures an experiment was carried out in the spring of 1992 in a summer cottage in the village of Vellerup 40 km from Risø. The cottage was a 1-storey wooden construction and covered an area of 36 m^2. The experiments took place from February to the beginning of April and the electrical heating was used. The weather was often windy during the experiments. For these reasons the air-exchange rate was high during the experiment, 0.8 - 1.5 h^{-1}. The window in a small bedroom was replaced with a plywood sheet and a centrifugal blower fitted, so that air could be sucked out and pressed into the house. Figure 3.8 shows the outline of the house and the position of the measuring equipment.

The experiment was carried out in three phases, each phase lasting two weeks. In the first phase, air was blown into the house maintaining a overpressure, then followed two weeks with natural air-exchange and in the last two weeks air was continuously pumped out of the house maintaining a reduced pressure. During the experiment the house was visited twice a week and filters changed in the air samplers, the flow rate of the blower was checked, indoor and outdoor temperatures recorded and the air-exchange rate was measured using SF_6 gas as a tracer.

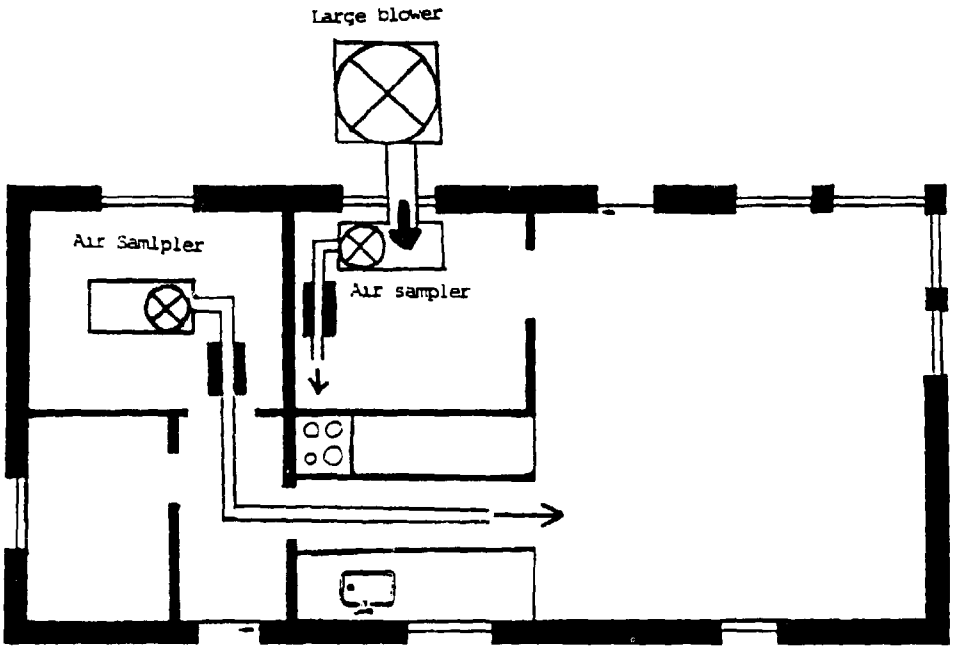

Figure 3.8 Plan of the summer cottage in Vellerup and the position of the equipment.

The air-exchange rate is an important parameter when the deposition constant is to be calculated. In the two periods with forced air-exchange, the air-exchange was controlled by the flow-rate of the blower and not influenced by the weather condition. The average air-exchange in the two periods were similar and an average value of 4.3 h^{-1} was used for the calculation of the deposition constant, λ_d. During the phase with a natural air-exchange six measurements were made of λ_r. The value of λ_r varied for these measurements with the weather conditions. An effort to extrapolate the measured air-exchange rates to cover the hole sampling period nas been made. Wind speed, wind direction and ambient indoor and outdoor temperature determine the rate of air-exchange in a given building. Since these data were not recorded at the site, data from the nearby Risø meteorological station have been used and the air-exchange was found to correlate with the wind speeds measured at the meteorological mast at Risø at 10 meters height. Compared to the variations in the wind speed data the relative changes in the indoor-outdoor temperature differences were small during the experiment (the temperature difference ranged from 14 to 17 C) and no correlation was found for these data. Also the wind direction were omitted as the number of air-exchange measurements was too small to permit this. The wind speed ranged from 4 to 10 ms^{-1} for the 6 air-exchange measurements made with the natural air-exchange situation. A good correlation, r = 0.95, was found despite the distance between the Risø meteorological mast and the test house. The air exchange was approximated by the following linear regression:

$$\lambda_r = 0.50h^{-1} + 0.08h^{-1}U_{wind\ speed}[m/s] \qquad (35)$$

This expression was then used to estimate the average air-exchange rate using the

average of wind speed measurements from the Risø meteorological mast during the natural air-exchange period. From the I/O ratios, an average deposition velocity, v_d was calculated from the deposition constant, λ_d, by multiplying it with the volume of the house, V, and dividing with the internal surface area of the house, S. λ_d was isolated from equation (2) and the term for the cleaning effect, λ_r, was included to allow for the filtering effect of the air sampling equipment in the test house. The equation used for the calculation of v_d was:

$$v_d = \frac{\lambda_d V}{S}, \lambda_d = \frac{\lambda_i - C_i/C_o(\lambda_r + \lambda_i)}{C_i/C_o} \tag{36}$$

The house in Vellerup had an internal volume of V = 84 m^3 and an internal surface area of S = 183 m^2. The results are shown in Table 3.4.The I/O ratio for the Be-7 concentration was 0.8 both when air was ducted air into the house and sucked out of the house. This is in agreement with the result found by Roed and Cannell(1986), i.e. the filter factor of the building envelop was close to one. The v_d was four times greater in the forced air-exchange phases than in the natural air-exchange phase. Apparently the increased air movement created by the blower significantly increased the deposition of the Be-7 labelled particles. This observation emphasized the difficulties in the interpretation of such I/O measurements.

Table 3.4 Levels of Be-7 in indoor and outdoor air. The air exchange rate for the natural air exchange configuration has been calculated using equation (35) and an average wind speed of 5.40 ms^{-1}. As the air exchange did not differ significantly between the over pressure and the reduced pressure situation an average value of 4.3 h^{-1} was used.

Configuration	λ_i [h^{-1}]	I/O ratio [ ]	Average v_d [10^{-4}ms^{-1}]
Positive pressure	4.2±0.4	0.80	1.4±0.13
Negative pressure	4.4±0.5	0.80	1.4±1.3
Natural exchange	0.93	0.77	0.35

3.4 Indoor/Outdoor Measurements using two Berner Impactors in Ferslev.

An impactor was used to sample air in a period overlapping the natural air exchange phase of the Vellerup experiment. The resulting Be-7 activity and the mass distributions are shown in Figure 3.5. The Be-7 had an AMAD of 520 nm in this experiment and this clear reduction of the concentration of larger particles compared with all the outdoor measurements suggested an experiment with two impactors measuring size specific I/O ratios.

In the summer of 1993 a second Berner impactor was obtained and it thus became possible to start an experiment with two impactors sampling simultaneously, one inside and one outside a house. The house in the village of Ferslev, that had been used in one of the experimental campaigns measuring indoor deposition described in chapter 4, was used for the measurements. The house is a Danish family house of one and a half storey in double brick construction. The natural air-exchange rate was 0.17 h^{-1} in average in August where the house was not heated and 0.37 h^{-1} in December

when the heat was on. These values are close to the average value for danish house of newer construction (0.2 h^{-1} with no mechanical ventilation and 0.4 h^{-1} with ventilation). It was decided to repeat the Vellerup experiment with the same three phases, but the natural air-exchange situation was performed both with and without heating of the house. In total, four series of measurements were made:

1. Four weeks with natural air exchange and no heating.

2. Four weeks with air pumped into the house and maintaining an over pressure.

3. Four weeks with air sucked out of the house maintaining a reduced pressure.

4. Three weeks with natural air exchange and indoor heating.

The impactor experiment in Vellerup had shown an excess mass especially in the stages 0.18, 0.35 and 0.71 μm logarithmic mean particle size. This extra mass in the indoor air might originate from the pump used air sampling and the impactor pump itself. To avoid any interference of the indoor mass measurements by fumes from the sampling equipment all equipment was placed in the bathroom of the house. The bathroom door was replaced with a plywood sheet through which tubes for air sampling and blowing and sucking air was fitted. This set-up of the instrumentation has been shown in Figure 3.9.

The air exchange rate was monitored with SF_6 tracer gas once or twice a week. The average air exchange rates measured during the four phases of the experiment are shown in column 2 of Table 3.5. These values were based on 4 or 5 measurements for each situation. For the phases with a forced air-exchange an average of the two exchange rates was used for calculating the deposition velocities, as the blower was pumping at the same flow-rate (verified with a weekly flow measurement) in the two phases and no significant difference can be seen between the SF_6 measurements.

In addition to the impactor measurements the absolute indoor and outdoor Be-7 levels were determined with air samplers operated at a flow rate of 100 min^{-1} using Whatman GFA filter papers. One sampler was placed outdoor next to the impactor inlet and two were placed indoors; one upstairs and one downstairs as shown on Figure 3.9.

The impactor samples were analyzed both gravimetrically and by gamma ray spectrometry. The I/O ratios of Be-7 and the airborne mass were thus measured for each size class. Teflon foils were used as collector surfaces in all tests. From the I/O ratio, the average deposition velocity to all internal surfaces was calculated from Equation (35). Due to the poor counting statistics for the outer stages deposition velocities are only calculated for stage 5, 6, 7 and 8. These measurements had a standard deviation ranging from 5 to 40 %. Especially stage 8 was associated with a high counting uncertainty. The larger number of samples, two impactors used, reduced the detector time available per sample. The internal volume, V, of the house was 278 m^3 and the area of the internal surfaces, S, was 485 m^2 excluding the furniture, but including floors, walls and ceilings.

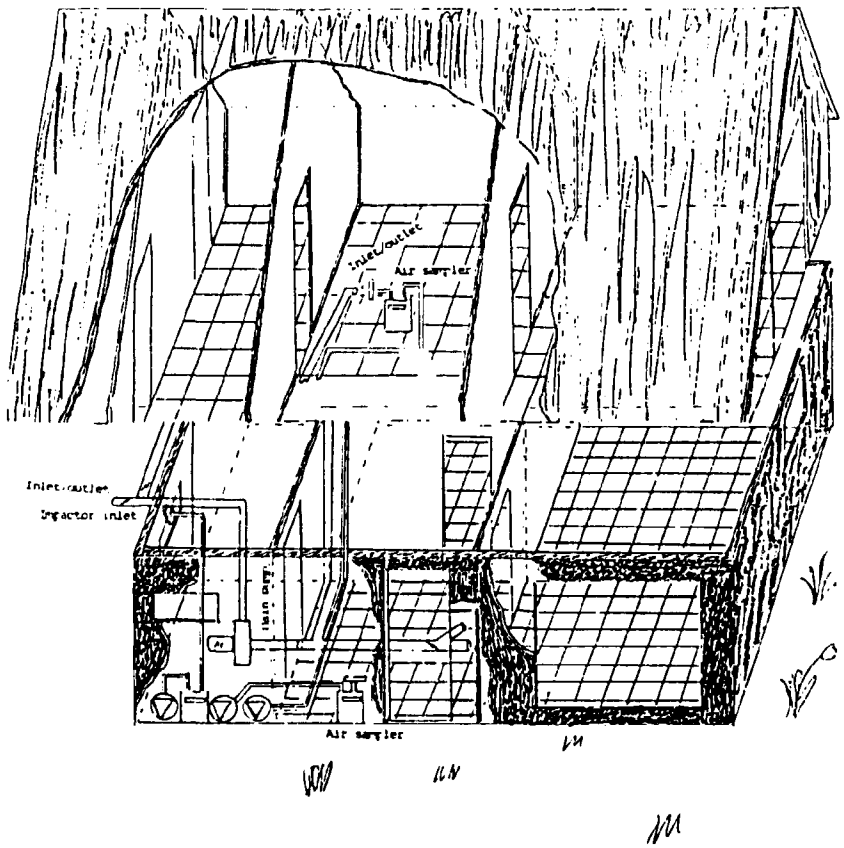

Figure 3.9 Plan of the experimental set-up in the Fersley test house. All pumps was placed in the bathroom to avoid disturbing the particle distribution in the test house with exhaust from the electro-motors. The drawing shows the inlet/outlet of the blower and the inlets of the air samplers and the impactors which was connected by tubes and pipes to the pumps in the bathroom. The outlet/inlet in the house of the big blower was divided into three tube: two downstairs for the kitchen and the living room and one for upstairs. This was done to ensure adequate mixing of the air blown into or out of the house.

Discussion of Results

The experiment progressed according to the plan until the last configuration with natural air-exchange and heating where the impactor pump suffered mechanical failure. As the test house was no longer available the experiment were terminated here. For the first three configurations a complete record of the monitored parameters were obtained. The important parameters and the overall results have been summarized in Table 3.5.

For the natural air-exchange rate situations the standard deviation on the average air-exchange rates ranged from 19 % to 29 %. Compared to the situation in the Vellerup test house where variations up to a factor three were observed this reasonably stable results and this relative insensitivity to the weather situation was attributed to the tight construction of the building. For the forced air exchange situations the

situation even improved and a standard deviation of 10 % was found on the average air-exchange rate. Overall the air-exchange was considered to be stable and the average values obtained were used to determine the deposition velocities of different particle sizes.

The I/O ratios of Be-7 obtained with GFA filters are shown in Table 3.5. For the indoor concentration an average of the upstairs and downstairs filter have been used. The pattern of these I/O ratios follows those measured with the impactor with the highest I/O ratio for the over pressure situation. But there are significant absolute differences between the impactor I/O ratio the I/O ratio obtained with GFA filters. These differences indicate that the internal mixing in the test was not complete and that there was consistent differences in the Be-7 concentration in different parts of the house. During the over pressure situation some additional filtering took place in the blower pumping air into the house and this must have reduced the indoor Be-7 concentration and thus the I/O, but the I/O ratio is higher in the over pressure situation. The filtering effect of the pump was measured by sampling air from the outlet and found to be 5 %.

The results were analyzed with the NMSIMPLX program. It was the hope that the fitting with a log-normal distribution would improve the predictions of the various data point and thus decrease the uncertainty. All the fits had low X^2 values as can be seen in Table 3.9. Some differences between the fitted I/O ratios and the measured I/O values were seen especially for the outer stages of the impactor and it was decided to use only the raw data in the analysis of the results.

Interpretation of the Mass Distributions

The out door mass distributions measured outside the Ferslev test house (see Figures 3.10 a, 3.11 a and 3.12 a) were similar to those at the RIMI test station (see Figure 3.4 a - e) with an accumulation mode peak around 0.7 μm and a coarse mode peak around 5.7 μm. The indoor mass distribution during the natural air-exchange situation (Figure 3.10 a) was similar to that found in the Vellerup test house (Figure 3.5). The coarse mode peak has nearly disappeared, but a large population of particles in the size range 0.18 to 0.35 exists in the indoor air causing the total indoor mass load to exceed the outdoor level. As the influence the electro-motors for the air samplers have been removed in this experiment by sealing them of in the bath-room other significant indoors sources of sub-micron particles must have existed in this house and probably also the Vellerup test house. No theories on the type of these indoor particle sources can be made here, but it the hope that future analysis of the impactor collector surfaces (chemical and PIXE) will yield further information on the origin of this excess mass.

Discussion of the Be-7 Measurements

The I/O level measured with GFA filters was 0.45 for the natural air exchange situation without heating. This corresponds to an average v_d of 0.33×10^{-4} ms^{-1}. This is close to the v_d of 0.35 ms^{-1} found in the Vellerup test house, but when the heating was turned on the air-exchange rate increased and the derived deposition velocity changed to 0.61×10^{-4}ms^{-1}. Again an example that significant changes can be seen in the deposition when the air flow is change, in this case due to the convective flows created by the central heating.

For situation number one with a natural air-exchange low indoor deposition velocities were found from the size specific I/O ratios obtained with the impactor as shown in Table 3.6. Similar to the Vellerup experiment the deposition velocities were

found to be much smaller when there was not any forced air exchange. The natural air exchange was 5 time smaller in Vellerup and the average deposition velocity was half that in Vellerup.

In the forced air exchange situations a clear decrease in the I/O ratio could be seen for increasing particle size as can be seen in Table 3.7 and 3.8. This corresponds to a increase in the deposition velocity with particle size. The I/O ratio was higher in the pressure situation than in the vacuum situation as would be the case if the air was filtrated during ingression into the building. But if ingression was the mechanism responsible for the larger reduction in indoor Be-7 concentration during the reduced pressure situation then it would be expected that the largest reduction occurred for the larger particles and this not the case as can be seen when comparing the Figures 3.11 b and 3.12 b and the geometric mean diameters in Table 3.9. The difference could also be coursed by the fact the inlet of the impactor was placed at points that was not representative of the average I/O. As can be seen in Figure 3.9 the impactor inlet was placed in the centre of the house were also exhaust of the air in the pressure situation and the outlet in the vacuum situation was situated. When ducting air out of the house it must be expected that particle concentration is lowest for the with longest residence time, that is the air in the centre of house. During the pressure situation the particle concentrations must be higher in the centre of the house as 'fresh' air is blown into the house here.

It is thus an oper question whether filtration or a difference in the equilibrium ratio at the measuring point is responsible for the different pattern in the vacuum and pressure situation. As earlier results, the Vellerup experiment and Roed and Cannell(1987), implied that there was no filtration no filtration factors have been calculated here and instead average deposition velocities have presented in Table 3.10 for the two situations. These values can then be compared with the deposition velocities found by direct measurements presented in the next chapter.

Table 3.5. Summary of important parameters for the I/O impactor experiment in Ferslev. Column three termed filter refers to measurements using GFA filters for determining the absolute indoor and out concentrations. The standard deviation of the gamma counting was 1 - 3 % for these measurements, but the week to week differences were greater than this (5 - 10 %). The 'impactor' column shows the I/O ratio for the total activity collected by the impactors. The stated uncertainties are those given by the NMSIMPLX programme.

Experiment	λ_r [h^{-1}]	Filter C_i/C_o [ ]	Impactor C_i/C_o [ ]
Natural air ex.	0.17+/-0.05	0.45+/-0.10	0.60+/-0.06
Pressured house	0.76+/-0.08	0.83+/-0.04	0.70+/-0.07
Vacuum on house	0.72+/-0.07	0.56+/-0.11	0.41+/-0.02
Nat. air-ex. Heat on	0.37±0.07	0.49±0.01	-

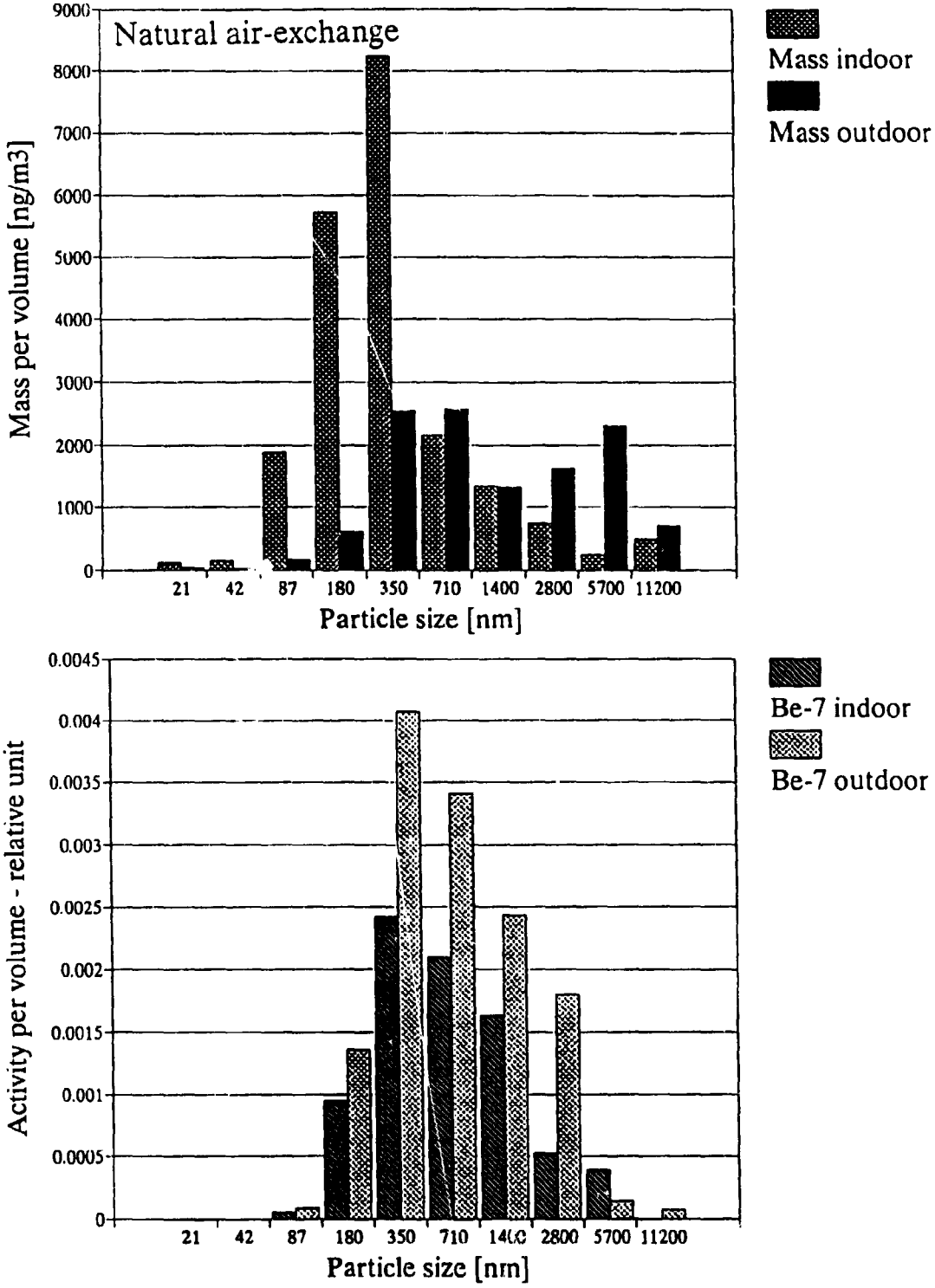

Figure 3.10 a & b. Mass and Be-7 distributions inside and outside the Ferslev house during the four weeks with a natural air-exchange. The outdoor mass distribution can be seen to follow the pattern of the measurements made at the RIMI meteorological station (Figure 3.4 b-e) with a accumulation mode peak around 0.7 μm and a coarse mode peak around 5.7 μm. The indoor mass distribution resembles that of the indoor impactor measurement made in Vellerup (Figure 3.5). Also the Be-7 distributions follows the pattern observed in the earlier measurements, but the clear shift towards a smaller indoor AMAD observed in Vellerup is not observed here.

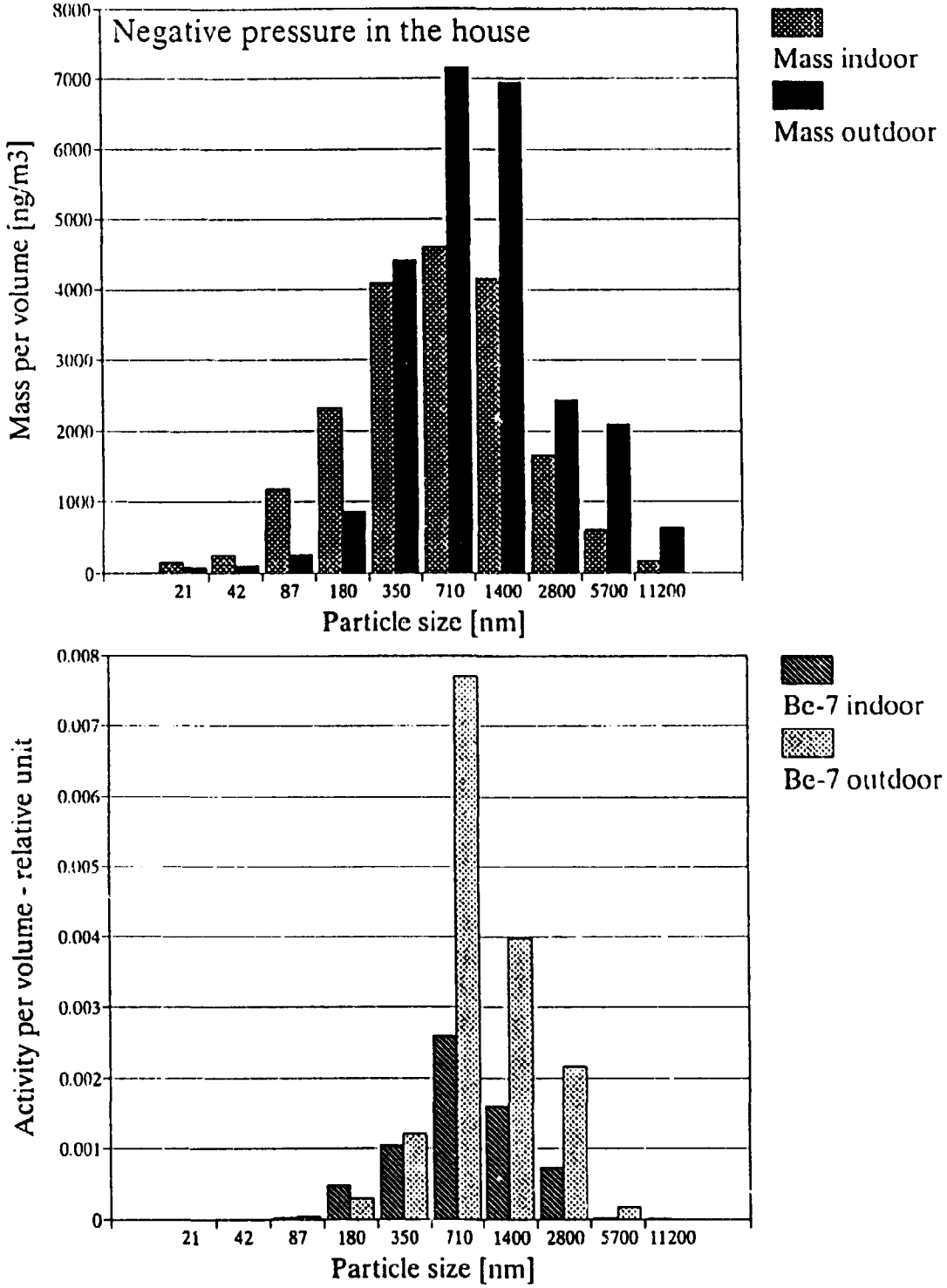

Figure 3.11 a & b. Mass and Be-7 size distributions inside and outside with reduced pressure in the test house. The increased air-exchange have reduced the excess mass observed for the fine particles, but the 0.087 and 0.18 μm stages the indoor concentration still exceeds the outdoor levels again suggesting the presence of significant internal sources of fine particles.. The Be-7 distribution shows a large and relative similar reduction for the 0.71, 1.4 and 2.8 μm stages and also for this configuration there was no overall difference in the AMAD of the indoor and the outdoor Be-7 distribution.

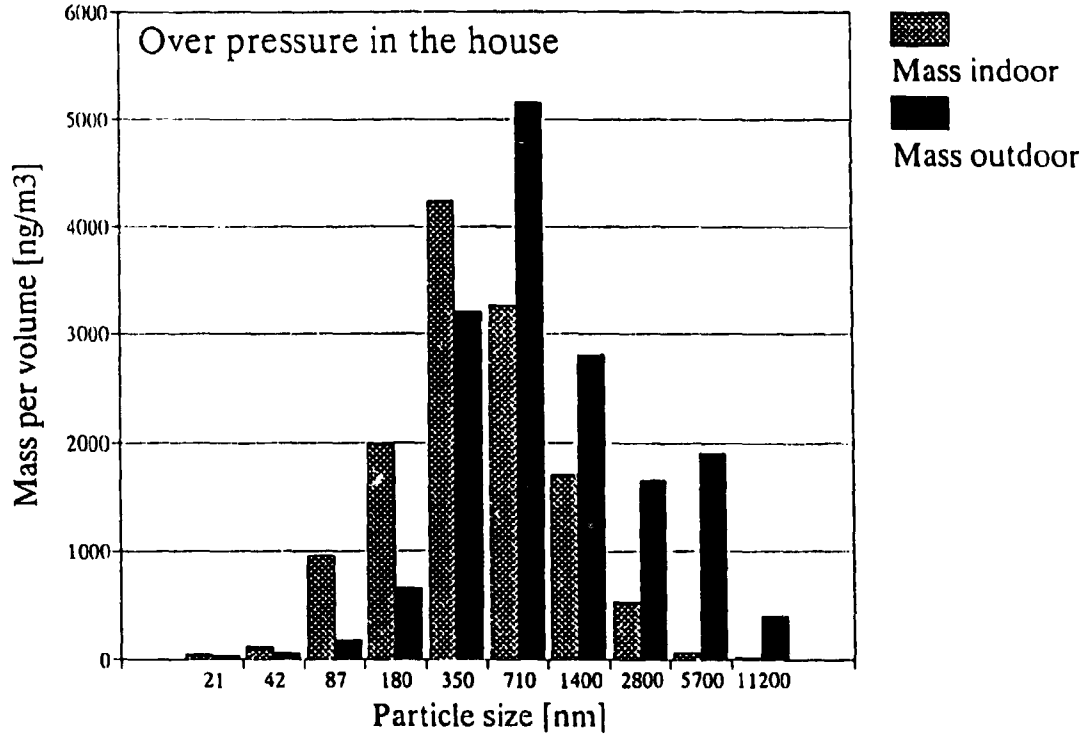

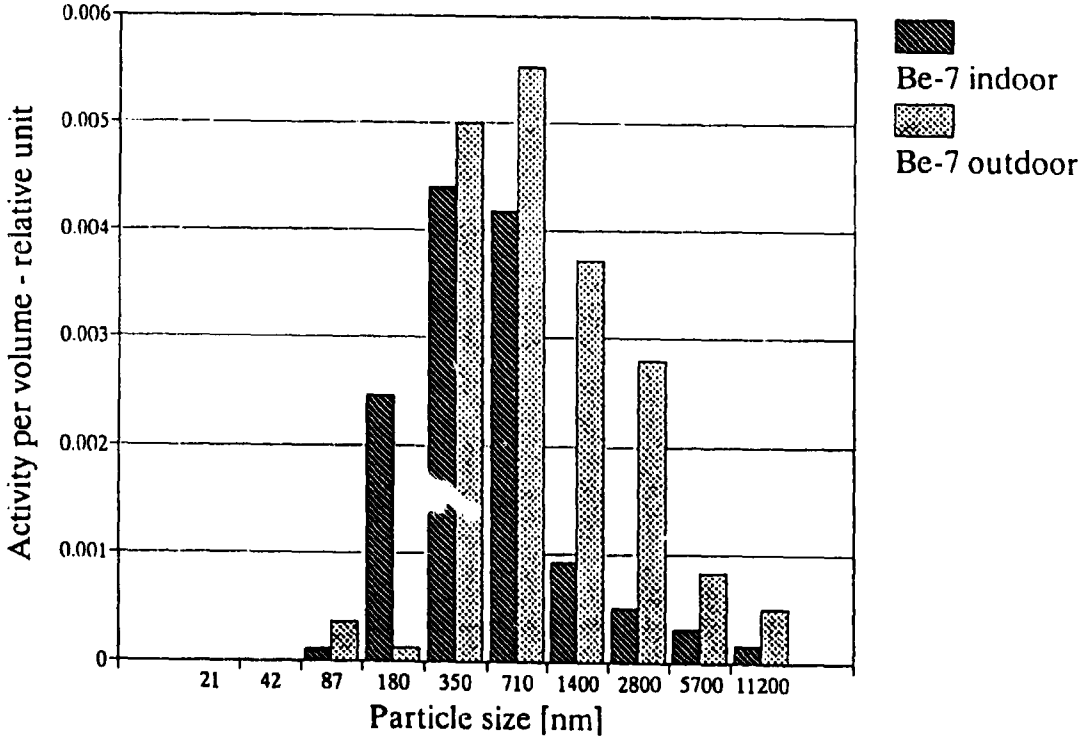

Figure 3.12 a & b. Mass and Be-7 distributions inside and outside during the over pressure configuration. The mass distribution follows the pattern seen in the previous measurements. Compared to the reduced pressure situation it can be seen that a reduced level in the accumulation mode of the outdoor aerosol corresponds with a reduced indoor mass concentration in the same size range. For Be-7 distributions a clear reduction of the AMAD can be seen for the indoor aerosols. This extra loss of larger particle may partly due to losses in the big blower.

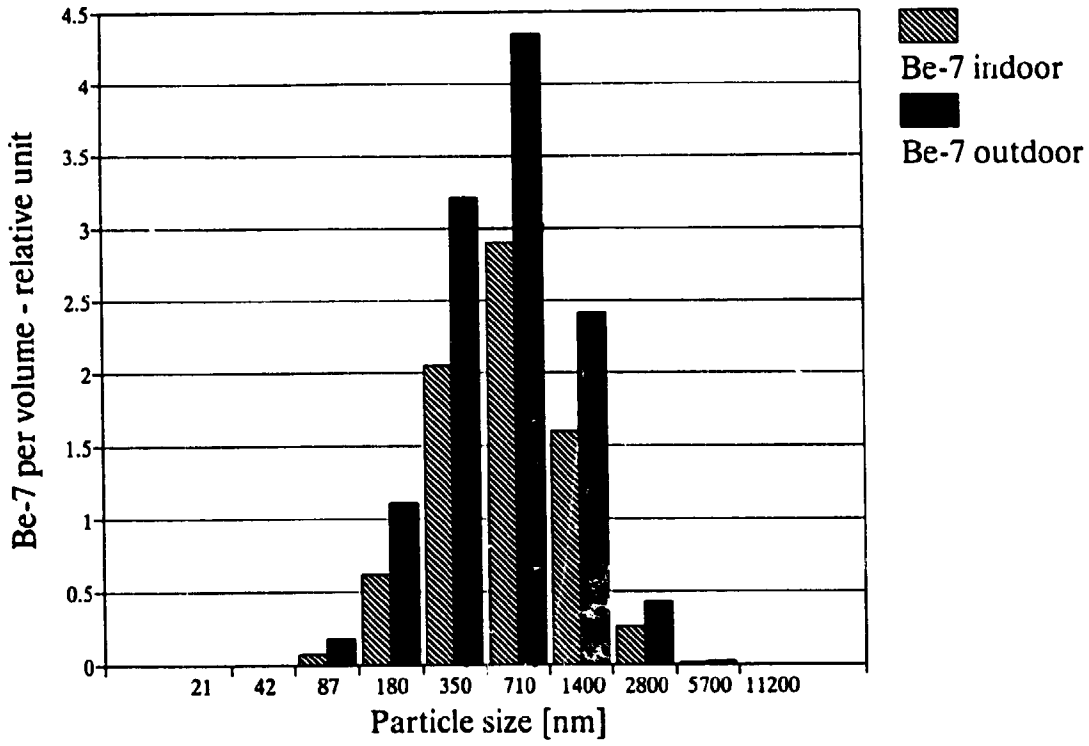

Figure 3.13. Fit with the NMSIMPLX programme for Be-7 data (Figure 3.10 b) from the natural air and no heating exchange situation. It was considered to use the fitted plot to calculate the size specific I/O ratios in order to improve the estimate of each data point, but the idea was discharged as the fitted distribution often differed significantly from the measured data in the outer impactor stages.

Table 3.6. Size specific I/O ratios for Be-7 for the natural air-exchange situation with no heating. The Air-exchange rate was 0.17+/-0.05 and the filter factor of the building envelop is assumed to be 1.0 for all particle sizes.

Mean size [μm]	Indoor Be-7 [10^{-3}cps]	Outdoor Be-7 [10^{-3}cps]	I/O [ ]	λ_d [ ]	v_d [10^{-4}ms^{-1}]
0.35	2.42	4.07	0.595	0.12	0.19
0.71	2.10	3.41	0.616	0.11	0.17
1.40	1.63	2.43	0.671	0.08	0.13
2.80	0.52	1.80	0.289	0.42	0.67

Table 3.7. Size specific I/O ratios for 3e-7 for the over pressure situation. The air-exchange used for calculating the deposition velocities was 0.74 h^{-1}

Size [μm]	C_{indoor} [Bqm^{-3}]	$C_{outdoor}$ [Bqm^{-3}]	C_i/C_o [ ]	λ_d [h^{-1}]	v_d [$10^{-4}ms^{-1}$]
0.35	4.40	5.00	0.88	0.10	0.16
0.71	4.18	5.52	0.76	0.23	0.37
1.40	0.91	3.72	0.24	2.27	3.61
2.80	0.49	2.79	0.18	3.45	5.49

Table 3.8. Size specific I/O ratios for Be-7 for the reduced pressure situation. The air-exchange is 0.74 h^{-1}. The relative uncertainty is 108, 35, 55, and 87 %, respectively.

Size [μm]	C_{indoor} [Bqm^{-3}]	$C_{outdoor}$ [Bqm^{-3}]	C_i/C_o [ ]	λ_d [h^{-1}]	v_d [$10^{-4}ms^{-1}$]
0.35	1.06	1.22	0.87	0.11	0.18
0.71	2.61	7.71	0.34	1.43	2.28
1.40	1.61	3.98	0.40	1.08	1.71
2.80	0.74	2.17	0.34	1.42	2.26

Table 3.9. Summary of the Be-7 distributions measured in Fersley analyzed on log-normal paper and with the NMSIMPLX programme. The error terms are those estimated by the NMSIMPLX code.

Name	GMD LN-paper [nm]	GSD LN-paper [ ]	Total measured [10^{3}cps]	GMD nmsimplx [nm]	GSD nmsimplx [ ]	Amount nmsimplx [10^{3}cps]	Chi [ ]
1O	662	2.81	13.37	614±56	1.89±0.11	11.7±1.3	11.3
1I	640	2.69	8.06	632±72	1.85±0.13	7.5±1.1	4.7
2O	855	2.85	18.65	965±50	2.35±0.12	18.2±1.8	10.2
2I	460	2.33	12.99	467±35	1.64±0.11	11.6±1.2	6.2
3O	975	2.29	15.82	909±59	1.62±0.13	14.7±1.5	11.4
3I	800	2.31	6.55	857±94	1.91±0.12	6.2±1.1	1.8

Table 3.10. Average deposition velocities for the pressure and vacuum situation.

Size [μm]	Average v_d [10^{-4} ms^{-1}]
0.35	0.17±0.01
0.71	1.33±0.96
1.40	2.66±0.95
2.80	3.88±1.62

4 Indoor Deposition Studies Using Rare-Earth Tagged Particles

Experiments with Be-7 had indicated that deposition is an important mechanism for removing particulate from indoor air. Very little information on indoor deposition can be found in the literature apart from some measurements made with particles labelled with radon progeny. The size of these particles were 10 to 100 nm in aerodynamic diameter, i.e. much smaller than the expected activity mean of the particles released after a (nuclear) accident. A knowledge of indoor deposition would clearly be valuable in assessment of the advantages of sheltering indoors during the passage of a toxic cloud. Information on size specific deposition velocities would enable us to predict protection factors for different sizes of particles. Senior scientist Jørn Roed and Professor A. Goddard discussed how to measure indoor deposition and an idea to use monodisperse silica particles labelled with neutron activatable tracers emerged. This technique is used to measure deposition velocities to plants at the Imperial College Reactor Centre in Sunningdale, Berkshire, United Kingdom.

This chapter describes experimental campaigns work carried out in four different houses. The first house was investigated using 2 and 4 micron silica particles. This experiment was carried out before I started working at Risø in September 1991. One of my first actions when I started at Risø was to discuss the experimental technique used and to participate in the preparation of the results for presentation (Roed et al. 1991). Later in the autumn of 1991 I went to England with the equipment used in the first house to participate in a series of experiments at the Building Research Establishment, BRE, in Watford. In the summer of 1993 a new house became available in the village of Ferslev Denmark. In the spring of 1994 another house became available in the village of Jersie in Denmark where a fourth and final series of measurements was made.

4.1 Theoretical Considerations and Experimental Technique

Jayasekeera et al.(1989) developed a technique where porous spherical monodisperse silicon-oxide particles (normally called silica) were labelled with the rare earth element dysprosium. The particles are detected by neutron activation of the Dy-164 to Dy-165 and subsequent gamma analysis. The advantages of this technique are:

- particles of a specific size can be dispersed in air and later be sampled and unequivocally identified since the abundance of dysprosium in the ambient aerosol is negligible.

- the high sensitivity of the neutron activation analysis means that only small amounts of silica particles are used, typically a few microgrammes, and the increase in loading of the ambient aerosol is negligible. The ambient burden is typically higher than 50 μgm^{-3}, Owen and Ensor(1992).

- the half-life of Dy-165 is only 139.2 minutes so no long term radiation hazard is created but the half-life is sufficient long to permit accurate measurements in the gamma-ray spectrometer.

The idea was to disperse these particles in a real house using a powder dispersion generator manufactured by Palas Gmbh and then measure the decrease in tracer concentration by taking consecutive filter samples. During the experiment, the air-exchange rate was to be measured and the deposition constant, λ_d was then to be found by subtracting the air exchange rate, λ_v, from the decay constant, λ_t:

$$\lambda_d = \lambda_t - \lambda_v \tag{37}$$

The air-exchange rate was measured by releasing SF_6 gas into the test room and monitoring the decrease in concentration by gas chromatography. The absolute decrease with time of both the tracer gas and the particle concentration is proportional to the concentration and the decay will thus follow an exponential curve if the experimental conditions are constant during the test. Both these decay constants are found by linear regression (e.g. Conradsen(1984)) of the logarithm of the tracer concentration, $C(t_i)$, at time, t_i, for n different points of time:

$$\lambda = \frac{n\sum t_i \log C(t_i) - \sum t_i \sum \log C(t_i)}{n\sum \log^2 C(t_i) - (\sum \log C(t_i))^2} \tag{38}$$

For this regression, the correlation coefficient is also calculated for each data set by the following formula:

$$r = \frac{n\sum t_i \log C(t_i) - \sum t_i \sum \log C(t_i)}{\sqrt{(n\sum \log^2 C(t_i) - (\sum \log C(t_i))^2)(n\sum t_i^2 - (\sum t_i)^2)}} \tag{39}$$

In both formulas all sums are for n points of time. Equations (38) and (39) have been used to calculate all decay constants and their regression coefficients.

Neutron Activation

All atoms have a probability to capture neutrons when colliding and thus increase the number of neutrons in the nucleus by one. Three things can happen then: the new nucleus may be stable and nothing further happens, an alpha particle can be emitted just after the capture or the new nucleus can be unstable and subject to beta decay. Usually a gamma photon will be associated with the beta decay and this can be detected without interfering with the sample. In order to use neutron activation combined with gamma spectrometry as a tracer technique several conditions must be fulfilled. A tracer that is sensitive to neutrons and emits gamma radiation with a reasonable half life after activation must be found. The particles that the tracer is incorporated into and the material used for sampling must have a low content of activatable isotopes in order to ensure a low background when analysing the gamma spectrum. The tracer itself should be present in negligible amounts in the sampling environment and for this reason rare earth elements are appropriate tracers.

The probability of capture is defined by the cross-section, σ, of the isotope and is measured in barns,(1 barn = 10^{-28} m^2). The flux, Φ, is defined as the number of neutrons in a small sphere multiplied with their average speed, while the cross section is determined by the percentage of an area that will cause an absorbtion of a neutron. With these definitions the total number of captures, A, can be calculated by multiplying the flux by the cross section, the number of relevant atoms, N, and the exposure time, T:

$$A \propto \Phi_{neutrons} \sigma_{target} N_{target} T_{exposure\ time} \qquad (40)$$

To avoid activation of isotopes that have gamma lines that will interfere with the gamma analysis of the samples some elements should avoided, e.g. sodium, chloride and metals. All elements lighter than sodium have a low cross section for neutron capture and subsequent beta decay. Even if a neutron is captured the new isotopes are either stable or have a short half live, $T_{\frac{1}{2}} < 1$ s, meaning that if the sample rests for a few minutes after activation all radiation from these elements will have disappeared. Some of the low mass elements have a large cross section for neutron capture and subsequent alpha emission. This is an instant process and it has no influence on the gamma analysis after irradiation. So in order to maximize the sensitivity of the gamma analysis the samples should consist of a tracer and elements such as C, N, O, H, F, S, Si and P. The last three elements are activated, but have no gamma rays associated with their beta decay. This means that all organic substances with a low sodium content can be analyzed with low interference from unwanted activation products by this technique; especially paper, plastics (not PVC though, because of the chlorine content), cotton, cellulose, hair, etc.

During this study two isotopes have been used at Risø and their data is shown in Table 4.1. At the Imperial College Reactor Centre europium, Giess et al.(1994), has also been used to label silica particles. By labelling different silica particle sizes with different rare-earths it would be possible to make house experiments with several particle sizes per experiment and thus increase the amount of information gained per test. Such improvements are considered in future experimental work.

From Table 4.1 it can be seen that for equal amounts of the elements irradiated with neutrons will result in an initially 50 % higher activity of the dominant gamma peak for dysprosium. Since dysprosium also has the longest half-life it will become more dominant with time after irradiation. The dysprosium labelled particles contain 5 to 16 mg of dysprosium per gram of silica particles and the indium particles contain 279 mg of tracer per gramme of particles. This means that if the two tracers are to be used together the silica particle concentration should be at least ten times higher than the indium particle concentration, considering mass, so that the Compton tail of the many high energy indium peaks does not blur the low energy Dy-165 peak.

Table 4.1. Isotopes used as tracers. Data is from Table of Isotopes(1967). Activity in the fifth column is calculated for 100 ng of the element irradiated for 10 minutes in a thermal neutron flux of 37 x 10^{15} $Nm^{-2}s^{-1}$. These are the conditions used at analysis by Risø. The intensity of the peak is noted under the energy. This percentage has been included in the activity calculation in the last column. There will also be a difference in detector efficiency for the two energies, but this has not been included as this difference depends on the detector system. The cross-section for dysprosium is the sum of the cross-section to Dy-165 and Dy-165ml. Dy-165ml has a half-live of 1.5 minutes before returning to ground state, Dy-165. As gamma counting starts 20 to 30 minutes after the neutron activation was finished the intermediate state has been assumed to have decayed.

Name	Target isotope	Natural abundance of isotope [%]	Cross-section of target isotope [$10^{-28}m^2$]	Main gamma peak [kev]	Activity of γ-line [event/s]	Half-Life [min]
Indium	In-115	96	151 barns to In-116ml	1293 80%	36000	54
Dysprosium	Dy-164	28	2800 barns to Dy-165	95 4%	52300	139.2

Supra-Micron Particles

The silica particles were labelled by shaking in a solution of dysprosium (using $DyCl_3$ or $Dy(NO_3)_3$ as compound). The porous surface of the particles gives them a large surface area for exchange of sodium in the silica particles with dysprosium. By heating the particles to 500°C, thus expanding the pores, and performing a second shaking with dysprosium chloride tracer content from 5 to 16 mg dysprosium per gram of particles can be achieved. As shown in Table 4.2 several different sizes of silica particles are available from the supplier. First column of the table states the size specified by the supplier. To verify the size of the particles, they have been sized by Miriam Byrne using a TSI Aerodynamic Particle Sizer, APS 33, at the Imperial College Reactor Centre. The APS is capable of particle size measurements in the range 0.5 to 30 μm and has a size resolution of 0.18 μm. This sizing, the second column of Table 4.2, shows that especially the 'one' and 'ten' micron particles differed from the specified size. Hereafter the particles will be referred to by their actual size as measured by the APS. A size distribution of 3 micron particles measured with the APS are shown in Figure 4.1.

To investigate whether if there is agreement between the mass distribution and the activity distribution a sizing of the particles using the Berner impactor at Risø have been tried. Unfortunately the Whatman 542 filter paper, which should be used when neutron activating the collectors surfaces after sampling, has a bad retention efficiency of the silica particles, Figure 3.1. Later impactor sizings have been made with teflon foils as collector surfaces, but the activity size distribution still appeared to be bimodal and this emphasised the need for using additional adhesive coatings when sampling supra-micron particles and an investigation of suitable substances are under way. The impactor samples showed that the 4 μm particles had 70 % of the mass in a peak with a AMAD of 5.3 μm and 30 % in a peak around 0.7 μm. The 2 μm particles had the

most mass in a peak with an AMAD of 2.6 μm. The impactor measurements thus agrees well with APS measurements when looking at the first peak, but due to the large number of particles that had bounced on to the lower stages the APS measurements have been considered the most reliable and used to characterize the particles. The impactor was used with success to size the sub micron particles as shown in Figure 4.5.

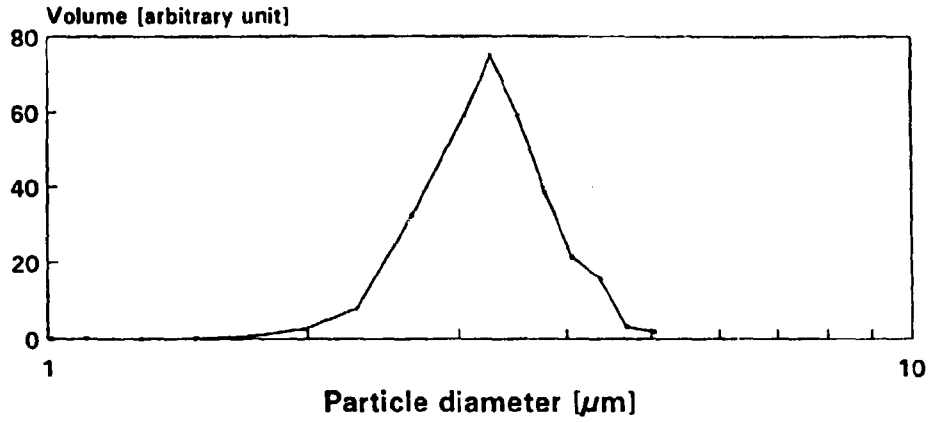

Figure 4.1. Result of APS sizing of the 'five' micron particles. An APS measures the aerodynamic diameter of the particles and this size information should thus be comparable to measurements made with impactors after the Chernobyl accident. Figure was prepared from data provided by M. Byrne.

Table 4.2. Review of silica particles used in the house experiments. The APS diameter is the median volume aerodynamic diameter. The Geometric Standard Deviation, GSD, is for a log-normal fit to the distribution.

Nominal size [μm]	APS dia. [μm]	APS GSD [ ]	Volume of one particle [μm^3]	Gram tracer per particle [10^{-15}g]	Number of particles for one 100 events s^{-1}
1	2	1.48	8.18	40.9	4670
3	3	1.20	14.14	70.7	2701
5	4	1.07	33.51	167.6	1140
10	5.5	1.18	87.11	435.6	440

Sub Micron Particles

After the APS sizing had shown that the nominal 1 micrometer particles are actually between 2 and 2.5 micrometer and the impactor experiments had shown that Be-7 had an AMAD that is closer to 0.7 μm than to 1.0 μm, the need for a tracer particle with

a diameter of one micron or less was obvious, if results were to be compared with the Be-7 measurements.

Attempts to incorporate rare-earth elements tracers in submicron polystyrene latex particles at Imperial College failed due to the lack of a suitable organic compound. Instead nebulization of a suspension of an indium-acetyl-acetonate powder in alcohol have been used successfully. The resulting particles have been sized with an impactor during an experiment in the Jersie test house. Subsequent neutron activation showed the particles to have an AMAD of 480 nm, which corresponds to a MMAD of 480±10 nm as the amount of tracer is proportional to the mass of the particle. The distribution of activity in the different stages can be seen in Figure 4.5. At Imperial College the indium particles have been sized using their Las-X particle sizer. The geometric particle size was found to be 670 nm GMD with a GSD of 1.6. The Las-X measures the geometric diameter of individual particles and the volume is calculated from a transformation of the number size distribution into a volume size distribution using an assumption of unit density spherical particles. If the measured particles are not spherical or have a unit density an error will arise in calculation of the median volume diameter and the GMD and MMAD will not be comparable. As we know, from microscopy, that the indium particles are not spherical and we have no knowledge on their density the two measurements agrees satisfactorily.

The nebulizer was used for three to five minutes before the tests and the tracer concentration obtain was from 2 to 4 $\mu g\ m^{-3}$.

The original idea of using indium powder was to evaporate it and make particles by the condensation method. Unfortunately the condensation generator at Imperial College operates at too high temperatures. The indium compound was oxidized when heated and the method was not successful. Another problem was that the particle condensation generator used was not mobile so particles would have to be recollected and redispersed in the test room or chamber.

At the Environmental Measurements Laboratory, EML, in New York a simple system for condensation generation of particles has been developed by Keng-Wu Tu(1982), Figure 4.2. The system has been used for testing the feasibility of making condensation aerosols from indium-acetyl-acetonate, $In(C_5H_7O_2)_3$. The principle for generating condensation aerosols is that a substance is heated in order to emit vapours, usually from the liquid phase. By subsequent cooling the air is supersaturated and the vapours condense. If small condensation nuclei is present in the air the condensation will primarily occur to these and monodisperse particles can be produced.

The indium compound was put in the glass ampoule and pure nitrogen was blown over the heated compound to prevent oxidation. In the set-up for producing monodisperse particles condensation nuclei consisting of NaCl (5 to 10 nm in diameter) are produced by spraying a salt water solution into the nitrogen flow. This improves the monodispersity of the produced particles as the condensation becomes more homogeneous. This was omitted during this experiment, since it was a test to see if particles containing indium could actually be produced from the compound in question. The nitrogen was blown into a test chamber and the size distribution in the chamber was measured with a differential mobility particle sizer, DMPS, from TSI at 5 to 10 minutes intervals. The chamber was not air-tight and a background of aerosols from the room air was present in the chamber. The lower curve in the two figures, Figure 4.3 a & b, shows the background in the chamber measured, before the test began. The two other curves show the distribution one and three hours after heating of the indium compound began. The number distribution, Figure 4.3 a, shows a clear peak at 25 nm in both cases. A second peak can be seen around 120 nm, especially after 3 hours.

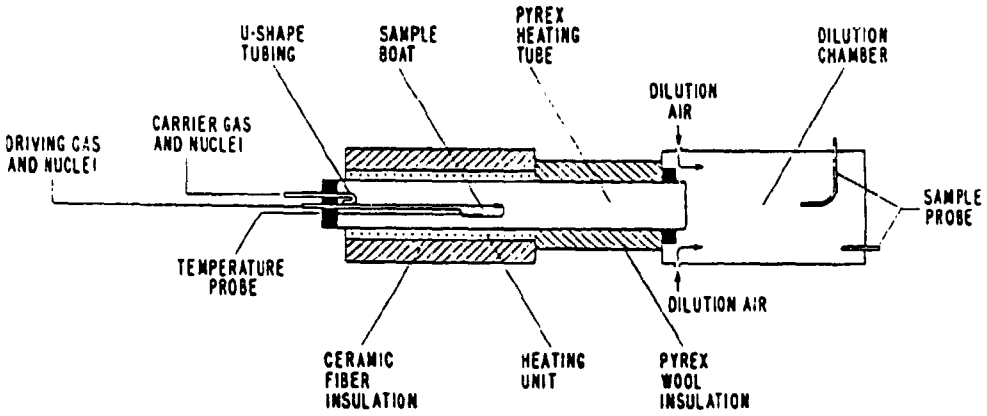

Figure 4.2. A simple aerosol generation system. The figure is from Tu(1982) This set-up has been used to test the feasibility of making condensation aerosols from the indium-acetyle-acetonate powder during the authors stay at the Environmental Measurements Laboratory in New York. The dilution chamber shown in the Figure was app. 10 m³ and the sample probes were used to suck air out for samples that were analyzed later by neutron activation in the Risø research reactor.

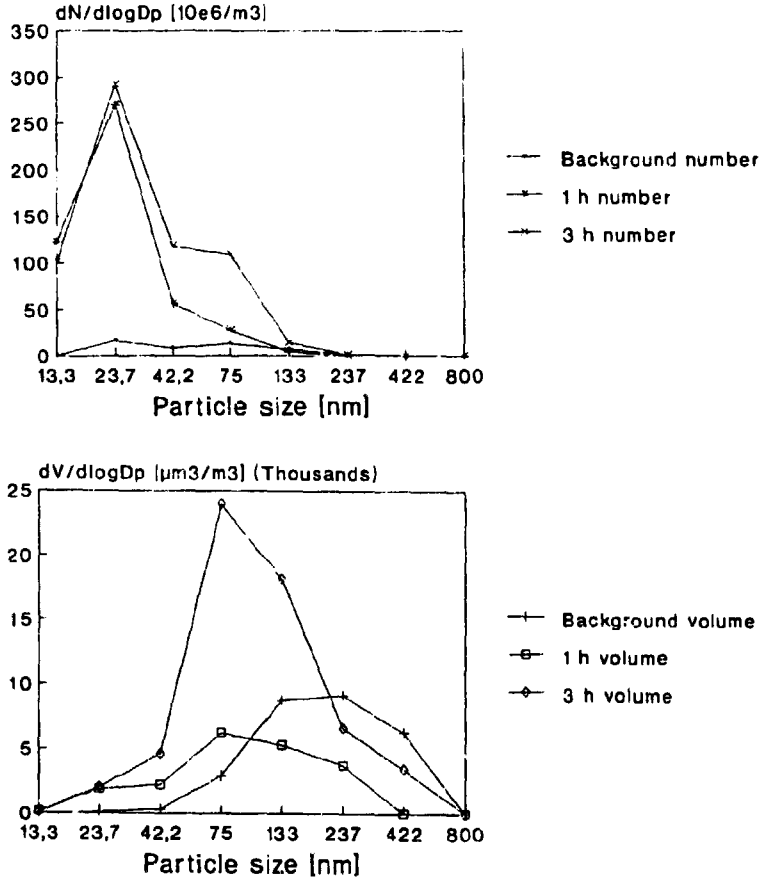

Figure 4.3 a & b. Number and volume distribution of particles produced in the EML test Chamber

When performing the experiment it was assumed that the indium powder would melt; a literature study later showed that the melting point of 165 C , stated in available chemical handbooks) in the chemical description was actually the temperature where a sublimation from the indium compound started. In an attempt to get the compound to melt the temperature was increased to 300 C°. This high temperature probably [illegible] condensation in the tube around the glass ampoule and small particles of 25 [illegible] n diameter was formed. Howe er, the high number concentration in the [illegible]er resulted in coagulation creating a volume peak around 120 nm. Air samples were made from the chamber and analyzed in the Risø research reactor. The Indium content in the air samples was 1.5 μgm^{-3} after three hours. Considering the small quantity of Indium powder used, this is a satisfactory level and it has demonstrated that this technique produces particles with a sufficiently high tracer concentration to be useful for experimental work. A commercial condensation generator from TOPAS in Dresden has been ordered and this method will be developed further.

Refinement of the Experimental Technique

During the development of the tracer technique some preliminary test were carried out in one of the staff houses at Risø. A 15 cm diameter Whatman 42 filter paper was used for making air samples using a vacuum cleaner as air pump. The used filter paper contained a significant amount of sodium which lead to the activation of Na-24 when the samples were neutron activated. A high background level was created due to the compton tail of the Na-24 decay and a very poor counting statistics were obtained for the Dysprosium peak at 95 keV. These experiments showed a need for improvements to be introduced before the next experiments in Risø Huse 27.

To improve the situation various filter papers were tested to find one with a low sodium content. By using a pump with more rigid characteristics a smaller filter paper could be used without reducing the volume of air sampled. Whatman 542 low ash hardpressed filter paper was chosen for the next experiments. This is a cellulose filter paper with a very low ash content, i.e. it is an almost pure organic filter and a tripod was mounted with two filter holders adjusted to carry 5.5 cm Ø filter paper. This enable one filter to be changed without interrupting the air flow through the other filter. Sample rates was from 20 to 25 /min with new filter paper and the stronger pumps.

The particles were released with a powder dispersion generator, RBG 1000, from Palas GmBh. This apparatus pushes the particles up through a cylinder with a slow moving piston and into a chamber with a fast rotating metal brush. From this chamber the particles is blown out through a nozzle in the top with pressured air. The emission time used range from 2 to 5 minutes depending on initial piston position and the chosen piston movement rate. At the end of the cylinder a fast rotating metal brush moved the particles up through a stream of pressured air and they were then dispersed from a nozzle at the top. In the disperser, the particles may pick up charges from the metal brush and the manufacture stated that some discharging might be necessary during dispersion. For this purpose a Kr-85 source in a glass ampoule was used in the first two houses. Kr-85 emits β-particles with a maximum energy of 800 keV. These beta-particles ionise the air that the particles flow through when leaving the disperser and the increased ion concentration in the air reduces the time it takes for a Boltzman charge equilibrium to be established, thus discharging the dispersed particles. Cooper and Reist(1973) showed that two condition should be fulfilled for this discharging to be efficient. (1) The ratio of the ion concentration to particle concentration should be considerably larger than the average number of elementary charges on the aerosol particles initially. (2) The residence time of each particle in the tube must be larger

than the time needed to reach a Boltzman charge equilibrium at the given ion concentration.

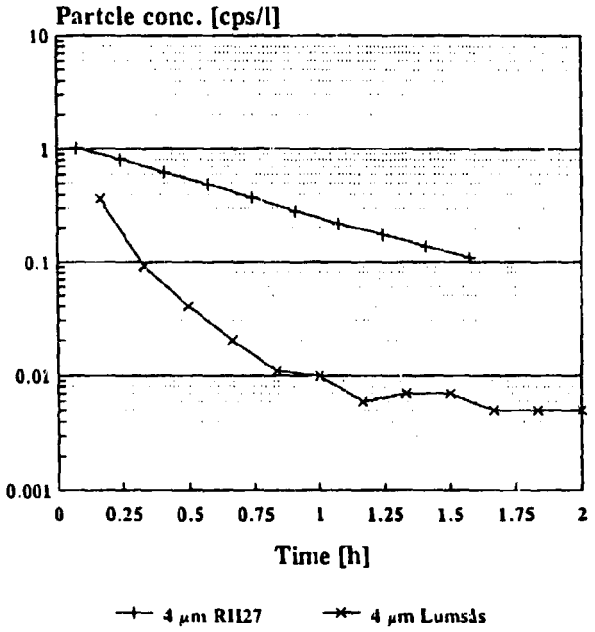

Figure 4.4. Particle experiment in Lumsås, Denmark, without a discharger compared with results from RH27. The Lumsås experiment showed the need for a discharger.

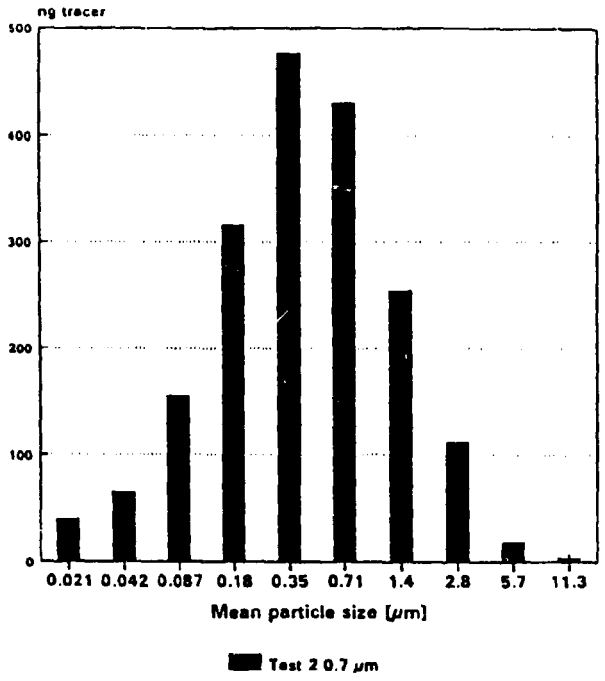

Figure 4.5 Impactor sizing of the indium particles. A fit with a log-normal distribution using the NMSIMPLX program gave an AMAD of 0.48 µm.

Some uncertainty remained as to whether the discharging was necessary, and an experiment was made without a discharger. As can be seen on Figure 4.4 the deposition is much higher without discharging and this experiment clearly showed the need for a discharger. A nickel, Ni-63, source were borrowed from the Technical University of Denmark and mounted in an aluminium tube. The source strength is 1.48 x 10^8 Bq and the beta particles have a maximum kinetic energy of 70 keV. Cooper and Reist(1973) gives empirical formulas for the efficiency of a discharger for a series of different discharger geometries using information on source strength and energy. With 34 ev required per ion pair produced in air the specific ionization for a beta spectrum with E_{max} = 70 keV becomes 305 ion pairs/cm. This gave an equilibrium of 3.9×10^{12} ion pairs m^{-3}. This distribution will bring an aerosol particle into a Boltzman charge equilibrium with a characteristic time of 0.07 s.

The highest number concentration occurs when the 2.5 µm particles are dispersed. Approximately 100 mg or 10^8 particles are emitted in two minutes with an airflow of 20 ℓ/min. This gives a particle concentration of 2.5×10^9 #/m^3 and an average residence time of 3.5 seconds in the discharger. Both criteria are thus fulfilled with the ion pair concentration exceeding the particle concentration by more than a factor of 1000 and the average residence time exceeding the average recombination (i.e. the time to reach a Boltzman charge equilibrium) time by a factor of 50.

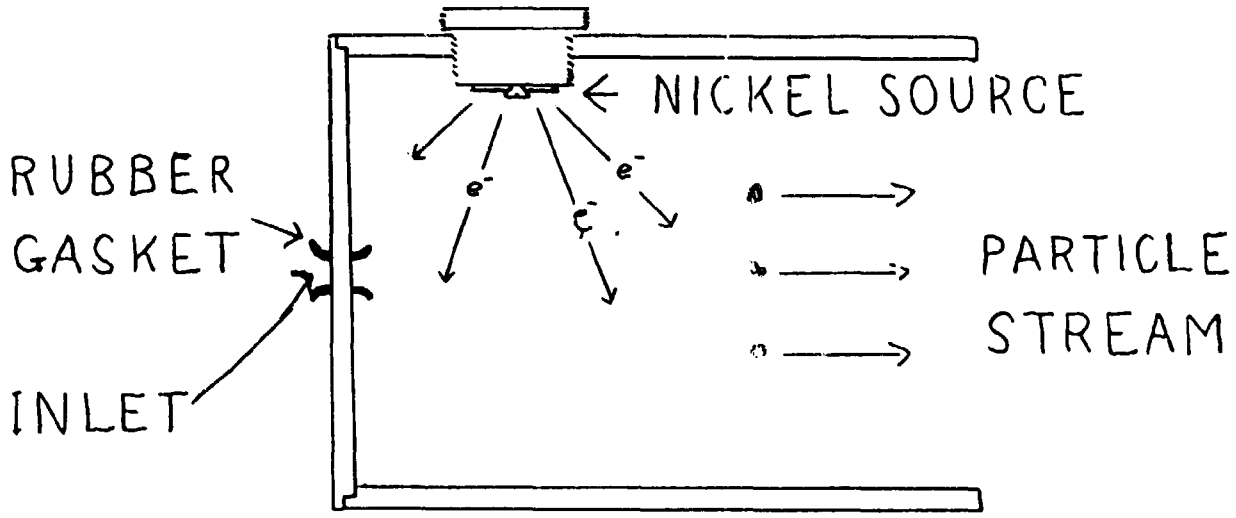

Figure 4.6. Aerosol discharger built with a 150 MBq Ni-63 source, $T_{\frac{1}{2}}$ = 92 year, E_{max} = 70 keV, mounted in an aluminium tube. The tube has a diameter of 9.4 cm and a length of 16.5 cm. The effect of this discharger have been estimated from the formulas given by Cooper and Reist(1978).

Summary of Experimental Technique

- Particles labelled with rare-earth elements is released in the test room.
- SF_6 tracer gas is released in the test room with all doors and windows closed.
- After the release 10 to 12 air samples are made each of 10 minutes duration. Each filter paper is handle with a forceps and sealed in separate bags right after use. The volume of air sucked through each filter is measured with a gas meter.

- The decay of the SF_6 tracer gas is monitored using gas chromatography. After the test the air exchange rate is worked out by a linear regression of the logarithm of the tracer concentration and the measurement time.

- The air samples are neutron activated and the cps content in each filter is determined by gamma spectrometry. The cps per volume of air is found by dividing with volume of air in the individual samples and the decay constant is found by linear regression.

- The deposition constant is found by subtracting the air exchange rate from the decay constant. The average deposition velocity is found by multiplying the deposition constant with the volume to surface ratio of the room.

4.2 Experiments in Risø House 27

At the end of November 1989 a series of four experiments was performed in Risø House 27, RH27. The results of these experiments have been reported by Roed et al.(1991). This is a house for Risø staff members and it was available for experiments for a few months in the Autumn of 1989. It is a typical Danish house built in the 1960s in double brick construction and a low air-exchange rate. All tests were made in the 98.8 m^3 living room with closed doors. The new filter papers and the new pumps were used. A series of 10 to 12 consecutive filter samples of 10 to 15 minutes duration was taken in the middle of the room. During the entire test small fans were running to make sure that the air was homogenously mixed. The samples were analyzed with a 21.3% Ge(Li) gamma detector after activation in Risøs research reactor. Two experiments were performed with 2 micron particles and 2 with 4 micron particles. Results are shown in Table 4.3. For each particle size an experiment was performed with and without furniture in the house.

Table 4.3. Result of experiments in RH27. The deposition constant has been found by subtracting the air exchange from the decay constant. From Roed et al.(1991).

APS size [μm]	λ_t [h^{-1}]	r [ ]	λ_r [h^{-1}]	v_d [$10^{-4} ms^{-1}$]	Furni-ture
2.5	0.84	0.9992	0.097	1.5	no
4	1.33	0.9997	0.007	2.4	no
2.5	0.95	0.9995	0.028	1.7	yes
4	2.10	0.9997	0.052	3.8	yes

In the first calculation of the average deposition velocity the ceiling was omitted from the room surface area as the deposition here was believed to be negligible. When results at Risø and Imperial College, see chapter 5, showed that the deposition to the ceiling was similar to the deposition on the walls, the average deposition velocity was recalculated including the ceiling area. For all the four houses the deposition velocity, v_d, has been calculated using the geometric surface, S, to volume, V, ratio. That is, no contribution from the surface of furniture, etc. has been included in the surface area of the furnished rooms. Such measurements would be difficult to make in an objective and reproducible way.

$$v_d = \frac{(\lambda_t - \lambda_v)V}{S} \qquad (41)$$

The deposition constant, λ_d, is found by subtracting the air exchange rate, λ_v, from the decay constant, λ_t. The average deposition velocity is found by multiplication with the volume to surface ratio, *V/S*, as shown in equation (41). The calculation of a v_d makes it possible to compare the results from different houses. For instance, the average ceiling height in Risø Huse 27 was half a meter higher than in the other test houses and this will give a different deposition constant, but the average v_d should be similar to that found in other houses. Further-more the average v_d can be used to estimate deposition constants in rooms with different S/V ratios than those used for the experiments.

The results of these experiments in shown in Table 4.3. The linear decay curves that can be seen in Figure 4.7 implied that the particles were sufficiently monodisperse for the purpose. With too broad a size distribution it can be expected that the difference in deposition velocity, v_d, would produce a decay curve with a decline in the decay rate with time as the particles with the lowest deposition velocity would become more and more dominating. The experiments showed an increased deposition in furnished rooms as could be expected and seen in experiments with Be-7, Roed et al. (1985). The four micron particles decayed faster than the two micron particles, as expected for particles larger than 1 μm for which gravity is the dominating loss force.

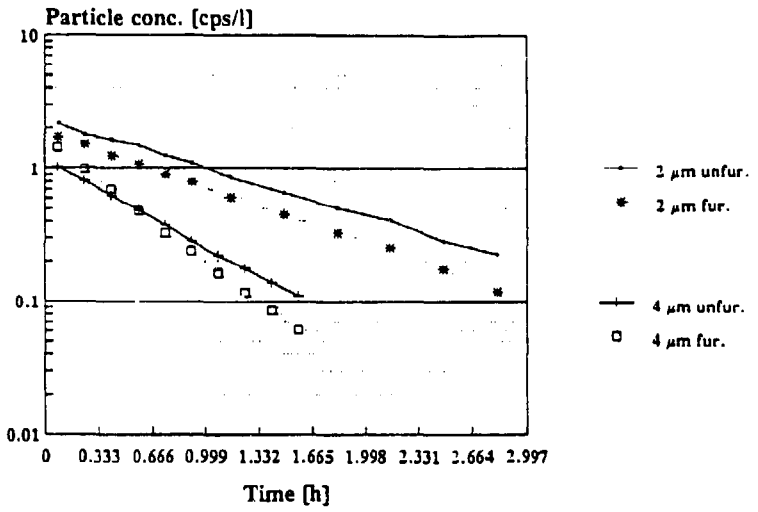

Figure 4.7. Decay curves from the experiments in RH27. The decay curves were steeper for the larger particles and when furniture was present in the room. This deposition pattern together with the straight decay curves implied that the experimental technique used produced reliable and usefull results. From Roed et al.(1991).

4.3 Experiments at the Building Research Establishment, UK.

A repetition of the RH27 experiments was carried out in the UK from 4th to 19th of November 1991. Christian Lange went from Risø by car to Watford to participate in the experiments and brought the equipment used in RH27 along. In Watford, the Building Research Establishment, BRE, had lent a research house to Imperial College.

The house was the middle one of three small two storey row-houses. The living-room was used for all except the last experiment, which took place in an upstairs bedroom. It was considered to be a house of average British standard. The air exchange rate was high and as it got windier the door and windows was closed and had to be sealed with scotch-tape to keep the air exchange rate below one change per hour. During the three weeks 18 tests were performed with two particle sizes. Experiments were performed with furniture and without furniture in the room. Some tests were made with big fans running to increase the turbulence and others with vacuum cleaners running. In one test enhanced human activity was tried, i.e. running and jumping in the room during the test.

The SF_6 equipment was set-up with 5 sampling locations and a switch box and tested twice before starting the particle tests. The switch box contained a pump that kept a flow through all 5 sampling lines. One line could be chosen as the inlet for the SF_6 detector and by using a short connection line between the switch box and the detector the continous flow on all lines facilitated faster switching between different sampling locations. The five sampling inlets were placed in the centre of the room, at the ceiling, in two corners and in the hall. The measuring apparatus was a laser gas chromatograph. To allow new air to enter the detector and to give the detector system time to stabilize 30-second intervals were maintained between measurements at the different sampling locations. The results as shown in Figure 4.8 confirmed that within two or three minutes after the release of the SF_6 the concentration had stabilized at all sampling locations in the room and that the decay curves were then identical for each location, though the absolute concentration level did vary a few percent from corner to corner. When fitted with exponential decay curves, as given by equations (38) and (39), all SF_6 measurements during the tests in BRE and the later tests have been linear with a regression factor better than 0.999. The mixing was tested at four points during the next 18 tests and it followed the same pattern in all tests. This mixing supported our belief that we would have a good particle mixing a few minutes after release. So in the basic tests the small mixing fans were switched off after the release of particles and before the beginning of the air sampling.

Three anemometers from Dantec A/S were used for monitoring air movement, turbulence intensity and room temperature during the tests. The anemometers contained low velocity transducers, type 54R10, which uses thermal anemotry and are designed specially for indoor use. The anemometers had not been calibrated recently and a consistent difference of 35 % between the highest and lowest reading was found when making an intercomparison of the anemometers. Readings during the tests ranged from 0.05 to 0.12 ms^{-1} for the air movement and 10 to 20 % for the turbulence intensity. These values increased to 0.20-0.25 m/s and 20-25 % in tests where large mixing fans were used. Melikov(1988) reported turbulence intensities of 20 % for unventilated rooms and around 30 % in ventilated rooms. The BRE values were lower than these and that may have been due to insufficient cleaning of the probes which would lead to a decreased sensitivity, which especially lowers the turbulence measurements.

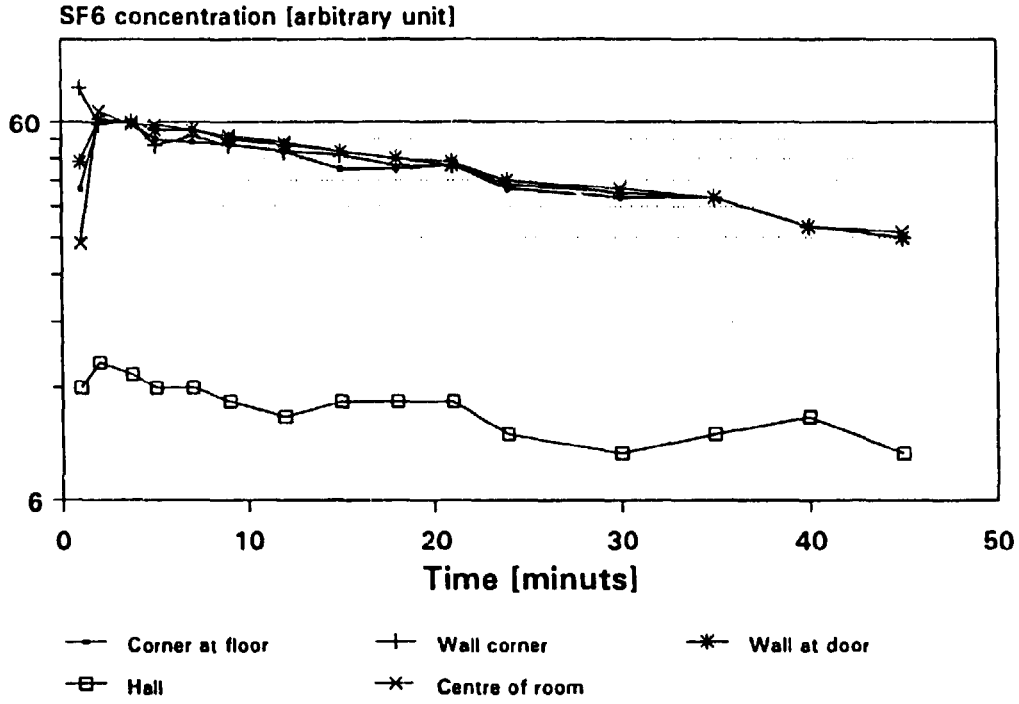

Figure 4.8. Air-exchange measurements in the BRE test house using multipoint sampling. The SF_6 was actually measured at 15 second intervals in these measurements and not simultaneously as shown. The first reading after one minute shows that the tracer gas still was not homogeneously mixed but already after two minutes this is the case. Hereafter the level is were constant throughout the room during the rest of the test though the rate of decline seems to vary.

Meteorological situation was monitored through the regular surveillance programme at BRE. Wind speed and direction, sun hours and temperature were monitored. The only use of this data sofar is to note that an increased air-exchange rate was correlated with an increased outdoor wind speed, as expected.

After the first four tests a trip to The Imperial College Reactor Centre was made to analyze the samples from the first tests. Some problems arose due to the lack of routine and equipment for fixing the samples in an uniform way above the detector. Decay curves were obtained for tests 1.1, 1.3, and 1.4 with correlation factors from 0.91 to 0.98 (see Table 4.4, UK results). After this first try fixed geometries were made both at Risø and Imperial College for gamma spectrometry analysis of the Whatman 542 filter papers. The samples from test 1.5 were analyzed at both Imperial College and at Risø with improved results, and a correlation coefficient of 0.9985 and 0.9990, respectively were obtained, see Figure 4.9. The slightly better correlation for the Risø analysis results are attributed to the higher neutron flux of the Risø research reactor, which produces a higher level of activated tracer and thereby a better counting statistics. It is interesting to note that even with the good correlation coefficients for the liniar regression analysis of the activation results of test 1.5 in the UK and Denmark there is a 7 % difference between the Imperial College and the Risø decay constant even though the counting uncertainty was better than 0.3 % for all samples

measured at Risø. Byrne(1994) used a weighted non-linear regression model and obtained estimates of the error term based on the standard deviation of the individual data points. She found a 2 % standard deviation for all the decay constants obtained from the Risø activation results and 8 to 10 % for results from the Imperial college reactor. The difference for test 1.5 between the Risø and Imperial College results were thus within the standard deviation. Also, tests 1.1, 1.3 and 1.4 were re-analyzed at Risø (see Table 4.4, DK results) and here the improved correlation coefficient was expected due to the improved control of the gamma ray counting geometry and the higher neutron flux.

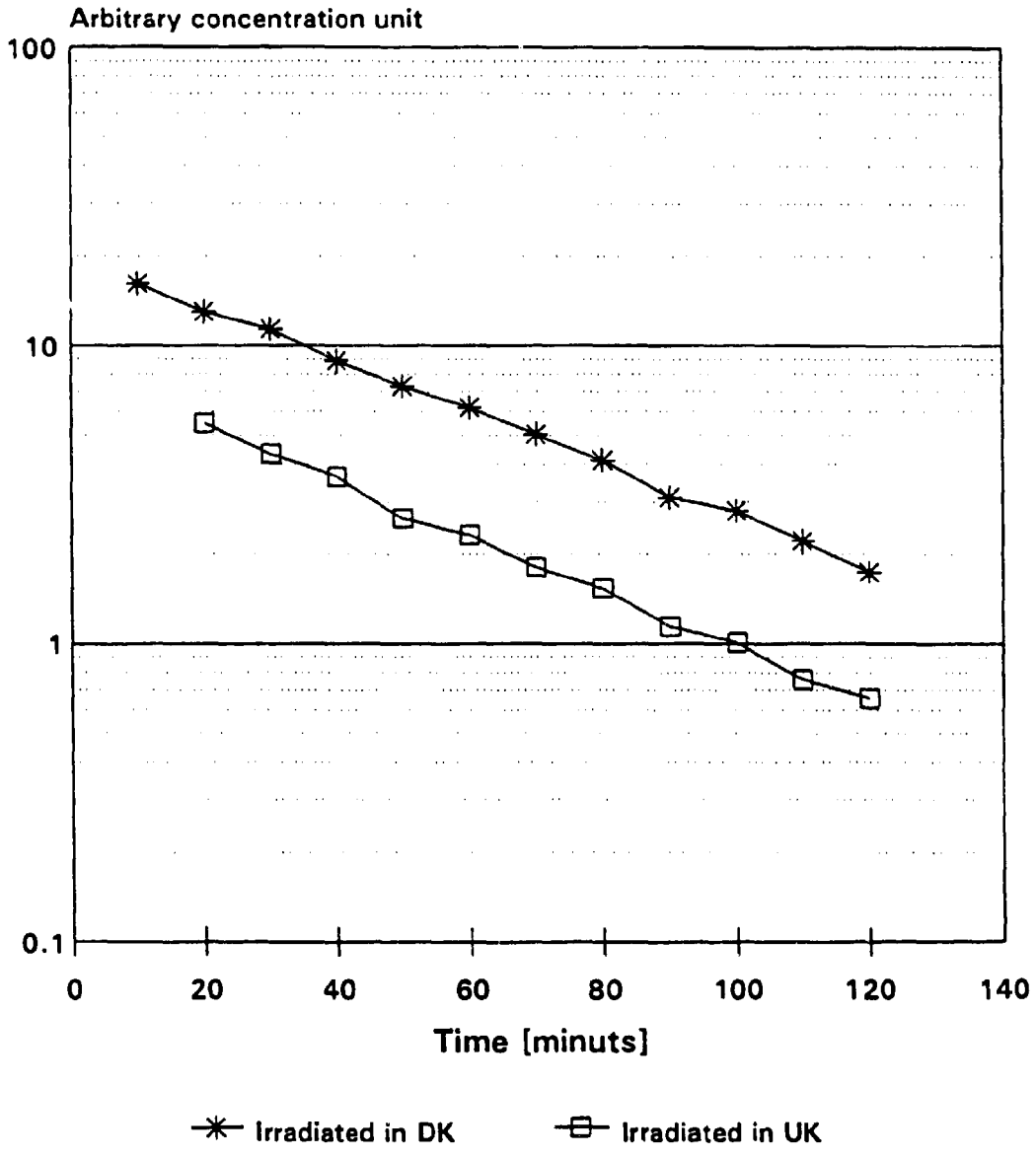

Figure 4.9 The results of activation of test BRE 1.5 in UK and Denmark. Despite the very good correlation coefficients, above 0.999, there is a difference of 7 % between the decay constants derived from the slope of the curves.

Table 4.4. Review of experiments in BRE. Tests 2.7 to 2.18 was performed by Miriam Byrne and only analyzed at Imperial College. r gives the correlation coefficient for the linear regression determining λ_t.

Name	Size [μm]	λ_t [h^{-1}]	λ_r [h^{-1}]	v_d [10-4ms^{-1}]	r [ ]	Notes
1.1UK	4	1.46	0.41	1.42	0.91	
1.1DK	4	2.32	0.41	2.59	0.992	
1.2DK	4	2.98	0.98	2.63	0.990	
1.3UK	4	2.49	0.40	2.83	0.98	
1.3DK	4	3.27	0.40	3.89	0.994	
1.4UK	2	1.38	0.40	1.33	0.977	
1.4DK	2	1.52	0.40	1.52	0.995	
1.5UK	2	1.28	0.25	1.40	0.9985	
1.5DK	2	1.20	0.25	1.29	0.9990	
2.7UK	4	1.77	0.27	2.03	?	furnished
2.11UK	2	1.11	0.33	0.95	?	furnished
2.17UK	4	1.57	0.20	1.86	?	

When analysing the next tests little or no dysprosium was found in the samples and examination of the particle disperser showed that it suffered from mechanical failure. The 13 experiments planned and carried during the experiment at BRE was later repeated and results are reported by Byrne(1994). These experiments included tests with high fan speeds, human activity and operation of a vacuum cleaner. Results of these tests are included in Table 4.4 for the data that has been included in the review of the average deposition velocities (tests 2.7, 2.11 and 2.17). For most of the other test it was concluded that the activities had been disturbing the air concentration decay so much that the obtained results could not be considered reliable.

4.4 Experiments in Ferslev

In the late spring of 1993 a new house became available in the villages of Ferslev 50 kilometres west of Copenhagen. Apparatus for producing sub-micron particles labelled with indium was used for the first time in a test house. New 3 and 5.5 micron silica particles labelled with dysprosium were also introduced in the tests. Now 5 monodisperse particle batches were available: 0.5, 2, 3, 4, and 5.5 μm.

The test house was an old barn, which had been converted to a residential house in the 1970s. The 30 m^2 living room was used for the experiments and internal doors was kept closed during the experiments. The room had a low air-exchange rate: between 0.03 to 0.12 h^{-1} in the 13 tests. Weather conditions were monitored with a mobile meteorological measurement station borrowed from the meteorological department at Risø. The weather was mild and sunny and with light winds during the

two weeks of experimental work. As a result no heating was on during the experiments.

Air speeds and turbulence were measured in the room using new Dantec A/S low velocity transducers calibrated in a wind tunnel at Dantec A/S. Measurements were made in the centre of the room and at two walls 1.2 meters above the floor. One of the 'wall' anemometers were placed in front of a large (4 m^2) panorama window. Air speeds ranged from 0.05 to 0.1 ms^{-1} with turbulence intensities from 20 to 30 %. When the sun shone through the window, the air speed increased to 0.24 ms^{-1} at the window probe and to 0.10 to 0.18 ms^{-1} at the other probes. Turbulence intensity remained unchange at around 25 %.

Relative humidity ranged from 32 % to 49 %. The relative humidity raised a few percent from the beginning to the end of each test probably due to the presence of the personal operating the equipment.

The three new particle sizes had average deposition velocities which agreed well with earlier results. The deposition velocity, v_d, of the submicron particles was half that found for the 2 µm particles. The 3 µm particles had a v_d between the values found for 2 and 4 µm particles. The 5.5 µm particles had the highest v_d measured so far, but not as high as could be expected if the increase were to be proportional to the square of the particle diameter (as is the case for the settling velocity).

Table 4.5 Decay constants and derived deposition velocities in Ferslev. The particle sizes are measured with APS, Las-x and a Berner impactor.

No	Size [µm]	λ_t [h^{-1}]	λ_v [h^{-1}]	v_d [$10^{-4} ms^{-1}$]	r [ ]	Furniture yes/no
1	2	0.583	0.052	0.917	0.79	no
2	3	0.71	0.113	1.036	0.97	no
3	5.5	1.856	0.122	2.995	0.98	no
4	4	1.198	0.077	1.937	0.93	no
5	0.5	0.451	0.050	0.693	0.94	no
6	3	1.052	0.067	1.700	0.99	no
7	5.5	1.821	0.046	3.07	0.97	no
8	0.5	0.308	0.046	0.531	0.84	no
9	5.5	2.002	0.128	3.24	0.97	yes
10	3	1.327	0.028	2.25	0.98	yes
11	4	1.996	0.077	3.315	0.995	yes
12	0.5	0.41	0.077	0.575	0.92	yes
13	2	0.47	0.025	0.726	0.97	yes

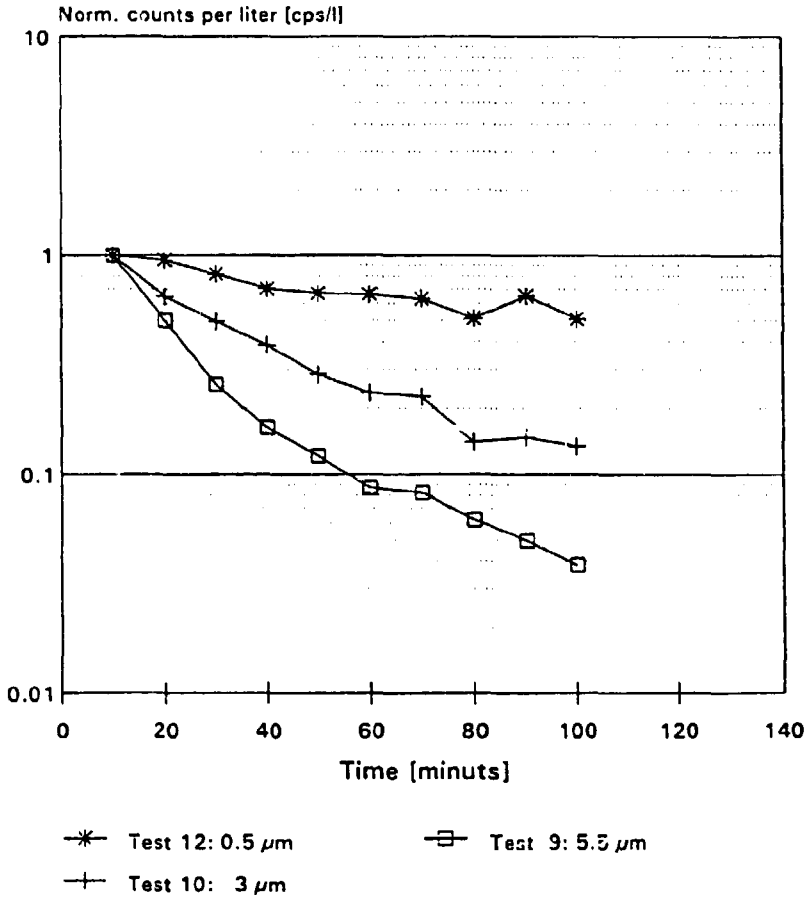

Figure 4.10. Decay curves from the house experiments in Ferslev for the three new particle sizes. The average deposition velocities derived for these particles agreed with results obtained for the first two particles batches. The 0.5 micron particle had a slower decay than the heavier particles and with 5.5 micron particles having the largest decay of all. It can be seen on the Figure that the decay lines are not as straight as in the earlier tests, due to problems with the filter holders. The decay constant of the 5.5 μm particles seems to change with time.

4.5 Experiments in Jersie

In March 1994, a fourth series of measurements took place in an old house in the village of Jersie. The house was built in 1900 and is of double brick construction. Not many insulatory improvements have been made to reduce heat losses in this house and the air exchange rate was between 0.7 and 1.1 h^{-1} during the seven tests performed. The living-room used for the experiments measured 4 by 8 meters. The house was inhabited during the experiments and for this reason only experiments with furnished rooms were carried out. The furnishing of this house was the most realistic since all the other test houses have been furnished for the tests and not by people intending to live there. The only experimental condition that was varied from test to test was that the small mixing fans were turned off during some of the tests to see if a influence of the change flow pattern could be seen in the deposition constants.

A large number samples were collected during the seven tests in Jersie. In addition to the air samples, samples from walls, ceiling, and floor were made to determine

deposition velocities for specific surface orientations. Other samples were made from cotton cloth, hair and skin wipes to determined the deposition to humans. In total, more than 300 samples were made The specific deposition results are presented in the next chapter.

No monitoring of the outdoor meteorological situation and the relative humidity indoors was made during these experiment. In general it was cold 0 to 5 °C (snow covered ground the first week), windy and cloudy during the two weeks. For this reason the central heating was on during all experiments The heating consisted of two radiators, 3 m long and 0.5 m high, with circulating hot water

During five of the seven tests, both indium particle nebulization and silica particle dispersion were used to increase the information obtain from each test. 80 to 100 mg of silica particles were released together with 3 minutes of nebulization from a suspension of 100 mg Indium-Acetyl-Acetonate in 15 ml of alcohol. The 3 µm particles were not used in these tests since they were found to be very similar to the 2 and 4 µm particles in the Ferslev tests. The 5.5 µm and some new nominal 20 µm particles were labelled at Risø. Unfortunately, only a weak solution of $DyCl_3$ was available and in the two tests where indium was nebulized together with these silica particles the 95 keV signal from dysprosium was lost due to the Compton tail of the In-116m and Na-24 higher energy gamma lines.

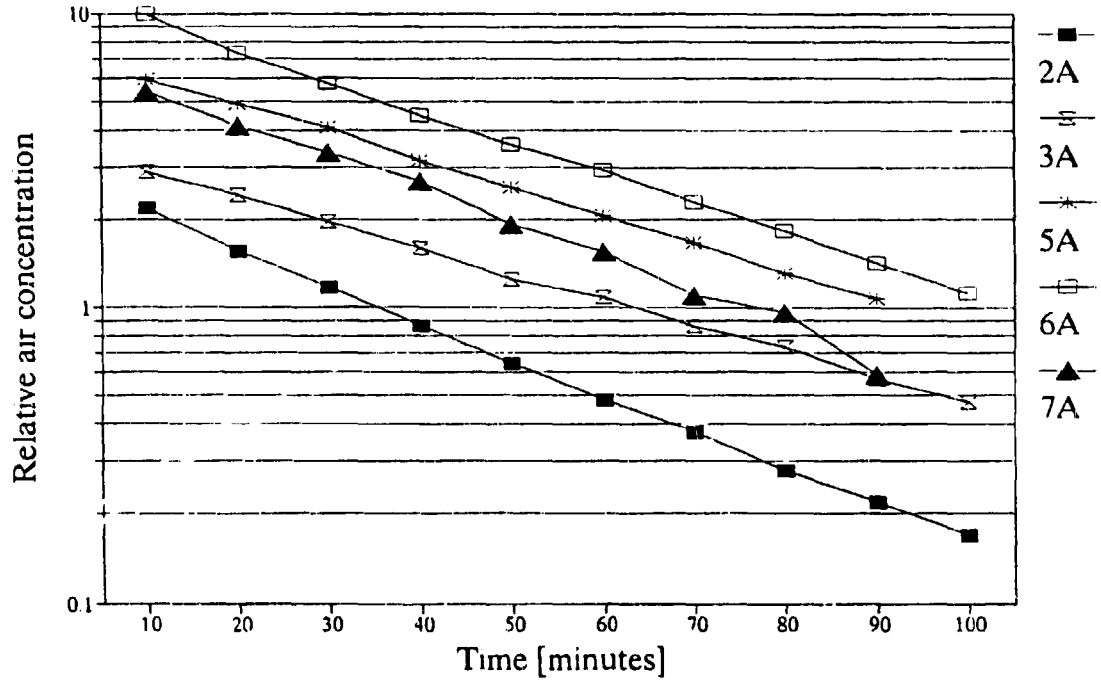

Figure 4.11 Decay curves for Indium particles in the Jersie test house.

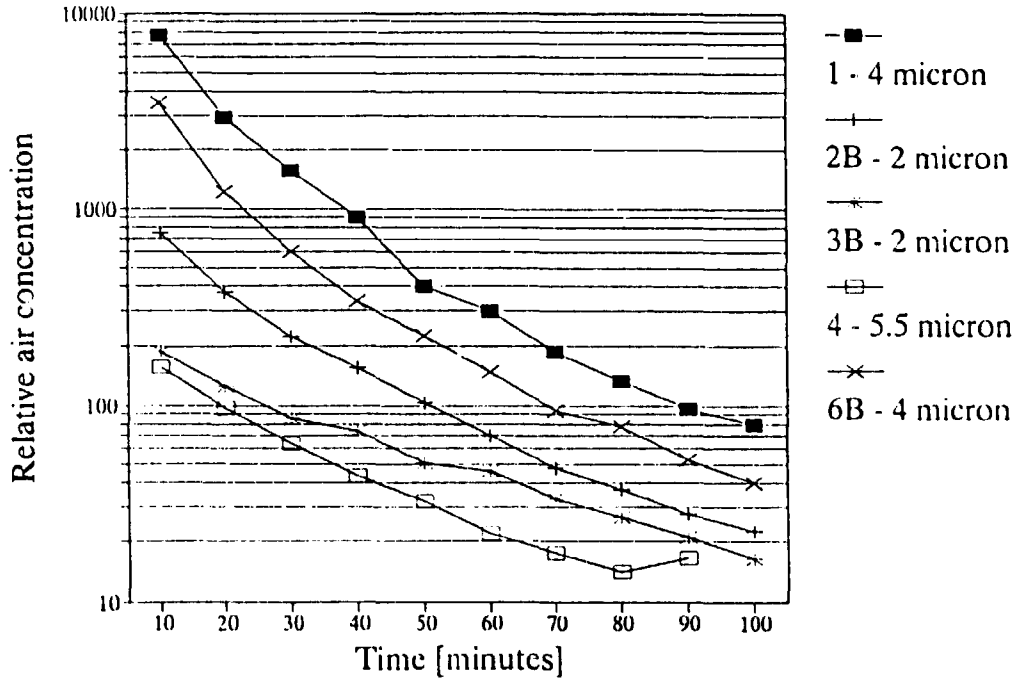

Figure 4.12. Decay curves for the Silica particles in the Jersie test house.

Table 4.6 Anemometer readings during the experiment in Jersie. A was in the centre of the room 1.5 meters above the floor. B was 20 cm from the north wall 1.8 meters above the floor over a hot water radiator which came on periodically during the experiments. C was placed in the middle of the south wall 20 cm from the wall and 1.8 meters above the floor.

Test	Fans	A Velocity [ms^{-1}]	A Turbulence [%]	B Velocity [ms^{-1}]	B Turbulence [%]	C Velocity [ms^{-1}]	C Turbulence [%]
1	on	0.355	44.9	0.183	31.2	0.197	29.3
2	on	0.173	26.3	0.162	30.7	0.341	37.8
3	off	0.066	37.1	0.090	38.0	0.058	53.4
4	off	0.074	43.1	0.155	38.0	0.094	41.3
5	on	0.178	21.2	0.143	38.0	0.114	32.1
6	on	0.199	18.5	0.188	39.9	0.094	43.8
7	on	0.222	27.2	0.126	35.4	0.176	35.9

A PMS model CSASP-200 light scattering aerosol sizer with 1-D Probe Adaptor Module PMS 1058B installed in a Toshiba PC/AT was used for monitoring the ambient aerosols in the test room. Size distribution data from all days with experiments was saved on the hard disk with 60 second intervals. This monitoring showed that the background aerosol level was so high, that the release of the tracer particles only increased the total number concentration by a few percent.

A 10-stage Berner impactor loaded with collector paper cut from Whatman 542 filters was operated during three tests. The impactor was operated in the exact same period as the air samplers to permit direct comparisons of the total amounts collected. The size distribution found for the indium particles is shown in Figure 4.5.

The three anemometers used in Ferslev were also used in these experiments in Jersie. During six days with experiments the average air speed and turbulence intensity were calculated every 30 minutes through out thel day. The values found during the tests are shown in Table 4.6, and Figure 4.13 shows the values during the day when tests 2 and 3 were performed. The influence of the small air fans for mixing can be seen on the Figure. It is interesting to note that the deposition was app 50 % higher both for the 0.5 and 2 µm particles used in these tests, when the mixing fans were on. In general, the air speeds and the turbulence intensities were higher in the Jersie test room than in the Ferslev test room. This is what would be expected due to the higher air-exchange rate and to the convective air currents created by the central heating.

Tne decay curves for the 12 tests are shown in Figures 4.11 and 4.12. The correlation coefficients were around 0.99 for all decay constants. This was an improvement compared to the Ferslev tests and is attributed to the new filter holders used in the Jersie tests. The derived deposition velocities, Table 4.7, were in good agreement with earlier measurements except for the 5.5 µm particles, which had a lower v_d than the 4 micron particles and the value found in Ferslev. As mentioned previously, the tracer content of the 5.5 µm particles was low and the tracer concentration in the room air may have been influenced by resuspended particles from previous experiments with a higher tracer content The 4 µm particles had the lowest correlation coefficients, 0.977 and 0.98, and from the decay curves it appears that the decay constant changes with time for these particles.

One explanation for this phenomena could be build-up of particle concentration in adjecent rooms and a subsequent lowering of the loss rate due to ventilation. If this

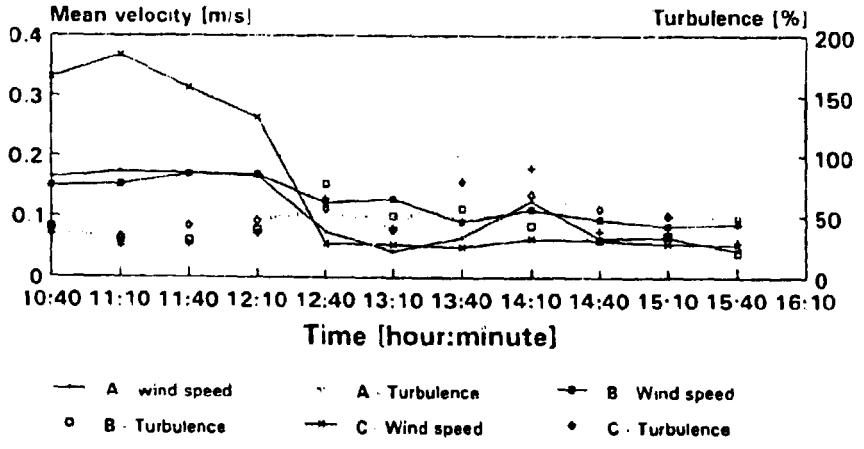

Figure 4.13 Air speed and turbulence measurements during Jersie tests 2 & 3. During the morning test the mixing fans were on They were turned off after the particle dispersion during the afternoon test

was the case a similar two component structure should also be seen for the SF_6 measurements during the test. As can be seen in Figure 4.13 the decay curve for the SF_6 concentration were perfectly straight during both experiments with 4 μm particles in Jersie and effect of internal build up of particles can be safely neglectedted. Another mechanisme that have been seen to give this two-component decay structure is insufficient decharging. The β-particles emitted from the Ni-63 source have a maximum energy of 93 keV giving them a very short range in solid matter (app. 100 μm). Although the discharger were cleaned after each test the sources itself was not cleaned and a thin layer of particles may have been present lowering the range of the β-rays and thus making the discharging insufficient at some distance from the source.

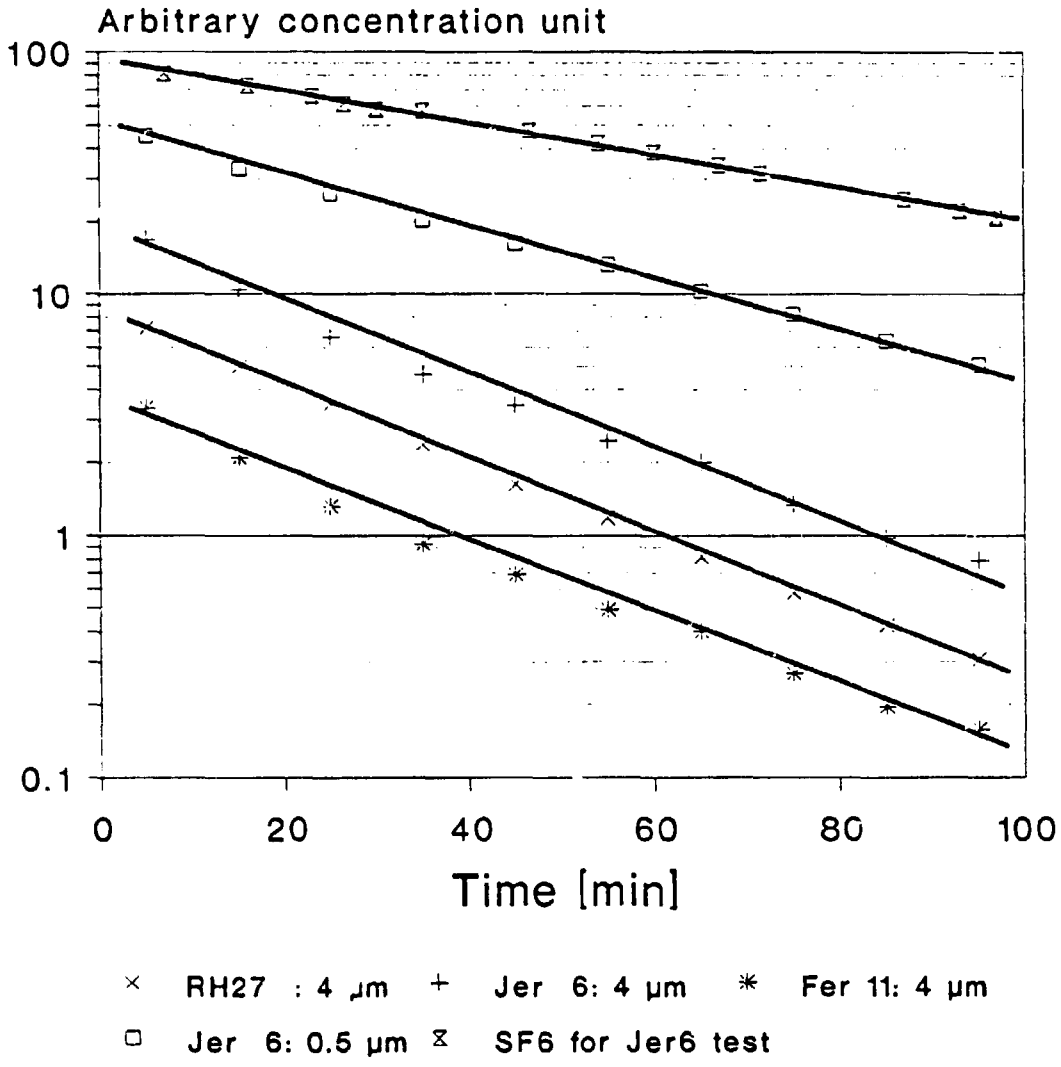

Figure 4.14. Decay curves for 4 μm silica particles in three test houses. This figure shows the similar deposition the 4 μm particles in three different test houses, but the Jersie curve has a bimodal decay curve. Maybe the decharging has become insufficient due to deposition on the Ni-63 source? The aluminium tube was cleaned between experiments, but the source itself was not cleaned. Another explaration might be that resuspended particles (maybe of particles from previous tests) was created during test by the peoble in the room.

Table 4.7. Results from the experiments in Jersie.

Test	Size [μm]	λ_s [h^{-1}]	$r(\lambda_s)$ [ ]	λ_r [h^{-1}]	$r(\lambda_r)$ [ ]	λ_d [h^{-1}]	v_d [$10^{-4} ms^{-1}$]	Fans on/off
1	4.0	3.0000	0.9808	1.1280	0.9998	1.8720	3.266	on
2A	2.0	2.2747	0.9892	1.0638	0.9999	1.2109	2.113	on
2B	0.5	1.7023	0.9993	1.0638	0.9999	0.6385	1.114	on
3A	2.0	1.5538	0.9995	0.7553	0.9972	0.7985	1.393	off
3B	0.5	1.2078	0.9945	0.7553	0.9972	0.4525	0.789	off
4	5.5	2.0063	0.9867	1.0980	0.9999	0.9083	1.585	off
5A	5.5	-	-	0.9490	0.9996	-	-	on
5B	0.5	1.3140	0.9995	0.9490	0.9996	0.3650	0.637	on
6A	4.0	2.7837	0.9773	0.9005	0.9988	1.8832	3.286	on
6B	0.5	1.4268	0.9994	0.9005	0.9988	0.5263	0.918	on
7A	20	-	-	1.1073	0.9998	-	-	on
7B	0.5	1.6059	0.9962	1.1073	0.9998	0.4986	0.870	on

4.6 Review of House Experiments

Deposition has been studied in five test rooms in four different houses. The houses differred widely in building standards. Two of the houses, RH27 and Ferslev, were tight constructions with a low air-exchange. The two other houses, BRE and Jersie, were leaky constructions with high air-exchange rates, as can be seen in Table 4.8. The surface to volume ratio, S/V, varied from 1.46 to 2.05 m^{-1} for the 4 test rooms included in the summary. The number of people in the test room varied from 4 people in one experiment in the 32.1 m^3 BRE test room to one man making a test in the large 98.8 m^3 RH27 test room. The degree of furnishing was also different in the four houses. The BRE test room was rather crowded (with equipment, scientists, and a shelve nailed to the wall) already when the unfurnished tests were made, whereas the Ferslev test room only became sparsely furnished when doing the 'furnished' tests. In general the furniture consisted of a sofa, sofa table, dining table with chairs, curtains, shelves, smaller tables and cupboards whereas smaller artifacts such as pictures, books, pieces of art or souvenirs was missing. Such smaller objects might increase the internal surface area significantly, but it is difficult to quantify the amount of such artifacts that is present in an average home.

Despite the differences between the test conditions in the various houses, the results are in good agreement. Table 4.9 shows the average results for furnished and unfurnished rooms. As tests only were made with furniture in the room during the Jersie experiment there is actually only 'unfurnished' results from three houses. In all experiments, the deposition velocity was highest in the furnished houses. In Table 4.9 the deposition can also be seen to increase with particle size as predicted by deposition theory for supra-micron particles, but the actual deposition velocities exceeds those predicted by the theories that only includes gravitonal settling(e.g. Corner and Pendlebury(1951)) by a factor 2 to 5 as can be seen in Figure 4.15 a & b.

When the results were compared with the measurements of indoor deposition presented in Roed & Cannell(1987): Table 2 good agreement was observed. For Be-7 which is associated with particles in the size range of 0.5 to 1.0 μm (see Chapter 3) they found a deposition velocity of 0.71×10^{-4} m/s as an average deposition velocity in the house. The indium particles had a AMAD of 0.5 to 0.7 μm, which is close to that ofBe-7, and the deposition velocity has been found to be 0.61×10^{-4} ms^{-1} for unfurnished rooms and 0.82×10^{-4} ms^{-1} for a furnished room in average. Roed and Cannell found a v_g of 3.1 to 3.9×10^{-4} ms^{-1} for Ce-144. This corresponds to the v_g of 4 or 5.5 μm particles in Table 4.9 and this would be reasonable size for cerium as it belongs to refractory group of release products as described in Rulik et al.(1987).

Table 4.8. Review of the test houses. Three Danish and one British house have been used for the experiments. Two leaky house and two tight house.

House	Volume, V [m^3]	Surface, S [m^2]	S/V [m^{-1}]	λ_i [h^{-1}]
RH27	98.8	145.2	1.47	0.03 - 0.10
BRE	32.1	65.8	2.05	0.25 - 0.98
Ferslev	74.0	121.5	1.64	0.05 - 0.13
Jersie	77.5	123.4	1.59	0.7 - 1.1

Table 4.9. Measurements of indoor Deposition Velocities in four houses. The first two columns show size and geometric standard deviation, GSD, of the test aerosol. The last two columns gives the average deposition to all surfaces measured in three different test houses. The numbers in the parentheses give the number of tests for each condition.

Size [µm.]	GSD [ ]	Avg. v_d Unfurnished [$10^{-4}ms^{-1}$]	Avg. v_d Furnished [$10^{-4}ms^{-1}$]
0.5	1.60	0.61±0.08(2)	0.82±0.08(6)
2	1.48	1.13±0.16(5)	1.36±0.(5)
3	1.20	1.33±0.37(2)	2.25±0.00(1)
4	1.07	2.42±0.17(5)	3.11±0.(5)
5.5	1.18	3.03±0.04(2)	3.24±0.00(1)

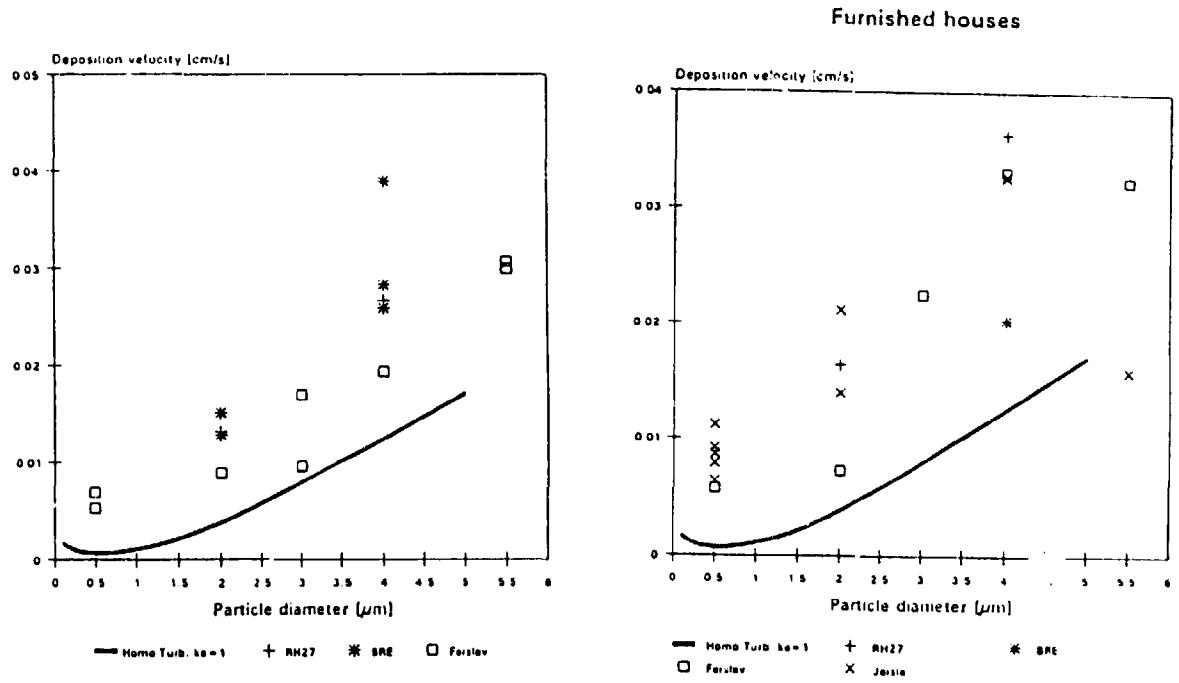

Figure 4.15 a & b. Average deposition velocities in unfurnished and furnished rooms. Review of results from the four test houses. The solid curves calculated from the formulas of Corner and Pendlebury(1951) with a Ke value of 1 s⁻¹.

5 Deposition to Surfaces

During the house experiments in Watford at BRE in 1991 the idea occurred that the sensitivity of the sample analysis permitted that other samples than air filters could be made. Some samples were taken to estimate the feasibility of this idea. A few filter papers were attached to the walls, wipes were made from different surfaces and pieces of cotton cloth were sampled after a test. No results from these preliminary tests are presented here, but these test showed that measurements of deposition to small surfaces, e.g. 10 cm², could be made with good accuracy.

This finding initiated a series of aerosol deposition studies, aimed at measuring the specific deposition velocities to various indoor surfaces. The average deposition velocity calculated from the decay rate of the tracer aerosol could then be compared with deposition velocities to individual surfaces. In the next house experiments this technique was used to measure deposition to specific surfaces as function of surface orientation. First in Ferslev and later in Jersie filter papers were attached to walls, floor and ceiling during the tests. The aim of these measurements was to establish a mass balance or in other words to determine how much of the aerosol becomes attached to individual surfaces in the room. This would enable a surface by surface comparison with current deposition models.

Jones(1990) brought to attention the fact that deposition to skin may be a pathway that would cause significant non-stochastic effects in the aftermath a nuclear accident but he lacked information on skin deposition velocities to decide if this was the case. It was proposed to use the tracer technique developed at Imperial College and Risø to make measurements of skin deposition and the second section of this chapter describes the results obtained.

Hair and clothing are other surfaces which we 'carry' close to the body and toxics

deposited here might cause damage by external radiation (in the case of radioactive materials) or by subsequent transport to the skin and absorbtion by the body. Deposition to these surfaces was also been investigated in this study

5.1 Deposition to Indoor Surfaces

When assessing the feasibility of measuring deposition to a 10 cm^2 area there are two limiting factors: the amount of tracer material must be above the lower limit of detection and the number of particles deposited on the area must be large enough for that stochastic processes to be negligible. If there is uniform deposition of a fixed number of particles to a given area the number particles in subsets of this area will follow a poisson distribution. This, for example, means that if for instance 1000 particles are expected to be deposited on a given surface then the standard deviation will be $\sqrt{1000}$, i.e. 33 particles or 3.3 %. This uncertainty must be added to the counting uncertainty of the gamma spectrometry measurements.

A Test Chamber Experiment

A test chamber was constructed in a basement at Risø. The far end of a cellar room was shielded with a plywood wall on a wooden frame. All apparatus was placed outside the chamber on shelves on the plywood wall. Openings/fittings were been made for aerosol injection, air sampling, data cables and power cables. The chamber was rectangular with a volume of 18 m^3 box with all surfaces painted in standard mat wall painting. The only equipment inside the chamber are four fans: the fan speed was controlled remotely with a variable transformer.

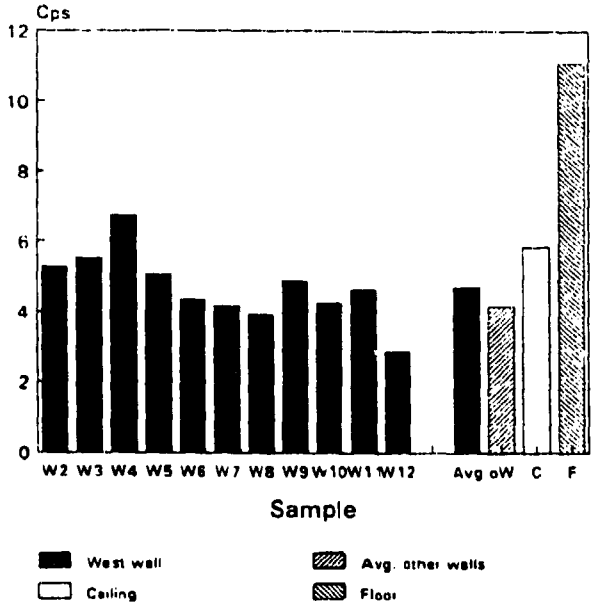

Figure 5.1 Vertical deposition pattern in still air for 4 μm particles in the Risø aerosol test chamber.

In one experiment the vertical deposition pattern on the west wall was studied. No fans were used in this experiment so air motion would be governed by slow convective motions. Deposition along a surface should be uniform when there are no significant variations in the flow patterns along the surface. So in this experiment the mass deposited on each filter paper along a surface should be similar.

In this experiment twelve collectors were attached along the centre line with 20 cm intervals from top to bottom. 5.5 cm diameter Whatman 542 filter papers were used as collector surfaces. The collectors were attached to the wall with double sided scotch tape. A load of 4 micron dysprosium labelled silica particles were released with the Palas particle disperser one hour after the door was closed, ie. amble time was allowed for the air inthe room to stabilize. The chamber was left until next morning when the filter papers were removed. With a typical decay constant of 1-2 h^{-1} for 4 micron particles this time interval should have been suffucient for essentially total deposition of the particles.

The results of this experiment showed that the technique gives stable results. The standard deviation on the mean deposition was close to that expected to occur due to the stochastic nature of the gamma analysis procedure and the deposition process. In other words:, if the assumption that deposition to the sampling surfaces in still air is uniform, we would expect to get a result like this. Similarly, if the standard deviation of the mean of the measured deposition on a series of collectors exceeds what is expected then this would indicate non-uniform deposition to the surface From Figure 5.1 it appears that the deposition was greater for w2 to w6, which were close to the ceiling, than for w7 to w12. The standard deviation within each of these two subsets actually corresponds closely to what can be expected from the uncertainty of the measurement technique.

Table 5.1 Result of test chamber experiment studying deposition pattern on a wall. The standard deviations, SD, of the average deposition to the collectors were app. twice the SD on the analysis of each filter The amount of tracer on each filter corresponds to approximately 2000 particles, i.e. the additional uncertainty is about 2.2%.

Surface	Mean [cps]	SD on mean [cps]	Av. SD on counts [cps]
West wall	4.71	0.95	0.45
West wall w2-w6	5.41	0.79	-
West wall w7-w12	4.13	0.64	-
Other walls	4.15	0.66	0.34
Floor	11.11	-	-
Ceiling	5.49	-	-

Deposition Velocities Measured to Individual Surfaces in the Ferslev Test House

After the preliminary experiments in BRE had shown that the developed particle technique was suitable for measuring deposition velocities to relatively small areas a regular sample program was introduced in the Ferslev test house. During the tests two collectors were attached to each surface in the room, i.e the floor, the four walls and the ceiling In total twelve collector paper samples were produced in each of the thirteen tests. As before the collectors were Whatman no 542 5.5 cm diameter filter papers. This filter paper is hard pressed and has a plane and not to rough surface and was regarded to have a surface roughness similar to (unpainted) wallpaper. The filter papers were attached with double-sided adhesive tape at marked points on the various surfaces. The filter papers were placed in position immediately before the particles were dispersed and placed in separate bags immediately following the end of the air sampling. The collectors were always handled with forceps in order to avoid the generation of extraneous gamma activity from the neutron activation process.. To limit the number of samples for the irradiation and the gamma counting the two filter papers from each surface were both placed in the same bag They were then irradiated and analyzed as a pair Typical counting times were 10 minutes to for a 6-8 % standard deviation

Table 5.2. Deposition velocities measured by 7 AA of filter papers attached to walls in the Ferslev test house. The floor and ceiling values are the average of measured for two collection surfaces. The wall deposition velocities are the average of 8 collection surfaces. The last coluomn of the Table shows the ratio between the decay constant found from the deposition velocities for the individual surfaces as per equation (3) and the actual observed decay rate of the tracer aerosol

Test no.	Size [μm]	v_d -floor [10^{-4}ms^{-1}]	v_d -walls [10^{-4}ms^{-1}]	v_d -ceiling [10^{-4}ms^{-1}]	$\lambda_{surface}/\lambda_{room}$ [ ]
1	2	2.16	1.04	1.12	1.38
2	3	10.14	3.99	13.71	7.39
3	5.5	17.95	2.56		
4	4	39.83	16.33	12.22	10.64
5	0.5	1.07	0.385	0.127	0.65
8	0.5	0.536	0.226	0.171	0.57
9	5.5	12.01	4.36	1.725	1.69
10	3	3.58	2.57	4.35	1.48
11	4	12.98	7.03	13.34	3.07
13	2	2.88	2.49	4.08	3.79

Table 5.2 shows the deposition velocities found for the the different surfaces in the thirteen tests in Ferslev. There were big variations from sample to sample for all particle sizes and surfaces. A similar pattern has been seen in the Risø and Imperial College test chambers when mixing fans were operated at medium to high speeds. An explanation in this case and maybe also in the experiments described here was that there were important local differences in the flow patterns. After this experiment it was, however, concluded that the collectors was not properly attached to the surfaces. The scotch tape used for attachment left a space of 1 to 3 mm between the filter paper and the surface and airborne particles may have reached the backside of the collectors by this route. Also, there may have been be deposition due to gravitation on upward-facing edges and to the backside of the ceiling collectors. For these reasons, major modifications were made for the next experimental campaign in Jersie.

The Results from Jersie

In the next test house, several improvements in the sampling technique were introduced. A 9 cm diameter Whatman 542 filter paper was fitted into a sheet of A-4 paper as shown in figure 5.2. This method prevented air flow behind the filter paper. To eliminate deposition caused by flow phenomena at the transition from A-4 paper to filter paper a circle was cut from the centre of each sample and packed for activation. Table 5.3 shows the deposition velocities for each of the ten sampling locations used in the Jersie test house during the seven tests

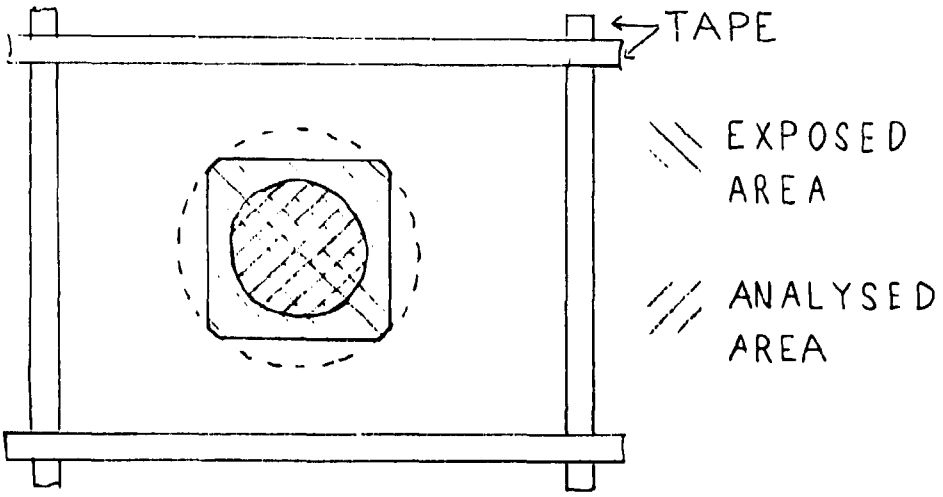

Figure 5.2. Sketch of a Whatman no. 542 9 cm diameter filter paper fitted into a sheet of paper attached to a indoor building surface. The dashed line shows the part of the collector that is covered by the paper. Only the centre circle of the filter paper was used for analysis. The A-4 paper that carried the collector was taped all around to the wall.

Table 5.3 Deposition velocities to surfaces in the Jersie test house. The last column shows the decay constant calculated from the deposition velocities measured to the individual surfaces divided with the actual deposition constant.

Test	Size [µm]	Ceiling 1 [10^{-4}ms^{-1}]	Ceiling 2 [10^{-4}ms^{-1}]	North 1 [10^{-4}ms^{-1}]	North 2 [10^{-4}ms^{-1}]	South 1 [10^{-4}ms^{-1}]	South 2 [10^{-4}ms^{-1}]	East [10^{-4}ms^{-1}]	West [10^{-4}ms^{-1}]	Floor 1 [10^{-4}ms^{-1}]	Floor 2 [10^{-4}ms^{-1}]	$\lambda_{surface}/\lambda_{room}$
2B	0.5	0.4981	0.3963	0.347	0.452	0.494	0.343	0.049	0.454	0.991	1.761	0.56
3B	0.5	0.1799	0.2730	0.559	0.344	0.216	0.238	0.322	0.286	0.936	0.737	0.54
5B	0.5	0.0339	0.1086	0.229	0.126	0.119	0.302	0.052	0.172	2.932	2.960	1.23
6B	0.5	0.0662	0.0665	0.172	0.1047	0.170	0.156	0.104	0.194	2.133	2.050	0.66
7B	0.5	0.0762	0.1026	0.175	0.1486	0.084	0.109	0.056	0.140	0.915	0.585	0.31
	Avg.	0.171	0.189	0.296	0.235	0.217	0.230	0.117	0.249	1.581	1.62	
	SD	0.190	0.141	0.163	0.154	0.154	0.098	0.117	0.127	0.914	0.981	
2A	2.0	9.093	11.14	4.860	10.99	26.85	28.18	6.111	8.510	14.18	32.7	4.3
3A	2.0	27.27	3.373	10.77	3.712	32.03	11.21	2.314	15.84	3.714	5.02	7.8
1	4.0	17.23	1.867	8.767	2.770	3.410	2.889	2.200	1.158	13.28	8.79	2.08
6A	4.0	26.61	3.692	47.85	6.067	30.44	7.937	2.708	32.92	44.81	8.65	6.28
4	5.5	2.735	1.147	1.096	3.057	2.002	1.632	2.077	1.254	5.115	10.9	2.14

Summary of Deposition Velocities Measured to Indoor Building Surfaces

In both the Risø aerosol test chamber and by Byrne(1994) it has been shown that the tracer technique described in Chapter 4 and 5 gives reproducible results when used for measuring deposition on surfaces. It has been used succesfully in two test houses. For the indium particles, the measured values were in good agreement with total deposition in the test rooms. However, for the silica particles, the high deposition velocities did not match-up with the total mass deposited. This was the case both in Ferslev and in Jersie where the sampling procedure had been improved. The conclusion here must be that the deposition to the whatman filter papers differed from that of the interior sufaces. Chamberlain, Garland and Wells(1984) found a similar differences between deposition to optically smoth surfaces and aerodynamically smoth filter paper for supra-micron particles in a series of wind tunnel experiments. Garland(1994) explained the increased deposition as particles being intercepted by small surface roughnesses. That is, even though the filter paper used as collectors had the same surface roughness as wallpaper, the different surface structure can and will cause a significant difference in the deposition of supra micron particles. In Table 5.4, average deposition velocities are shown for tests where there is an agreement between the surface deposition and the total deposition.

In deposition theory, it is often stated, see chapter 2, that deposition to the ceiling should be smaller than than deposition to the walls as the settling velocity should be subtracted from the deposition velocities for walls. In none of the tests was such a reduction in deposition to the ceiling was observed. For the indium particles (Table 5.4), a little reduction was seen in deposition to the ceiling, but for all the silica particles a similar or larger deposition was observed to the ceiling compared to the walls. Knutson et al.(1992) also found a slight increase in deposition to the ceiling when measuring the deposition of particles labelled with radon daughters. This can be explained by the fact that for larger particles the deposition to walls and ceilings occurs due stocastics processess such as inertial impaction and interception on surface roughnesses and the drag from gravity becomes of minor importance.

Table 5.4. Average deposition velocities to walls, floor and ceiling in the Jersie and Ferslev tests. Selected results. Number in parenthesis represents number samples used for the average.

Size [µm]	Floor [10^{-4} ms^{-1}]	Wall [10^{-4} ms^{-1}]	Ceiling [10^{-4} ms^{-1}]
0.5	1.5±0.8(14)	0.24±0.07(40)	0.16±0.02(14)
2	2.16±0.08(2)	1.04±0.41(8)	1.12±0.04(2)
5.5	11.3±5.2(4)	1.95±0.65(10)	1.94±0.79(2)

5.2 Skin Deposition

During the last three tests in the Ferslev test house, samples were taken for deposition measurements by wiping the skin of a human volunteer. The purpose of this was to see if wiping the skin would remove enough deposited material to give a good estimate of a lower value for a deposition velocity to skin. As wiping of the skin with a filter paper soaked in alcohol not can be expected to remove 100 % of the deposited tracer particles the obtained deposition velocities must be lower or conservative values

conservative values of skin deposition. The wipes were made on the upper side of the lower left arm of a test person wearing a T-shirt, i.e. the arm was not covered by clothes during the course of the test. The test person was doing light activities during the test; reading instruments and changing filter papers. The results showed surprisingly large values of deposited matter. For the 2 μm particles a deposition velocity of 1.8×10^{-3} ms^{-1} was found with a standard deviation of ±20 %. This observation showed that the experimental technique was sufficiently sensitive to yeild conservative values for deposition to skin and it is the approach which has been used in later experiments.

Measurements of Skin Deposition During the Tests in Jersie

For the deposition experiments to be made in the Jersie test house a protocol for making samples by skin wiping was discussed thoroughly. We decided to use a no. 542 filter paper 9 cm diameter Whatman for wiping and soaked it in ethanol. The filter paper was chosen to keep the background count rate as low as possible when the wipes were neutron activated. Ethanol was chosen as detergent as domestic research revealed this as the major ingredients in skin tonics for make up removal. Alcohol is also used by doctors and nurses when cleaning an area of the skin before injections, etc. The sampling procedure was as follows:

- Before the experiment an area of 40 cm^2 was marked on the lower left arm and the right cheek of the face. The areas were then washed and cleaned with a paper tissue soaked in ethanol.

- During the experiment, the test person performed light activities such as reading instruments and typing on a portable PC with a TFT-screen.

- After the experiment, the test person and an assistant went to an adjacent room, where the assistant put on clean gloves, soaked a filter paper in alcohol and cleaned a marked area thoroughly. This sample was placed in a sealed bag and the second area was cleaned with a new filter paper.

- To test the wiping efficiency a second wiping of the marked area of the arm was made after the first wipe in some tests.

The skin deposition velocities were calculated by the following formula:

$$v_{d,skin} = \frac{Mass\ deposited}{40\ cm^2\ \overline{C}_{water}\ Exposure\ time} \qquad (42)$$

Table 5.5. Deposition velocities to skin, hair and cloth found in the seven tests in Jersie. The number in parenthesis represents the number of samples that the average is based on. The deposition velocities to the arm and face were measured to the same test subject, CL, in all tests. The cloth was cotton pieces cut from a laboratory coat. The deposition velocity to hair was found from hair samples taken from the head of CL.

size, d_p [µm]	v_d -arm [$10^{-4}ms^{-1}$]	v_d -face [$10^{-4}ms^{-1}$]	v_d -cloth [$10^{-4}ms^{-1}$]	v_d -head [$10^{-4}ms^{-1}$]
0.5	2.07±0.67(5)	2.61±1.05(5)	2.63±0.77(6)	3.41±1.77(8)
2	16.70±3.67(2)	19.41±4.27(2)	24.2±5.2(2)	37.2±4.56(2)
4	16.22±4.14(2)	21.17±0.0(1)	39.8±13.8(4)	35.2±15.1(4)
5.5	39.45±0.0(1)	60.16±0.0(1)	78.1±35.6(2)	28.0±7.4(2)

Table 5.5 gives the average skin deposition obtained from the samples from the Jersie test house. The results showed a clear increase in deposition with increasing particle size, as would be expected due to the increased effect of gravitation, and deposition to the arm and face of the test person were similar for each particle size. In all tests the same test person, CL, was used. The variations in these data exceeded the standard deviation due to the gamma analysis by a factor of 4 to 6. When discussing the test procedures, several problems were identified. The outline drawn of the test area did not provide a satisfactory control of the sample areas. Especially it was difficult to keep within the outlined areas when performing a thorough scrubbing. Secondly, differences in wiping efficiency are believed to have caused variations, as different persons did the wiping after the tests. This was confirmed by the observation that on several of the wipes made to test the wiping efficiency carried just as much tracer as the first wipe of the area. Another source of error was the determination of the average concentration of tracer aerosol in the test room. The dispersion of the indium and dysprosium tracers were started some minutes before the air sampling made to determine the decay constant of the tracers. To better determine the total integrated room concentration a 'pre-filter' was made by air sampling during dispersion and included when calculating the deposition velocities to individual surfaces. Another question is whether the measurements of the room air concentrations were absolute. Here, especially the filter efficiency of the Whatman no. 542 filter papers used for air sampling was important. The filter efficiency was measured by passing the air-aerosol mixture through a series of filters and measuring the relative amounts of particulate collected by each filter. A filter efficiency of 97 % were found and in all calculations, a filter efficiency of 100 % has been assumed.

Measurement of Deposition to Skin in an Office

To improve the protocol for measuring skin deposition some changes were introduced and measurements made in an office at Risø. Metal templates were made to encircle a selected area of the arm after exposure. The frame had a rectangular opening of 8 cm^2. This enabled us to wipe a fixed area much more thoroughly.

To minimize the risk of contaminating the samples one person handled the equipment and dispersed the aerosol and an other person waited in a laboratory, two closed doors away from the test room, to do the sampling. When the aerosol had been dispersed the test persons entered the room and carried out the agreed activities for 20

minutes. A single air sample was made during the exposure period. After exactly 20 minutes the test persons left the office and went to the clean laboratory. Here, all the sampling was performed by the unexposed person. This procedure should ensure well defined exposure time and average air concentration.

During the office experiment the two test persons were typing on PCs, one, CL, in front of an EIZO colour screen with a normal static field and one, KGA, in front of a TFT screen with no electrical field. CL had sparse hair growth and KGA had rich hair growth on the arm. The facial hair of both test persons had been freshly shaven. Skin wipes were made from the lower right arm of KGA and both CLs arms. 2 micron particles labelled with Dysprosium and 0.5 micror particles labelled with Indium were used in the test. The results, as seen in Table 5.6, were consistent for all samples The samples from faces and CLs arm had approximately the same deposition velocity and the hairy arm of KGA had the largest deposition for both particles sizes. No significant changes in deposition pattern can be seen due to the different PC-screens in front of the test persons.

Table 5.6 Skin deposition velocities for 2 and 0.5 micron particles from experiment in an office Exposure time was 20 minutes.

Description of sample	Amount [µg m^{-2}]	Air C. [µgm^{-3}]	v_d 2 µm [10^{-4}ms^{-1}]	Amount [µgm^{-2}]	Air C. [µgm^{-3}]	v_d 0.5 µm [10^{-4}ms^{-1}]
KGAs face	1.74	0.22	66.1	2.31	3.26	5.92
KGAs arm	2.15	0.22	81.6	5.26	3.26	13.47
CLs face	0.88	0.22	33.3	2.83	3.26	7.25
CLs right arm	1.67	0.22	63.4	2.92	3.26	7.48
CLs left arm	1.68	0.22	63.6	3.47	3.26	8.89

During the test the air movement and turbulence intensity was measured with three anemometers from Dantec A/S. The air speed at the three measuring points ranged from 0.1 to 0.25 m/s and the turbulence intensity ranged from 45 % to 20 %, with the highest intensities for the slowest air movement.

Discussion

The values found in the office test are 3 to 4 times larger than the values found in the Jersie test house. The improved experimental protocol combined with the consistency of results make the later values more reliable.

Recently Gudmundsson et al.(1992) have presented measurements of deposition velocities to the eye and forehand of a human mannequin for particles with an aerodynamic diameter from 2.7 to 28.7 µm. These measurements have been used in the formulation of semi-empirical model by Schneider et al.(1994). For the 2.7 µm particles and a turbulence intensity of 20 % a deposition velocity of 1.4 x10^{-3} ms^{-1} was found. This is approximately 1/4 (it is 1/2 of the v_d found to CLs face) of what the average v_d found in the office test for the 2.5 µm particles. Several aspects may be responsible for the difference between the obtained values.

- The particles used were different and though they were sized with the same instrument both shape and density differs.

- The sample surfaces have a different surface roughness. The mannequin is smooth and has no hair growth at all.

- The mannequin is not heated. A study by Bell(1994) at Imperial College found the deposition velocity to a unheated metal cylinder to be 17 % to that of the deposition velocity to an arm. For the same flow conditions the deposition velocity was 4.4 times larger to a heated cylinder or 74 % of what he found to an arm.

5.3 Deposition to Hair

Another surface considered is the hair. During the Jersie tests samples of hair were made. For these samples the amount of tracer per gram of hair was determined. The problem was now to convert these numbers into deposition velocities. A proposal was that if the deposition occurred mainly on the outer layers of hair the total deposition to a head could be determined by collecting the hair after a major hair cut. To look at the deposition pattern some hair samples were cut at bottom of the head. They were then divided into 3 - 6 samples of app. 1.5 cm's length. Figure 5.3 shows a typical situation with little deposition close to the head and more than 50 % deposition in the outer fifth of the hair. The weight of the first hair cut was used to estimate the total deposition to the head. The area of the head covered with hair was determined by fitting a piece of paper to the head of the test person. Equation 43 shows the formula used to calculate the deposition velocities for the Jersie samples shown in the last coloumn of Table 5.5:

$$v_{d,head} = \frac{[ng\ of\ tracer]\ x\ [Total\ mass\ of\ outer\ hair]}{[weight\ of\ hair\ sample]\ x\ [Area\ of\ head]\ x\ T_{exposure}} \qquad (43)$$

The total mass of the outer hair was 5.75 g and the hair covered area of the head was estimated to be 0.09 m^2. Each of the hair samples used in this calculation was taken from the outer 1.5 cm hair layer. Due to the uncertainties on the average deposition profile the head and the many rough estimates a uncertainty of a factor of two must be assume for the numbers presented. Also, the test person in these tests had short very smooth hair and significant differences must be expected in the deposition pattern to persons with curly hair or long hair.

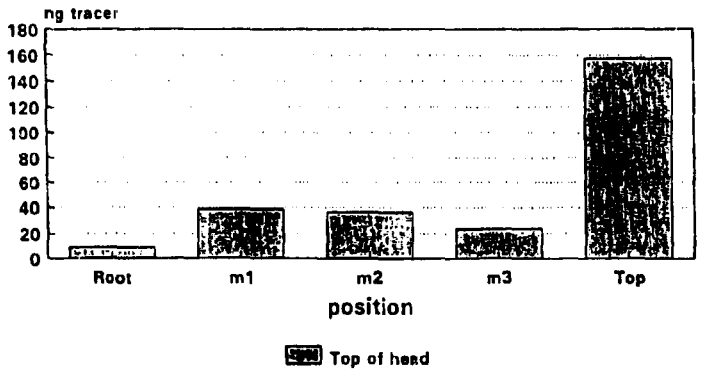

Figure 5.3. Profile of deposition to hair. Each sample is app. 1.5 cm long.

Table 5.7. Deposition velocities measured to hair. The deposition velocity to hair is given per surface of a single hair. Hair diameter 50 μm and density is 1.5 gcm^{-3}. 5.75 g = 0.0244 m^2 The deposition velocity to the head is found by dividing the 'v_d' with the area of the test persons head: app. 0.09 m^2.

Size	Amount of tracer [n/g]	Total weight of hair [g]	Total Deposited [n]	Air conc. [μgm^{-3}]	v_d to the head [10^{-4}ms^{-1}]	v_d-hair [ms^{-1}]
0.5	214	5.75	1200	3.26	34.1	0.0126
2.0	3.49	5.75	20	0.22	8.44	0.0031

To collect material for major haircut a volunteer test person let his hair grow for two months after the Jersie tests. After the test in the office the test person had a complete hair cut to measure the total deposition to the head. The hair was cut twice and approximately one third of the hair was removed each time. Each of the two samples were weighed. Then each sample was cut into small pieces and mixed in a bag. Three samples for activation were taken from each bag of hair. The results are shown in Table 5.7.

5.4 Deposition to Clothes

During the tests in Jersie an effort was made to measure the deposition of particles to clothes. 150 cm^2 pieces of cotton fabric was attached to the upper and lower sleeve of the right arm of the test person during six of the tests. 6-8 cm^2 pieces were cut from the centre of each sample and analyzed by neutron activation. The deposition velocities was found as by equation (42). Standard deviation for the gamma counting was 8-10 % and the standard deviation on the average deposition velocity for each particle size are 20 to 30 %. The average deposition velocity was a little higher to the lower sample but the difference was much less than the standard deviation on the averages and thus not significant. So the average deposition velocity for all samples at both locations are the figure which are presented in the second last coloumn of Table 5.5.

6 Modelling of the Protective Value of Houses

The litterature (reviewed in Chapter 2) failed to reveal a model or code suitable for describing or predicting the deposition rates of supra-micron particles to indoor surfaces. In an effort to improve the situation in support of predictive modelling of accident scenaries, a number of experiments were carried out to obtain deposition rates for specific particle sizes and they were described in Chapter 4 Since all the important transport processes for particles (diffusion, settling and inertial impaction) depend on the particle diameter the relationship between deposition velocity and particle size has been examined by fitting linear and power functions to the measured data.

The empirical expressions derived for indoor deposition velocities have then been used in a simple model in order to predict dose reduction factors. The knowledge obtained through the measurement of size distribution for different isotopes after the Chernobyl accident was used to predict isotope-specific protection factors

6.1 Empirical Models for Indoor Deposition

Loss-rates of airborne particles were measured in four different houses and the results presented in chapter 4. A special effort has been made to determeine the effect of furniture in the test rooms. An attempt was made in the BRE test house to examine the effect of increasing the turbulence by running large fans during some tests, but the results from these tests showed a lower than expected tracer concentration in the test room and had slower decay than the tests without fans. It was concluded after these tests that the fan speeds used had been too high and that after a fast initial deposition resuspension caused the slowly declining low level tracer concentration in the room. In the next experiments smaller mixing fans were used at lower fan speeds and good data was collected on the air motion and turbulence in the Ferslev and Jersie test house, but the amount of data is insufficient to enable an analysis of the relationship between turbulence intensity, particle size and deposition velocity. Single cases in the two tests houses indicated an increased deposition when the turbulence level was increased.

Two data sets were selected were the correlation coefficients were better than 0.95 for the tracer aerosol decay curves. Twelve results from unfurnished houses and fifteen results from furnished houses were chosen. Experiments where small mixing fans were operated during the test have been included in these data sets. A power regression and a linear regression have been made for the two data sets, expressing the deposition velocity as a function of the particle size. Average deposition velocity was chosen rather than the deposition constant in order to take the different surface to volume ratios of the test rooms into account. Equations (44) and (45) shows the linear regression and the power regression expressions found for the unfurnished rooms. The correlation coefficients are given in the parentheses:

$$V_d = 0.54 d_p + 0.40 \quad (r = 0.90) \tag{44}$$

$$V_d = 0.946 (d_p)^{0.71} \quad (r = 0.96) \tag{45}$$

and equation (46) and (47) shows the results for the furnished rooms:

$$V_d = 0.64 d_p + 0.53 \quad (r = 0.95) \tag{46}$$

$$V_d = 1.23 (d_p)^{0.65} \quad (r = 0.96) \tag{47}$$

where v_d is the average deposition velocity to all surfaces and d_p is the particle diameter. In both the unfurnished and the furnished rooms the power regression had the best correlation coefficient, i.e. 0.96 compared to 0.90 and 0.95. The deposition velocity was found to increase with the 0.71 and the 0.65 power of d_p. This clearly is not in line with the theoretical predictions of Nazaroff and Cass(1989) that for particles larger than 1 µm the deposition velocity should increase according to the square of the diameter of a particle. Also the deposition velocities found were much greater than those predicted by the theories presented by Nazaroff and Cass. However, the findings are in good agreement with the experimental results by Schneider et al.(1994) and Sehmel(1973). They found that the deposition velocity increased linearly

with the particle size in the particle size range investigated. Since the formulae presented in equations (44) to (47) are purely empirical, it must be emphasized that they are not valid outside the particle size range investigated, i.e. 0.5 to 5.5 μm.

The regression lines are shown together with the data points in Figures 6.1 and 6.2. It can be seen that the data obtained in the four different houses are in good agreement. The fact that the gradient of the line declines as the particle size increasesis in line with a hypothesis that inertial turbulent mixing is the process responsible for the larger than expected deposition. Such an effect would decrease with increase in particle size, where the increased inertia makes the particles less susceptible to turbulent eddies and more likely to have a steady downwrd motion resulting in a high deposition to the floor.

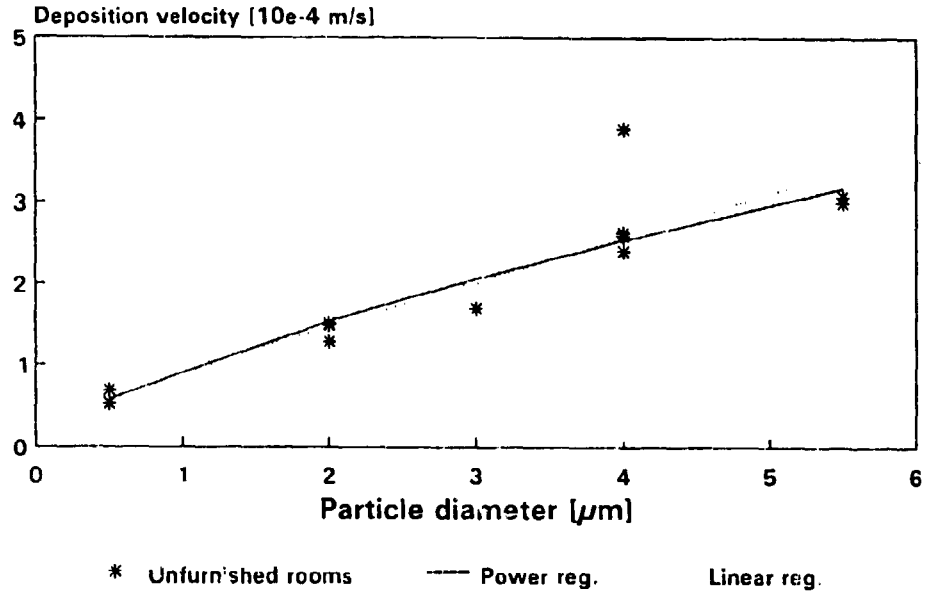

Figure 6.1. Linear and power regression line of the deposition velocity data from the four unfurnished test rooms. Only the twelve data points with correlation coefficients better than 0.95 for the decay constant are included in the regression The regression formulae are shown in equations (44) and (45)

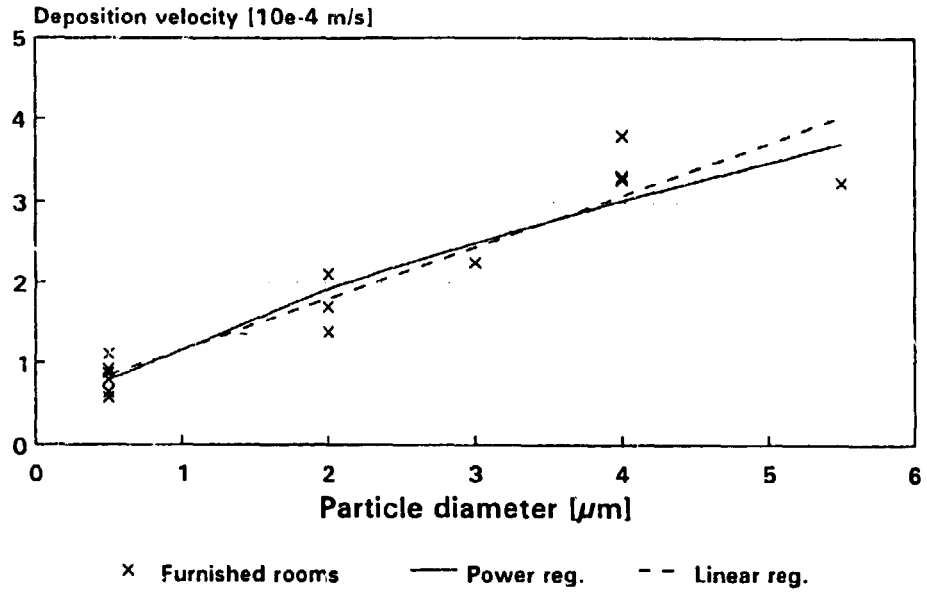

Figure 6.2. Linear and power regression line of the deposition velocity data from the four furnished test rooms. Only the fifteen data points with correlation coefficients better than 0.95 for the decay constant are included in the regression. The regression formulae are shown in equations (46) and (47).

6.2 A Simple Model for the Protective Value of a House

Engelmann(1992) made an important point when he noted that estimates of the protection offered by buildings in case accidents involving releases to the atmosphere should be realistic and not conservative if an optimum emergency response is to be achieved. When the civil defense authorities need to decide between evacuation or sheltering they need to have a realistic picture of the consequences in order to make the correct decision. Present models of the effect of sheltering during releases of radioactive materials to the atmosphere consist of a single factor giving a common dose reduction factor, *DRF*, for all nuclides. A value of 0.5 is currently used in probabilistic accident consequence assessment codes, Brown(1989) (except noble gases for which *DRF* = 1.0, i.e. no reduction in inhalation due to indoor residence). In order provide a more realistic model that takes into account properties of the released material the empirical formula for indoor deposition is used together with equation (8) to calculate dose reduction factors, *DRF*s. equation (48) shows the derived formula:

$$DRF = \frac{\lambda_r(U_{wind}\Delta T)}{S/V \cdot 1.23(d_p)^{1.65} + \lambda_r(U_{wind}\Delta T)} \qquad (48)$$

where the deposition constant, λ_d, is found by multiplying the average deposition velocity with an average *S/V* ratio for the buildings in question. In the review by Engelmann(1992) surface to volume ratios were summarized for a number of different buildings: 1.74 m^{-1} for apartment buildings/houses, 1.3 m^{-1} for office buildings and 0.66 m^{-1} for industrial buildings. These values do not include contributions from furniture and eqiupment in the room. The S/V ratios of the test rooms used indoor deposition measurements were also determined without including furniture and were presented in Table 4.8. The average S/V of the test rooms was 1.69 m^{-1} and a value of

1.7 m^{-1} has been used in the model calculations shown in Figure 6.3.

The air-exchange rate can be expressed as a function of the weather conditions, outdoor temperature and wind speed. The temperature difference over the building envelop can be expressed as the difference between the outdoor temperature and the indoor temperature, typically about 21 °C. The air-exchange rate was determined as a function of these parameters for a typical Danish houses by Kvisgaard et al.(1984). Engelmann(1992) quoted several references and used an equation similar to equation (12) for calculation of air-exchange rates for houses in the USA from data on wind speeds and temperature difference.

In Figure 6.3 the *DRF* is plotted as a function of particle size for three different values of the air-exchange rate. An assumed surface to volume ratio of 1.7 m^{-1} was used in these calculations. It can be seen that the *DRF* decreases significantly with particle size. The three values for the air-exchange rate used (0.25, 0.5 and 1.0 h^{-1}) represents a low, medium and high value and the DRF varies between 0.1 and 0.7 or factor of seven depending on the particle size for these air-exchange rates. These relatively large variations in DRF clearly justifies a more detailed model for the DRF.

In 1986 the reactor unit no. 4 at the Chernobyl nuclear power plant blew up and the biggest release to the atmosphere of radioactive material from a nuclear power plant occured. As discussed in Chapter 1 detailed information was obtained on the size distribution of the released nuclides. Partly to investigate what isotope specific DRFs that could be assumed for the release products and partly to suggest DRFs that might apply in future situations. With the equation derived here for the protective effect of houses and the protection factors were calculated for the three main groups of Chernobyl aerosol for a house with λ_v =0.5 h^{-1}:

- Particulate iodine: The AMAD of particulate iodine was about d_p= 0.5 µm (e.g. Tschiersch and Georgi(1987)) and from this a *DRF* of 0.5 is obtained

- The volatile group: Cs-137 had an aerodynamic diameter of d_p = 1.0 can be assumed (e.g. Jost et al.(1986)), and that leads to a DRF of 0.4.

- The refractory: For this group that includes the fuel fragments an AMAD of 4 µm can be assumed (e.g. Rulik et al.(1989)) leading to a DRF of 0.2.

Current accident models assume a uniform *DRF* of 0.5 for indoor residence. The results presented here suggest that an isotope-specific *DRF* would be justified with lower *DRF*'s for the refractory group. Particle size measurements closer to the accident site plant would probably have recorded an even larger AMAD for this group and subsequently a even better *DRF*. The variation in the *DRF* depends on the size the activity size distribution of the isotope, and that is dependent on the properties of the corresponding chemical element

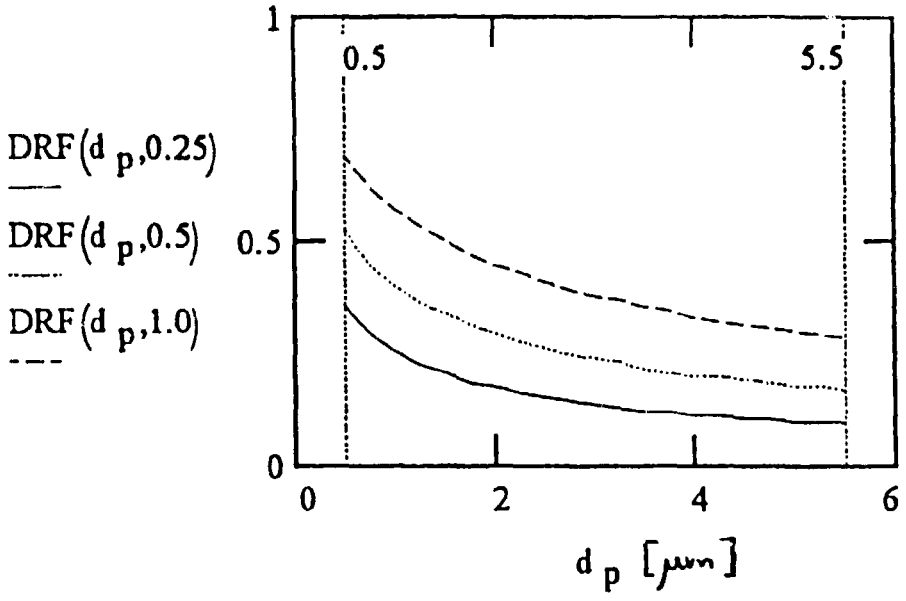

Figure 6.3. DRF's as function of particle size and air-exchange rate. The number after 'd_p' in the left margin of the figure is the air-exchange rate for that line style. A surface to volume ratio of 1.7 m^{-1} have been used corresponding to a medium sized living room. The vertical lines indicate the valid particle size range, i.e. 0.5 to 5.5 μm.

Ventilation of Buildings After the Passage of a Cloud

Several authors (as discussed in chapter 1) believed that increased ventilation after passage of a cloud of radioactive particles is an important part of the potential *DRF*. To examine this view, equation (5) has been solved numerically for a non-rectangular cloud passage. As the effect of ventilation will be greatest for particles with a lower deposition velocity (they remain airborne longer) a deposition constant of λ_d = 0.4 (corresponding to the minimum deposition velocity observed for a 0.5 μm particle, app. 0.6×10^{-5} ms^{-1}) was assumed in the calculations. The cloud passage has been described by a stepwise linear function (the dotted line in Figures 6.4 a & b). For 100 minutes the outdoor concentration was assumed to increase linearly to a pollutant concentration of 100 in arbitrary units, it then stayed constant for 100 minutes and then it declined linearly for 100 minutes. A solution has been found for two values of λ_r: 0.4 h^{-1} corresponding to the average for Danish houses and 0.8 h^{-1}, which is a suitable value for a British houses. The equilibrium ratio between indoor and outdoor concentration is shown by the broken line and the indoor concentration is shown by the solid line in Figures 6.4 a & b.

By comparing the indoor and outdoor concentrations shown in figure 6.4 it can be seen that there will be a significant time delay from the start of the decline of the outdoor concentration until the indoor concentration is actually higher than the outdoor concentration. The exact time for this will under all circumstances be impossible to detect in case of an accident as it will differ from house to house. From a practical point of view the earliest time for advising the public to open doors and windows must be when the outdoor concentration approaches zero. If it is assumed that the persons under shelter breathe clean air from this moment a reduction in inhalation dose of 19 % will be achieved. This value is for nearly optimal conditions: a slowly depositing particle in a reasonably well sealed house and for a cloud passage of short

duration (Figure 6.4 a). If the air-exchange rate is increased to 0.8 h^{-1} (Figure 6.4 b) a reduction of only 10 % will be obtained. In all these calculations it has been assumed that the indoor pollutant concentration could be reduced imeadiately by opening door and windws but even in this case the air exchange might be rather slow especially in weather with little or no wind and the acheived reduction will be lower For cloud passages of longer duration, for larger particles with a higher deposition velocity and for more leaky houses the reduction due to ventilation after the cloud passage becomes neglicible.

Such uncertain possibilities for dose reduction do not justify the incorporation of ventilation after cloud passage as a inherent part of the Dose Reduction Factor, but of course the civil defense authorities should keep the positive effect in mind in case of an accident and encourage ventilation after a toxic release has passed an inhabited area, especially if the release involves slow deposition gases.

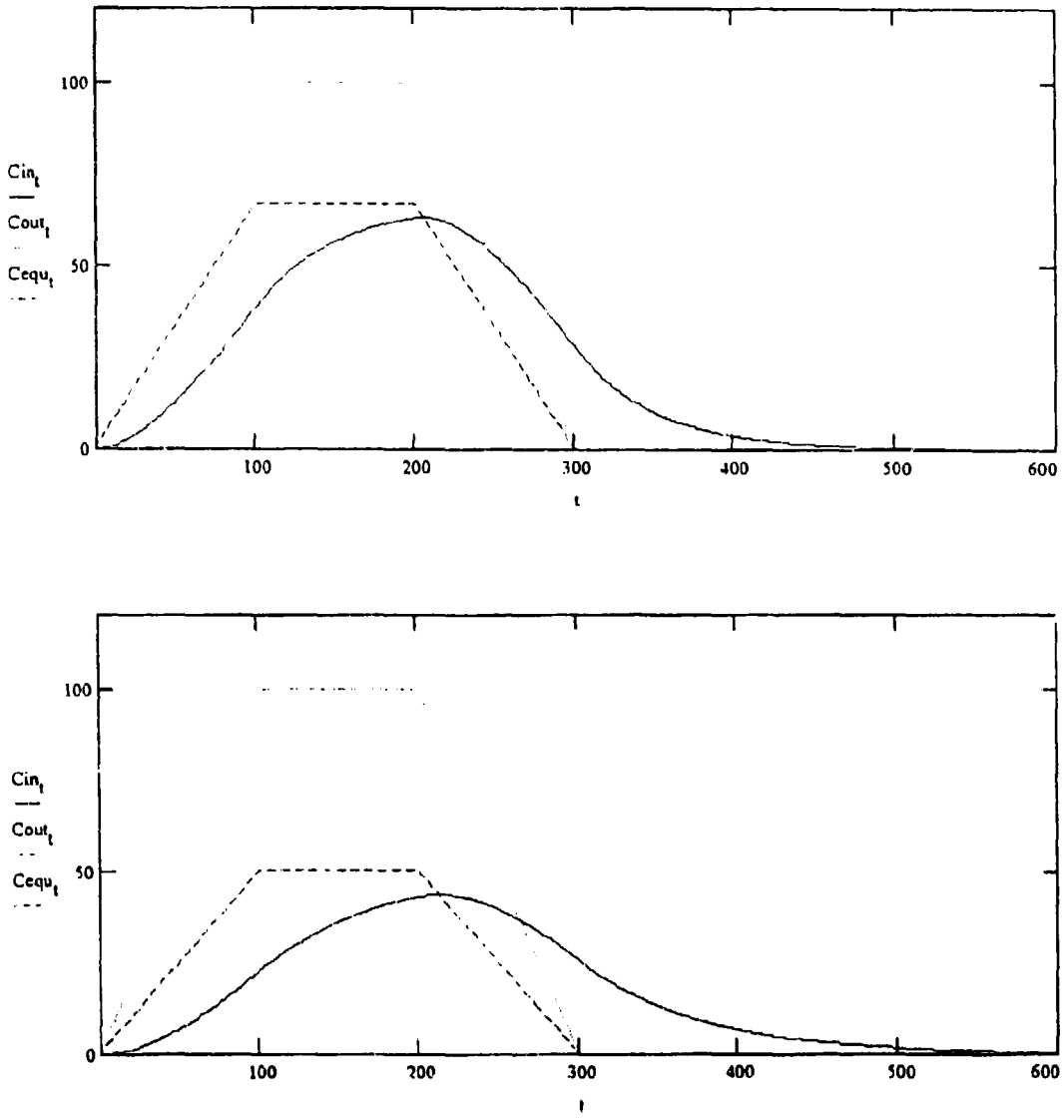

Figure 6.4 a & b. Non-rectangular cloud passage and equilibrium ratio for λ_r = 0.4 h^{-1} (a) top figure, and λ_r = 0.8 h^{-1} (b) bottom Figure

6.3 Comparison of Results

In Table 6.1 the experimental results obtained from the Be-7 experiments and from the indoor deposition measurements using artificial tracers are compared with the theoretical results obtained by Nazaroff & Cass(1989) and the wind tunnel results of Sehmel(1973). In general the theoretical predictions Nazaroff & Cass are similar to the deposition velocities measured in the unoccupied houses with Be-7 as a tracer and a natural air exchange. The deposition velocities measured with artificial tracers were about 4 times larger than these values in the size range from 0.5 to 2.8 μm. This increase in deposition velocity must be attributed to the presence of scientist, pumps and other equipment in the test room created an increased air motion and additional surface for deposition. When a forced air-exchange is applied the deposition velocities increased both in Vellerup and Ferslev and again it must be attributed to the increased air motion.

Table 6.1. Review of experimental results and theoretic values of average indoor deposition velocities. The second and third column gives the values obtained by the I/O impactor experiment in Ferslev. The column termed silica particles have been obtained by using the empirical formula given by equation (47). The 'Nazaroff & Cass' and 'Sehmel' column was obtained by reading the figures in the respective papers. The last column gives the sedimentation velocity calculated from equation (20).

Size [μm]	Be-7 Natural air-ex. [10^{-4}ms^{-1}]	Be-7 Forced air-ex. [10^{-4}ms^{-1}]	Silica particles [10^{-4}ms^{-1}]	Nazaroff & Cass [10^{-4}ms^{-1}]	Sehmel [10^{-4}ms^{-1}]	v_s [10^{-4}ms^{-1}]
0.35	0.19	0.17	-	0.04-0.07	0.08-0.25	0.05
0.71	0.17	1.33	0.98	0.06-0.09	0.3-0.4	0.19
1.4	0.13	2.66	1.53	0.2	1.0-1.5	0.66
2.8	0.67	3.88	2.40	0.6	3-10	2.48
5.5	-	-	3.03	2.2	15-100	9.29

7 Summary and Conclusions

State of Art

In order to determine the protective effect offered by houses in case of radioactive or toxic releases to the atmosphere, a the literature rewiev was carried out and the key parameters identified. It was found that most authors agreed on an expression like equation (8) to describe the potential dose reduction factor, *DRF*. Indoor deposition is an important part of this equation, but very little was known about this subject. As a result, little explanation or modelling has been possible for the numerous references dealing with I/O ratios of pollutants. A primary objective in the project reported here

was to measure indoor deposition for particles of different sizes in order to enable the construction of models for predicting potential DRFs in emergency situations

Modelling of Indoor Deposition

Through a review of papers modelling deposition inside vessels it was concluded that only the paper by Nazaroff and Cass(1989) provided formulae that could be used for prediction of deposition velocities from directly measurable physical parameters. Unfortunately, the model was not valid to the for larger particles of interest in this study. Nazaroff and Cass predicted that the deposition velocities to walls and ceilings would approach zero as the particle size increased, whereas the measurements of deposition velocities to walls and ceilings presented in chapter 5 clearly showed an increase in deposition to these surface for particles above 1 μm. The results of the study reported here were in line with the experimental results obtained by Byrne(1994), Sehmel(1973) and others.

Indoor/Outdoor Measurements Using Atmospheric Be-7 Labelled Particles as a Tracer

The size distribution of particles carrying Be-7 in the atmosphere has been measured and found to vary between 0.7 and 1.0 μm It was observed that the activity distribution of Be-7 followed that of the mass distribution in the atmosphere. Reineking et al.(1987) came to the same conclusion.

Using natural aerosol particles carrying Be-7 as a marker, it was shown that there were no significant loss of particulate during the ingression of air into the test house. No such filtration has been found and no filtration has been assumed in modelling the protective value of a house, though some uncertainty still exists, especially for larger particles.

Two impactors were used to determine simultaneously the size specific I/O ratio of Be-7 labelled particles. The deposition velocities derived from these measurements, assuming no filtration, agreed well with the deposition velocities measured with artificial tracers. This supports the view that filtration by the building envelop is of little or no importance for the particle size range studied: 0.35 to 2.8 μm.

Indoor Deposition Measurements

Indoor deposition rates have been measured in four different houses with 5 different monodisperse aerosol tracers in the size range 0.5 μm to 5.5 μm. The results were divided by the surface to volume ratio of the test rooms in order to obtain comparable results. Results from the four test houses are in good agreement both for unfurnished and furnished rooms. Linear and power regressions for the two cases all had correlation coefficients better than 0.9. The deposition velocities were found to increase linearly or with the 0.7 power of the particle diameter, but not with the square of the particle diameter.

In general, deposition velocities were 3 to 4 times greater than what has been predicted by the models presented by Nazaroff and Cass(1989). This can be explained by the higher deposition velocities to vertical surfaces found by the passive sampling method described in Chapter 5. Low values of deposition velocity were found in the unoccupied test house in Ferslev where impactors were used to determine the size-specific I/O ratio determination of Be-7 labelled particles. When the air movements in the Ferslev test house were elevated due to increased air exchange or central heating,

the deposition velocities for different size classes of Be-7 labelled particles were found to be in good agreement with those found with the artificial tracers.

Skin Deposition

As a spin-off of the particle tracer technique developed, skin deposition velocities were measured for five particle sizes. The deposition velocities found were larger than expected (up to 7×10^{-4} ms^{-1} for 0.5 μm particles and 6×10^{-3} ms^{-1} for 2 μm particles). These results means that up to 10 times as much toxic material is deposited on the skin as is inhaled. For radionuclides emitting β-particles or for toxics that can be absorbed through the skin this means that the largest contribution to dose could come from deposits on the skin. This observation clearly has implications in occupational health.

Modelling the Protective Effect of Houses

The study of the effect of ventilation following thassage of a cloud of radioactive material showed that this effect was of minor importance when non-rectangular cloud passages were considered, even for optimal conditions, compared to the uncertainties due to variation of air-exchange rates and deposition constants. It is concluded that ventilation after cloud passage should not be included in the calculation of the *DRF*s, but should be kept in mind as a possible means of further dose reduction after a cloud has passad.

After the Chernobyl accident measurements of size distributions of atmospheric particles a distinct pattern was found for three classes of radio-nuclides. As the activity size distributions for the diferent isotopes depended on the chemical properties of corresponding element it can be assumed that the activity distribution of a future radioactive release to the atmosphere will resemble that of the Chernobyl aerosol. Using the size information obtained from the measurements of the Chernobyl aerosol and the empirical expression for the indoor deposition derived in chapter 6 it is concluded that different dose reduction factors can be obtained for different classes of radio-nuclides. For the standard of buildings prevailing in the northern part of Europe typical values would be 0.5 for particulate iodine, 0.4 for volatile elements, e.g. Cs-137, and 0.2 for refractory elements, e.g. strontium, plutonium. These values depend on the air-exchange rate, which in turn will depend on the weather conditions and the tightness of the buildings considered.

Acknowledgements

I want to thank Professor Uffe Korsbech for recommending me for a PhD position at Risø and for taking on the administrative burden of being my university tutor.

Senior scientist Jørn Roed has been my tutor at Risø National Laboratory and I owe him much, for his interest in and support throughout the project. He has made my PhD study at Risø a fruitful and enjoyable experience and it has always been a pleasure to discuss science with him.

Dr. John Garland was acting as the external examinor at the PhD lecture. He made a tremendous effort in making corrections and suggestions for improvements. I must express my gratitude for the many valuable contributions.

Chief of Laboratory Henrik Prip has offered his vast knowledge on instrumentation and experimental science from my first day at Risø and has been a good friend together with Dr. Kasper G. Andersson and Sven Olsen. I must thank them together with the rest of the ecology section for their support of my work.

Dr. Miriam Byrne has been a pleasant partner through two series of experiments and a vivid participant in discussion of results through e-mail.

I would like to thank Dr. Carl Gogolak for organizing my stay at the Environmental Measurements Laboratory, EML, in New York and for giving me a really nice welcome.

Dr. Earl Knutson was an inspiring tutor during my stay at EML and it was great fun to speak/listen to Norwegian while away from Denmark.

I want to thank Kim Pilegaard and Poul Hummelshøj for letting us borrow equipment (especially the Berner impactor) and use their RIMI field station.

A special thank to Ulf Jacobsen for his help and patience with the many neutron activations he handled.

References

Aarkrog, A.; Bøtter-Jensen, L.; Chen Qing Jiang; Dahlgaard, H.; Hansen, H.; Holm, E.; Lauridsen, B.; Nielsen, S.P.; Strandberg, M. and J. Søgaard-Hansen. Environmental Radioactivity in Denmark in 1990 and 1991. Risø-Report-621-(EN), 1992.

Alzona, J.; Cohen, B.L.; Rudolph, H.; Jow, H.N. and J.O. Frohliger, Indoor-outdoor relationships for airborne particulate matter of outdoor origin, Atmospheric Environment, Vol. 13, pp. 55-60, 1979.

Andersen, Ib. Relationship between outdoor and indoor air pollution, Atmospheric Environment, Vol. 6, pp. 275-278, 1972.

Bell, K.F., Investigation of the effect of heating and air movement on the deposition velocity of aerosol to body surfaces. M.Sc. dissertation, Imperial College, 1994.

Biersteker, K.; Graaf, H. de and C.A.G. Nass, Indoor air pollution in Rotterdam homes, International Journal of Air and Water Pollution, Vol. 9, pp. 343-350, 1965.

Berner, A. and C.J. Lürzer, Mass Size Distributions of Traffic Aerosols at Vienna, Journal of Physical Chemistry, Vol. 84, pp. 2079-2083, 1980.

Bondietti, E.A. and C. Papastefanou. Aerodynamic size associations of natural radioactivity with atmospheric aerosols. AEROSOLS: Formation and Reactivity, 2nd Int. Aerosol Conf. Berlin, 1986.

Brenk, H.D. & H. De Witt, Indoor Inhalation Exposure after Nuclear Accidents. Report from Brenk Systemplanung, 1987.

Brown, J., Sheltering in the event of an accident. Atom Vol. 389, pp. 17-19, 1989.

Byrne, M. An experimental study of the deposition of aerosol on indoor surfaces, Ph.D. dissertation, Imperial College, London, 1994.

Chamberlain, A.C. Radioactive Aerosols, Cambridge University Press, 1991.

Chamberlain, A.C.; Garland, J.A. and A.C. Wells, Transport of Gases and Particles to Surfaces with widely Spaced Roughness Elements, Boundary-Layer Meteorology, Vol. 29, pp. 343-360, 1984.

Christensen, G.C. and R. Mustonen, The Filtering Effect of Buildings on Airborne Particulate Matter. Report from Institute of Energy Technology in Norway, IFE/KR/E-87/002, 1987.

Coblentz, C.W, and P.R. Achenbach, Field Measurements of Air Infiltration in Ten Electrically-Heated Houses, ASHRAE, No. 1845, 1963.

Cohen, A.F. and B.L. Cohen, Infiltration of particulate Matter into Buildings, SAND79-2079, NUREG/CR-1151, 1979.

Collet, P.F., Boligers luftskifte, Teknologisk Institut, 1976. In Danish.

Colome, S.D. and J.D. Spengler, Instrumental Neutron Activation Analysis of Indoor/Outdoor Respirable Aerosols, 72nd Annual Meeting of the Air Pollution Control Association, Cincinnati, Ohio, 1979.

Cooper, D.W. and P.C. Reist, Neutralizing Charged Aerosols with Radioactive Sources, Journal of Colloid and Interface Science, Vol. 45, No. 1, pp. 17-26, 1973.

Corner, J. and E.D. Pendlebury, The Coagulation and Deposition of a Stirred Aerosol, Proceedings of the Physical Socie ',Vol. B64, pp. 645-654, 1951.

Crump, J.G.; Flagan, R.C. and J.H. Seinfeld, Particle Wall Loss Rates in Vessels, Aerosol Science and Technology, Vol. 2, pp. 303-309, 1983.

Crump, J.G. and J.H. Seinfeld, Turbulent Deposition and Gravitational Sedimentation of an Aerosol in a Vessel of Arbitrary Shape, Journal of Aerosol Science, Vol. 12, pp. 405-415, 1981.

Davies, C.N. Definitive Equations for the Fluid Resistance of Spheres, Proceedings of the Physical Society, Vol. 57, pp. 259-270, 1945.

Davies, C.N. in Aerosol Science, C.N. Davies, Ed., Academic Press, New York, 1966.

Dibb, J.E. and J. Jaffrezo, Beryllium-7 and Lead-210 in Aerosol and Snow in the Dye 3 Gas, Aerosol and Snow sampling program, Atmospheric Environment, Vol. 27A, No. 17/18, pp. 2751-2760, 1993.

Dingle, A.N. and E.W. Hewson, An Experimental Study of Ragweed Pollen Penetration, Journal of the Air Pollution Control Association, Vol. 8, pp. 16-22, 1958.

Dockery, D.W. & J.D. Spengler. Indoor-Outdoor relationships of respirable sulphates and particles. Atmospheric Environment, Vol. 15, pp. 335-343, 1980.

Ede, A.J. Advances in free convection, Advances in heat transfer, Vol. 4, pp. 1-64, 1967.

Engelmann, R.J. Sheltering effectiveness against plutonium provided by buildings. Atmospheric Environment, Vol. 26A, No. 11, pp. 2037-2044.

Engelmann, R.J.; Pendergrass, W.R.; White, J.R. and M.E. Hall, The effectiveness of stationary automobiles as shelters in accidental releases of toxic materials. Atmospheric Environment, Vol. 26A, No. 17, pp. 3117-3125, 1992.

Gadgil, A.J.; Kong, D. and W.W. Nazaroff, Deposition of Unattached Radon Progeny from Enclosure Flows, Radiation Protection Dosimetry, Vol. 45, No. 1/4, pp. 337-341, 1992.

Garland, J. Personal communication, AEA Technology, United Kingdom, 1994.

Giess, P.; Goddard, A.J.H.; Shaw, G. and D. Allen, Resuspension of Monodisperse Particles from Short Grass Swards: A Wind Tunnel Study, Journal of Aerosol Science, Vol. 25, No. 5, pp. 843-857, 1994.

Gudmundsson, A.; Schneider, T.; Petersen, O.H.; Vinzents, P.S.; Bohgard, M. and K.R. Akselsson, Determination of Particle Deposition Velocity onto the Human Eye, Journal of Aerosol Science, Vol. 23 S1, pp S563-S566, 1992.

Harrison, R.M., Some important air pollutants and their chemical analysis. In Harrison, R.M. (Ed.) Pollution. causes, effects and control: Royal society of chemistry, Cambridge, 1990.

Hillamo, R.E. and E.I. Kauppinen, On the Performance of the Berner Low Pressure Impactor, Aerosol Science and Technology, Vol. 14, pp. 33-47, 1991.

Halpern, M., Indoor/Outdoor Air Pollution Exposure Continuity Relationships, Journal of the Air Pollution Control Association, Vol 28, No. 7, pp. 689-691, 1978.

Holub, R.F.; Raes, F.; Dingenen, R van and H. Vanmarcke, Deposition of Aerosols and Unattached Radon Daughters in Different Chambers; Theory and Experiment, Radiation Protection Dosimetry, Vol. 24, No. 1/4, 217-220, 1988.

Hummelshoj, P. Dry Deposition of Particles and Gases. Ph.D. Thesis. Risø-R-658(EN), DK, 1992.

Jayasekeera,P.N.; Aerosols Containing Activatable tracers for Deposition Studies, Proc. 3rd Annual Conf. U.K. Aerosol Society, 1989.

Jenkin, M.E.; Cox, R.A. and D.E. Candeland, Photochemical Aspects of Tropospheric Iodine Behaviour, Journal of Atmospheric Chemistry, Vol. 2, pp. 359-375, 1985.

Jensen, H.E Matematisk Analyse, Bind 1, p 129. (In Danish)

Jones, J.A., The Importance of Deposition to Skin in Accident Consequence Assessments, Proceedings of the Seminar on methods and codes for assessing the off-site consequences of nuclear accidents, Athens, 7 to 11 May 1990.

Jost, D.T.; Gäggeler, H.W.; Baltensperger, U.; Zinder, B and P. Haller, Chernobyl fallout in size-fractionated aerosol, Nature, Vol. 324, pp. 22-23, 1986.

Knutson, E.O. Modelling Indoor Concentrations of Radon's Decay Products, in Radon and Its Decay Products in Indoor Air, Editors: Nazaroff, W.W. and A.V. Nero, Wiley. New york, 1988.

Knutson, E.O.; Gogolak, C.V.; Scofield, P. and G. Klemic, Measurements of Radon Progeny Activity on Typical Indoor Surfaces. Radiation Protection Dosimetry, Vol. 45, No. 1/4, pp. 313-317, 1992.

Knutson, E.O.; Hubbard, L.M. and B.M. Bolker, Determination of the surface to Volume Ratio in Homes from Measurements of Radon and its Progeny, Radiation Protection Dosimetry, Vol. 42, No. 2, pp. 121-126, 1992.

Koch, J. & J. Tadmor. Sheltering - a protective measure following an accidental atmospheric release from a nuclear power plant. Health Physics, Vol. 54, No. 6, pp. 659-667, 1988.

Kocher, D.C., Effects of indoor residence on radiation doses from routine releases of radionuclides to the atmosphere, Nuclear Technology, Vol. 48, pp. 171-179, 1980.

Kolima, H.; Abe, S. and K. Fujitaka, Semi-empirical Estimation of Deposition Velocity of Unattached Radon Daughters in a Room, Radiation Protection Dosimetry, Vol. 46, No. 2, pp. 103-109, 1993.

Kritz, M.A. and S.W. Rosner, Air Mass Origins and Troposphere-to-Stratosphere Exchange Associated With Mid-Latitude Cyclogenesis and Tropopause Folding Inferred From ^{7}Be Measurements, Journal of Geophysical Research, Vol. 96, No. D9, pp. 17405-17414, 1991.

Kvisgaard, B.; Collet, P.F. and J.Kure. Research on fresh-air change rate: 1. Building Technological institute in Denmark, 1984.

Megaw, W.J., The Penetration of Iodine into Buildings, Harwell Report, AERE-R-3827, UK, 1961.

Melikov, A.K. Quantifying draft risks. Technical review No. 2. Brüel & Kjær, Nærum, Denmark, 1988.

Nazaroff, W.W. and G.R. Cass, Particle Deposition from a Natural Convection Flow onto a Vertical Isothermal Flat Plate, Journal of Aerosol Science, Vol. 18, pp. 445-455, 1987.

Nazaroff, W.W. and G.R. Cass, Mathematical Modelling of Indoor Aerosol Dynamics,Environmental Science and Technology, Vol. 23, No. 2, 1989.

Nazaroff, W.W. and G.R. Cass, Mass-transport Aspects of Pollutant Removal at Indoor Surfaces, Environment International, Vol. 15, No. 1/6, pp. 567-584, 1989.

Nazaroff, W.W. Mathematical Modelling and Control of Pollutant Dynamics in Indoor Air, Ph.D. Thesis, California Institute of Technology, Pasadena, California, 1988.

Offermann, F.J.; Sextro, R.G.; Fisk, F.J.; Gimsrud, D.T.; Nazaroff, W.W.; Nero, A.V.; Revzan, K.L.; and J. Yater, Control of Respirable in Indoor Air with Portable Air Cleaners, Atmospheric Environment, Vol. 19, pp. 1761-1771, 1985.

Okuyama, K.; Kousaka, Y.; Yamamoto, S. and T. Hosokawa, Particle Loss of Aerosols with Particle Diameters between 6 and 2000 nm in a Stirred Tank, Journal of Colloid and Interface Science, Vol. 110, pp. 214-223, 1986.

Osuch, S.; M. Dabrowska; P. Jaracz; J. Kaczanowski; Le Van Khoi; S. Mirowski; E. Piasecki; G. Szeflinska; Z. Zszeflinski; J. Tropilo and Z. Wilhelmi, Isotopic Composition of High-activity Particles Released in the Chernobyl Accident. Health Physics. Vol, 57, No. 5, pp. 7007-7016, 1989.

Owen, M.K. and D.S. Ensor, Airborne Particle Sizes and Sources Found in Indoor Air, Atmospheric Environment, Vol. 26A, No. 12, pp. 2149-2162, 1992.

Poet, S.E.; H.E. Moore and E.A. Martell. Lead-210, bismuth-210 and Polonium-210 in the atmosphere: accurate ratio measurement and and application to aerosol residence time determination. Journal of Geophysical Research, Vol. 77, pp. 6515-6527, 1972.

Porstendörfer, J. and A. Reineking, Radiation Protection Dosimetry, Vol. 45, No. 114, pp. 303-311, 1992.

Rasmussen, N.C. et al. Reactor Safety Study - WASH 1400. U.S. Nuclear Regulatory Commission, Washington, D.C. 1975.

Reineking, A.; Scheibel, H.G.; Hussin, A.; Becker, K.H. and J. Porstendörfer, Measurements of Stage Efficiency Functions Including Interstage Losses for a Sierra and a Berner Impactor and Evaluation of Data by a Modified Simplex Method, Aerosols in Science, Medicine and Technology, The eleventh Annual Conference of the Association for Aerosol Research, 1984.

Reineking, A.; Becker, K.H.; Porstendörfer J. and A. Wicke, Air Activity Concentrations and Particle Size Distributions of the Chernobyl Aerosol, Radiation Protection Dosimetry, Vol. 19, No. 3, pp. 159-163, 1987.

Reineking,A., H.G.Scheibel, A.Hussin and J.Porstendorfer. Radioactive Aerosols in the Lower Atmosphere. Proceedings from 3rd Int. Aerosol Conf., Vol. II, pp. 1217-1221, Kyoto, Japan, 1990.

Reist, P.C., Introduction to Aerosol Science, Macmillan Publishing Company, New York, 1984.

Roed,J.; Gjørup, H.L. & H.Prip. Huses beskyttende virkning ved luftforureningsuheld, Risø-M-2484. 1985. (in Danish)

Roed, J., Relationships in Indoor/Outdoor Air Pollution, Risø-M-2476, 1985.

Roed, J. & R.J. Cannell. Relationship between Indoor and Outdoor aerosol concentration following the Chernobyl accident. Radiation Protection Dosimetry, Vol. 21, No. 1/3, pp. 107-110, 1987.

Roed, J.; Goddard,A.J.H.; MacCurtain,J.; Byrne, M. & C. Large. Reduction of Dose from Radioactive Matter ingressed in Buildings. Cadarache, 1991

Rulik, P.; Bucina, I. and I. Malatova, Aerosol Particle Size Distribution in Dependence on the Type of Radionuclide after the Chernobyl Accident end in the NPP effluents, Proceedings of the XVth Regional Congress of IRPA on the Radioecology of Natural and Artificial Radionuclides. Sweden, FS-89-48T, 1013-4506, 1989.

Sandalls, F.J.; Segal, M.G. and N. Victorova, Hot Particles from Chernobyl: A Review. Journal of Environmental Radioactivity, Vol. 18, pp 5-22, 1993.

Schneider, T.; Bohgard, M. and A. Gudmundsson, A semi-empirical model for Particle Deposition onto Facial Skin and Eyes. Role of Air Currents and Electrical Fields, Journal of Aerosol Science, Vol. 25, No. 3, pp. 583-593, 1994.

Schumann, T.; Gysi, H. an S. Kaelin, Coating of Impaction Surfaces of cascade impactors: Necessary for Sampling Ambient Aerosols in Rural and suburban Areas? Journal of Aerosol science, Vol. 19, No. 7, pp. 993-996, 1988.

Sehmel, G.A. Particle Eddy Diffusities and Deposition Velocities for Isothermal Flow and Smooth Surfaces, Journal of Aerosol Science, Vol 4, pp. 125-138, 1973.

Shimada, M.; Okuyama, K.; Kousaka, Y.; and K Ohshima, Turbulent and Brownian Diffusive Deposition of Aerosol Particles onto a rough Wall, Journal of Chemical Engineering of Japan, Vol. 20, pp. 57-64, 1987.

Siren, K. A Computational Approach to the Penetration of Gaseous Pollutants into Buildings, Part I: Single Family Hous. Helsinki University of technology, Department of Energy Engineering, 45, 1992.

Table of isotopes, sixth edition, John Wiley & sons, New York, 1967.

Talbot, L.; Cheng, R.K.; Schefer, R.W.; and D.R. Willis, Thermophoresis of Particles in a Heated Boundary Layer, Journal of Fluid Mechanics, Vol. 101, pp. 737-758, 1980.

Tschiersch, J. and B. Georgi, Chernobyl Fallout Size Distribution in Urban Areas, Journal of Aerosol Science, Vol. 18, No 6, pp. 689-692, 1987.

Tu, K. A Condensation Aerosol Generator System for Monodisperse Aerosols of Different Physio chemical Properties, Journal of Aerosol Science. Vol. 13, No. 5, pp. 363-371, 1982.

Whitby, K.T., The Physical Characteristics of Sulphur Aerosol. Atmospheric Environment, Vol. 12, pp. 135-159, 1978

Willeke, K. and K.T.Whitby, Atmospheric Aerosols: Size Distribution Interpretation, Journal of the Air Pollution Control Association, Vol. 25, No. 5, pp. 529-534, 1975.

Yocom, J.E.; Clink, W.L. & W.A. Cote. Indoor/Outdoor air quality relationships. Journal of the Air Pollution Control Association. Vol 21, No. 5, pp. 251-259, 1971.

Yocom, J.E. Indoor-Outdoor Air Quality Relationships. Journal of the Air Pollution Control Association. Vol. 32, No. 5, pp. 500-520, 1982.

Bibliographic Data Sheet **Risø-R-780(EN)**

Title and author(s)

Indoor Deposition and the Protective Effect of Houses against Airborne Pollution

Christian Lange

ISBN	ISSN
87-550-2024-0	0106-2840

Dept. or group	Date
	May 1995

Groups own reg. number(s)	Project/contract no.(s)

Pages	Tables	Illustrations	References
114	26	46	87

Abstract (Max. 2000 characters)

The protective value of a house during a release of toxic materials has been investigated to the atmosphere. A review of the relevant literature revealed wide agreement on dose reduction factors from 0.5 to 0.2. According to the literature indoor deposition rather than filtration by the building envelope was the main cause of the reduction, but very little information on indoor deposition exists.

The main topic for this work has been the measurement of indoor deposition using monodisperse particles in the size range 0.5 to 5.5 μm, labelled with neutron activatable tracers. The decay of aerosol concentration was measured and average deposition velocities were recorded in four houses. The results were consistent with increasing deposition velocities for increasing particle size and increasing degree of furnishing.

Neutron activatable particles have been used for measurements of skin deposition velocities to a human volunteer. The deposition velocity was found to be $7.4 \pm 1.1 \times 10^{-4}$ ms^{-1} for the 0.5 μm particles and $57 \pm 14 \times 10^{-4}$ ms^{-1} for the 2.5 μm particles. These values of skin deposition velocities imply that the amount of pollutants deposited to the skin of a dressed person is more than an order of magnitude larger than the amount deposited in the lungs, and that skin deposition is an important pathway for toxics that can penetrate through the skin.

Beryllium-7 was used as a tracer in a series of experiments. The activity distribution of this isotope was determined using a Berner low pressure impactor. Median diameters ranged from 0.7 to 1.1 μm and it was found that the activity distribution followed the mass distribution of the accumulation mode for atmospheric particles. I/O measurements have been made with two impactors. The results showed that the reduction in indoor air concentration was largest for supra micron particles.

Descriptors INIS/EDB

AEROSOLS; AIR INFILTRATION; BERYLLIUM 7; BUILDINGS; DEPOSITION; DYSPROSIUM 165; INDIUM 115; INDOOR AIR POLLUTION; NEUTRON ACTIVATION ANALYSIS; PARTICLE SIZE; PARTICULATES; SAMPLING; SILICA; SKIN; SPATIAL DISTRIBUTION; TRACER TECHNIQUES

Available on request from Information Service Department, Risø National Laboratory
(Afdelingen for Informationsservice, Forskningscenter Risø), P O Box 49,
DK-4000 Roskilde, Denmark
Telephone (+45) 46 77 46 77, ext. 4004/4005
Telex 43 116 · Telefax (+45) 46 75 56 27

RISØ

Objective

The objective of Risø's research is to provide industry and society with new potential in three main areas:

- *Energy technology and energy planning*
- *Environmental aspects of energy, industrial and plant production*
- *Materials and measuring techniques for industry*

As a special obligation Risø maintains and extends the knowledge required to advise the authorities on nuclear matters.

Research Profile

Risø's research is long term and knowledge-oriented and directed toward areas where there are recognised needs for new solutions in Danish society. The programme areas are:

- *Combustion and gasification*
- *Wind energy*
- *Energy technologies for the future*
- *Energy planning*
- *Environmental aspects of energy and industrial production*
- *Environmental aspects of plant production*
- *Nuclear safety and radiation protection*
- *Materials with new physical and chemical properties*
- *Structural materials*
- *Optical measurement techniques and information processing*

Transfer of Knowledge

The results of Risø's research are transferred to industry and authorities through:

- *Research co-operation*
- *Co-operation in R&D consortia*
- *R&D clubs and exchange of researchers*
- *Centre for Advanced Technology*
- *Patenting and licencing activities*

To the scientific world through:

- *Publication activities*
- *Co-operation in national and international networks*
- *PhD- and Post Doc. education*

Risø-R-780(EN)
ISBN 87-550-2024-0
ISSN 0106-2840

Available on request from:
Information Service Department
Risø National Laboratory
P.O. Box 49, DK-4000 Roskilde, Denmark
Phone +45 46 77 46 77, ext. 4004/4005
Telex 43116, Fax +45 46 75 56 27

Key Figures

Risø has a staff of just over 900, of which more than 300 are scientists and 80 are PhD and Post Doc. students. Risø's 1995 budget totals DKK 476m, of which 45% come from research programmes and commercial contracts, while the remainder is covered by government appropriations.